Project Report No. 103

EXPERIMENTAL STUDY OF WARM WATER FLOW INTO IMPOUNDMENTS
PART III:
TEMPERATURE AND VELOCITY FIELDS NEAR A SURFACE OUTLET IN THREE-DIMENSIONAL FLOW

by
Heinz Stefan
and
Frank R. Schiebe

Prepared for
Department of the Interior
Federal Water Pollution Control Administration

December 1968

PREFACE

Under a grant from the Department of the Interior, Federal Water Pollution Control Administration, a study was made of the hydromechanics of flow of heated water into natural lakes and reservoirs. The study was essentially experimental and confined to the immediate vicinity of the outlet. It had three phases, the results of which are presented in three project reports by the St. Anthony Falls Hydraulic Laboratory, University of Minnesota.

1. Project Report No. 101, Experimental Study of Warm Water Flow into Impoundments. Part I: Flow and Heat Exchange Near a Surface Outlet in Two-Dimensional Flow, December 1968.

2. Project Report No. 102, Experimental Study of Warm Water Flow into Impoundments. Part II: Temperature and Velocity Instrumentation and Data Processing for the Three-Dimensional Flow Experiments, December 1968.

3. Project Report No. 103, Experimental Study of Warm Water Flow into Impoundments. Part III: Temperature and Velocity Fields Near a Surface Outlet in Three-Dimensional Flow, December 1968.

The principles of the instrumentation have also been described in a separate publication entitled "The Measurement of Low Fluid Velocities with the Aid of a Tethered Sphere," by Heinz Stefan and Frank R. Schiebe, published in Water Resources Research, December 1968.

Results of a literature survey on stratified flow were assembled in an Internal Memorandum, No. IM-93, entitled The Role of Mixing in Stratified Flows - An Annotated Bibliography, by N. Hayakawa and F. R. Schiebe.

Internal Hydraulic Jump in Co-Current Stratified Flow, by N. Hayakawa, is the title of another Internal Memorandum, IM-94, July 1969, prepared under this program.

A sound-motion picture (20 min.) entitled "Warm Water Flow into Impoundments" has been produced. It shows some features of stratified flow of heated water from a channel over cold water in a reservoir.

SUMMARY

The investigation reported herein was undertaken in order to obtain some experimental information on the physical processes producing temperature and velocity distribution when heated water is discharged from a channel into a wide and deep tank. The outlet channel was built with a rectangular cross section. The receiving tank also had a rectangular cross section, but its depth and width were more than ten times larger than those of the channel. The facility was provided with instrumentation to measure temperature and velocity in a three-dimensional stratified flow. Measurement of the latter proved to be very difficult, and a large amount of effort was necessary to achieve the goal. The facility was used to carry out a number of experiments, as shown in Table I. Reduced Froude numbers and Reynolds numbers at the outlet ranged from 0.62 to 7.2 and 1500 to 9400, respectively. Strong stratification of the flow could be observed in all experiments. Surface spreading patterns of the plumes were also recorded photographically. The effects of buoyancy and turbulence on temperature and velocity may be inferred from the data, which are reported at the present time without analysis. The data are useful for comparison with analytical models. The facility and its instrumentation can now be used for further, more complicated, three-dimensional stratified flow studies.

EXPERIMENTAL STUDY OF WARM WATER FLOW INTO IMPOUNDMENTS PART III: TEMPERATURE AND VELOCITY FIELDS NEAR A SURFACE OUTLET IN THREE-DIMENSIONAL FLOW

1. Scope of Investigation

In the course of a study on the circulation of condenser cooling water from a steam generating plant through a lake [1]*, it became apparent that not enough information is available in the literature on the mixing and stratification of liquids of different densities. This deficiency in knowledge has also been pointed out by others; for example, it is mentioned several times in the Proceedings of the Twelfth Pacific Northwest Symposium on Water Pollution Research [2]. In the condenser cooling study reported in Ref. [1] it was clear that where warm water entered the lake it would form a stratified layer on the surface in spite of some mixing at entry, but the thickness of the layer and the temperature gradient between the layer and the natural lake could not be predicted satisfactorily. Furthermore, there was considerable doubt as to the relative importance of stratification and turbulent mixing as the warm water layer spread and cooled. If stratification persisted to a high degree even for small temperature differences, the added heat would be dissipated to the atmosphere relatively rapidly and there would be no increased temperature at the plant intake (usually located at some depth below the water surface). On the other hand, if turbulent mixing of sufficient intensity occurred at the interface, the stratification could be destroyed. Then heat dissipation to the atmosphere would be less rapid and the plant might ingest warmer water.

Prediction of the areal extent and profile of the warm water regime is generally important not only to the operation of a plant, but also to the study of the effects of the warm water on the biology and potential pollution of the lake.

Temperature distribution is not the only problem area involving stratification and mixing. Related problems occur, for example, in the spreading of sewage water discharged into the ocean, in the discharge of aerated domestic sewage and certain industrial wastes into lakes and rivers, in the flow

---

*Numbers in brackets refer to the List of References on page 21.

of sediment-laden water into clear water, in estuaries where fresh and salt water meet, and even in the spreading of smoke in the atmosphere. Better knowledge of the fundamentals of combined problems in stratification and turbulent mixing will ultimately contribute to the solution of problems in all these areas.

Under a grant from the Department of the Interior, Federal Water Pollution Control Administration, a laboratory study was made of the hydro- and thermodynamics of the flow of heated water into natural lakes and reservoirs. This part of the final report deals with experimental results on temperature and velocity distributions near a surface outlet of heated water into a wide tank filled with colder water.

The results show the degree of stratification that can be expected at an outfall where fluid of one density joins fluid of another density. The characteristics of the outfall, the difference in density between warm and cold water, the rate of surface cooling, and to a certain extent the size of the tank influence these results.

Discharges from a rectangular outlet channel placed at a right angle into the wall of a rectangular tank were investigated. The channels ended either flush with the wall of the tank, as shown in Fig. 1, or projected into the tank, as shown in Fig. 2.

While the research reported upon here was being carried out, two publications appeared which refer to similar flow configurations. The study by Jen, Wiegel and Mobarek [3] deals with warm water discharged from a pipe at fairly high speeds. The effect of stratification is considerably different from that found in outlets at lower speeds. The reduced Froude number at the outlet, $Fr_o' = U_o(\frac{\Delta\rho}{\rho_o} g d_o)^{-1/2}$, may be used for comparison, where U_o is the average velocity at the outlet $Q_o(b_o d_o)^{-1}$, ρ_o is the density of the water at the outlet, $\Delta\rho$ is the density difference between warm and cold water at the outlet, d_o is the water depth in the outlet channel, and g is the acceleration of gravity. The studies in Ref. [3] used reduced Froude numbers from 18 to 180, while the results reported herein refer to values from 0.6 to 7.2. The latter values are more commonly experienced in application to thermal power plants. There is also some difference between the type of flow from a pipe and that from a rectangular channel.

The second study was made by Hayashi and Shuto [4]. Hayashi and Shuto investigated a problem very similar to the problem being considered here. Temperature data only were obtained in their study, whereas velocity fields were also investigated in the present study. An analytical model to describe such a stratified flow from an outlet is proposed in Ref. [4]. As is usual with mathematical models of physical processes, simplifications and assumptions had to be employed. Results in Ref. [4] show that for a case where no vertical mixing is assumed in the analytical model and inertial forces are small, there is good agreement with experimental results for the case where mixing is expected to be very small. In Ref. [4] a similarity hypothesis was made with regard to temperature and velocity distributions in the surface current. Results to be presented herein show that these assumptions may be justified only in a limited area.

There are numerous other studies on stratified flow which are related to this investigation. A bibliography of publications dealing with the hydrodynamics of stratified flow was prepared in 1968 by members of the staff of the St. Anthony Falls Hydraulic Laboratory [5]. A limited number of copies is available for distribution.

2. Experimental Facility and Experimental Procedure

The three-dimensional facility was designed and built so that the spread of warm water discharged horizontally from an outlet at the surface of a near quiescent pool of cooler water could be studied. Provision was made for the continuous addition of a small flow of cool water to make up the water being entrained by the surface flow so that a steady-state condition could be maintained. The facility used is shown schematically in Fig. 3 and photographically in Figs. 4 and 5. It consisted essentially of a large rectangular tank 40 ft long, 17 ft wide, and approximately 2 ft deep. Warm water was carried to the tank in an open channel. The outlet was located at the center of one end of the tank. The outlet channel used had a rectangular cross section, the wetted part of which was maintained at 0.5 ft wide and 0.165 ft deep in this laboratory study. Experiments were carried out with outlet channels either ending flush with the wall or projecting 4.86 ft into the tank.

The tank was entirely lined with two inches of styrofoam covered with 1/4 inch of asphalt to prevent heat transfer through the bottom and walls of the tank. However, heat was lost from the warm water in the tank to the atmosphere.

The volumetric flow rate of the heated water and the water temperature at the outlet were steady in all experiments. Outlet flow was turbulent. The experimental facility was located in a several-storied building. The room temperature and humidity could not be controlled, and there were some variations of these quantities over a period of several days. Temperature and velocity profiles were measured in approximately 30 to 50 locations distributed over the entire pool in every experiment. Temperatures to be measured ranged from 50° to 95°F. Thermistor probes (Yellow Springs Instrument type 8436) with a time constant of 0.7 seconds were used for this purpose.

The development of suitable instrumentation for the measurement of point velocity vectors in the range between 0.01 and 0.2 ft per second was a major problem. The requirements of the velocity sensor were very difficult to satisfy. The sensor had to be inserted through the free surface from above and had to have the capability of measuring velocity gradients in water layers which were relatively thin. This required that the probe be very small. The probe also had to be sensitive to very low velocities and work in a temperature gradient. In addition, the direction of the velocity vector was unknown and variable. Several methods were tried: probes based on a photoelectric principle, probes using a thermal disturbance principle, miniature fluid amplifiers, and photographing dye streaks. All these methods gave unsatisfactory results for various reasons.

The tethered sphere was then developed. It is described in Ref. [6] and in Part II of this series of reports, listed in the Preface. Basically, the instrument statically balances the drag and the buoyancy forces of a tiny sphere against the tension in the tethering line. The sphere is formed from wax or plastic and is approximately 1/16 inch to 1/8 inch in diameter. The line is rayon 0.0002 inches in diameter. The displacement of the sphere from zero velocity position gives, with proper calibration, the magnitude and direction of the point velocity. The size of the sphere and its specific gravity determine the range of velocities in which the instrument is useful.

3. Range of Variables and Parameters Investigated

The study reported herein was paralleled by a similar study in a two-dimensional flume. In the part of the report which covers the two-dimensional flow of warm water into a reservoir--listed as Part I in the Preface--the dimensionless groups of physical parameters which control the flow and the heat exchange in such an experiment have been derived and discussed. The results are immediately applicable to the three-dimensional tank experiments. The only difference is that in tank experiments two additional ratios of geometrical lengths had to be used. They describe the width of the outlet channel b_o and the width of the tank b_ℓ. Thus the dimensionless groups likely to affect three-dimensional flow into the tank are the geometrical ratios,

$$\frac{b_o}{d_o}, \quad \frac{b_\ell}{d_o}, \quad \frac{d_\ell}{d_o}, \quad \frac{\ell_\ell}{d_o}$$

the temperature ratios,

$$\frac{T_\ell}{T_o}, \quad \frac{E}{T_o}$$

and the Reynolds number Re_o, reduced Froude number Fr_o', and Biot number Bi_o at the outlet. The symbols d, b, ℓ, and T designate the depths, widths, lengths, and temperatures, respectively, and the subscripts o and ℓ refer to the outlet and the reservoir or lake, respectively; E is the equilibrium water temperature or the temperature at which the net heat transfer between the water surface and the atmosphere will be zero; the internal Froude number was defined previously. The outlet Reynolds number and the Biot modulus are

$$Re_o = U_o d_o \nu_o^{-1} \quad \text{and} \quad Bi_o = k_s d_o k^{-1}$$

respectively, where U_o is the average flow velocity at the outlet, d_o is the outlet depth, ν_o is the kinematic viscosity of the water at the outlet, k_s is the average coefficient of surface heat transfer, and k is the conductivity of water.

In the experiments some of the dimensionless groups were constant, while others varied. The dimensions were all maintained very nearly constant at

$$d_o = 0.165 \text{ ft}$$

$$d_\ell = 1.60 \text{ ft}$$

$$b_o = 0.50 \text{ ft}$$

$$b_\ell = 17.0 \text{ ft}$$

$$\ell_\ell = 40.0 \text{ ft}$$

The range of various variables, such as the outlet flow rate of warm water Q_o, the heated water outlet temperature T_o, the cold water temperature T_ℓ in the tank, and the air temperature T_a, can be found in Table I. The range of T_a roughly approximates that of the equilibrium temperature E, which was usually a few degrees below the room temperature. Q_o and T_o could be controlled arbitrarily within the limits provided by the available heat exchangers.

The Biot modulus Bi_o cannot be calculated exactly, because the average surface coefficient of heat transfer k_s is unknown, but it can be estimated to be between 1.0 and 4.0, most likely close to 2.0. The Reynolds numbers investigated ranged from 1200 to 9600 and the densimetric Froude numbers from 0.6 to 7.2. Temperatures and velocities in the plume as well as surface spreading patterns were investigated. In some experiments only partial measurements were made. Extensive temperature and velocity measurements were made in seven experiments, one of which was a preliminary experiment, as shown in Table I. In these experiments approximately forty temperature and velocity profiles, consisting on the average of 30 and 20 points in each vertical, respectively, were taken in the tank for every run. Thus the temperature and the velocity field near the surface outlet are described by approximately 1200 and 800 points, respectively. This applies to each of the flow conditions tested.

The instrumentation was not developed to its full extent, and voltages equivalent to local temperature and the deflections of the tethered sphere were read from a digital voltmeter, recorded manually, punched on cards, and

Table I - SUMMARY OF EXPERIMENTS

TEST NO.	TYPE	OUTLET Q_o (cfs)	OUTLET d_o (ft)	OUTLET T_o (°F)	TANK T_ℓ (°F)	AIR T_a (°F)	Re_o	Fr_o'
	GROUP 1. EXPERIMENTS WITH TEMPERATURE AND VELOCITY RECORDS							
				Preliminary Test				
101	FLUSH	0.0228	0.088	90.9	79.2	80	5,700	7.2
				Main Tests				
215	FLUSH	0.00645	0.162	91.0	70.0	78	1,590	0.62
207	FLUSH	0.0131	0.165	76.5	51.5	78	2,700	1.38
216	FLUSH	0.376	0.162	92.0	73.0	81	9,370	3.73
214	PROJ.	0.00645	0.155	87.0	68.0	80	1,520	0.72
211	PROJ.	0.0141	0.159	84.0	60.0	76	3,190	1.43
217	PROJ.	0.0376	0.155	92.5	73.5	81	9,400	3.98
	GROUP 2. EXPERIMENTS WITH PARTIAL TEMPERATURE RECORDS							
201	FLUSH	0.0220	0.158	72.6	44.9	74	4,320	2.61
202	FLUSH	0.0217	0.156	74.7	53.0	76	4,370	2.68
203	FLUSH	0.0214	0.163	72.7	47.0	76	4,210	2.44
204	FLUSH	0.0217	0.164	75.0	49.3	74.5	4,310	2.30
205	FLUSH	0.022	0.165	81.5	46.3	76	4,900	1.97
	GROUP 3. EXPERIMENTS WITH SURFACE FLOW PATTERN RECORDS							
				Still Pictures (black and white)				
208	FLUSH	0.0131	0.164	82.2	58.0	75	2,890	1.29
209	PROJ.	0.0131	0.166	82.2	58.8	75.6	2,980	1.31
210	PROJ.	0.0142	0.166	78.0	57.3	78.0	2,990	1.52
212	PROJ.	0.0143	0.154	80.2	63.1	78.0	3,180	1.80
				Motion Pictures (color)				
213-b	PROJ.	0.0074	0.154	85.6	60.5	73.0	1,740	0.76
213-a	PROJ.	0.0140	0.154	85.3	62.0	73.0	3,200	1.48
213-c	PROJ.	0.0408	0.154	84.7	59.6	80.0	9,600	4.23

The data gathered for the preliminary test were accumulated and reduced. Figures 6, 7, and 8 are examples of these data. The net excess heat flow--i.e., the heat energy flux in the x-direction--was also determined. This calculation was based upon locally measured temperature and velocity data at various distances from the outlet. Figure 9 shows the result of this calculation. The excess heat is decreasing with distance from the warm water outlet by the amount of heat being lost to the atmosphere. The accuracy of the data at locations farther than 8 ft from the outlet in this case was not sufficient for their use in this calculation.

With the experience gained from this initial test the instrumentation was modified and the remainder of the tests were planned.

4.2 Results of Main and Other Tests

Six main tests were run, as shown in Table I. It is impossible in the context of this report to present all the experimental data obtained. The main features of the flow and of the temperature distribution are shown and interpreted, first for the flush outlet and then for the projecting outlet.

4.21 Temperatures -- The development of the temperature profile with distance from the outlet is shown in a series of isotherms in a vertical plane through the centerline of the outlet channel. In locations where temperature is actually a time-dependent fluctuating quantity due to turbulence, time-smoothed values have been reported. Figures 10a, 11a, 12a, 13a, 14a, and 15a clearly show the effect of buoyancy forces on the thickness of the warm water layer. Low internal Froude numbers at the outlet indicate a high degree of buoyancy. Heat loss at the water surface had an effect on the temperature distribution, and this effect increased with distance from the outlet. The amount of heat lost at the water surface was not measured and is likely to be different from one experiment to another. Water temperatures approach an equilibrium temperature which is somewhat lower than the air temperature. The humidity of the air was near one hundred per cent in all cases. The temperature difference between the water at the surface and the atmosphere may therefore be taken as a qualitative measure of the amount of heat lost.

The first series of figures (Figs. 10a, 11a, and 12a) refers to outlets ending flush in a vertical wall, while the second series (Figs. 13a, 14a, and 15a) was obtained with a projecting outlet. Differences between the two types appear to be only minor as far as temperatures are concerned. It had been expected that the projecting outlet would show a smaller amount of mixing at the outlet and hence stronger stratification. The shear of the warm water stream on the colder sublayer was expected to produce a horizontal cold water current in the positive x-direction into which the warm water would discharge from the projecting outlet. Without projection no such cold water current could form; instead, the cold water attracted by the warm water jet would have to make something like a right-angle turn at the outlet, and there would be a tendency toward stronger mixing at the outlet. The isotherm patterns did not provide enough information from which to decide whether these expectations were correct. It appears to be more likely that there are no major differences between the two types of outlets.

The temperature at the water surface decreases with distance from the outlet due to heat loss and mixing. The decrease in temperature measured can be quite drastic. Two examples are shown in Fig. 16. These refer to two special experiments which were run after the completion of Test 216. As the water flows downstream there is continuous heat loss through the water surface. Temperatures can be expected to tend toward an equilibrium temperature at which the rate of surface heat transfer will have dropped to zero. This temperature was estimated to be close to 79.5°F, the temperature which the water in the tank assumed when left in it over a period of several days without flow. The two curves in Fig. 16 can be reduced to one if temperature differences above the equilibrium temperature E are plotted in the form $(T - E)/(T_o - E)$ versus distance from the outlet, as shown in Fig. 17. When a logarithmic scale is used for the dimensionless temperature differences, the data plot fairly close to a straight line, suggesting an approximately exponential temperature decline along the centerline of the tank. According to an equation derived in Ref. [1],

$$\frac{T - E}{T_o - E} = \exp\left[-\frac{K\Lambda}{Q\rho c_p}\right] \qquad (1)$$

where T is the temperature at an isotherm on the water surface, T_o is the outlet temperature, E is the equilibrium temperature, K is the average coefficient of surface heat transfer for area A, A is the water surface area between any two streamlines, the outlet and an isotherm of temperature T, Q is the volumetric flow rate between the two streamlines, ρ is the density of water, and c_p is the specific heat for constant pressure. Velocities as well as temperatures are assumed to be uniform over the depth of the warm water layer.

If the experimental data shown in Fig. 17 and in Eq. (1) are to agree it is necessary that

$$\frac{KA}{Q\rho c_p} = nx$$

where n can be determined from the slope of the temperature profile in Fig. 17. For a specific experiment at a given flow rate Q and in a specific environment all variables in this equation become constants except A and x. Thus A is required to be proportional to x, which is substantially correct along the centerline because the flow shows only a small amount of lateral spread. Streamlines are very nearly parallel, as will be shown later.

The flow conditions of the experiments which produced the results shown in Fig. 16 were similar to those of Test 216. Figure 12 reveals that the isotherms are nearly horizontal. The warm water layer is not well mixed along a vertical, and there is no two-layered system. Surface temperatures nevertheless show an exponential decline, suggesting that the heat transfer process at the water surface along the centerline is similar to that of a warm water layer which is vertically well mixed.

It is also of interest to examine some of the vertical temperature profiles. Figures 18a through 18c represent an example of measured temperature distributions at various distances from the outlet for Test 201 with the outlet flow conditions shown in Table I. This particular series of graphs shows the decrease in surface temperature from $72.6^{\circ}F$ at $x = 0.5$ ft to approximately $58^{\circ}F$ at $x = 32.0$ ft. It is interesting to examine the extent and magnitude of turbulent temperature fluctuations. Such

fluctuations are found in locations where flow is turbulent and temperatures are nonhomogeneous due to incomplete mixing of warm and cold water. The disappearance of the temperature fluctuations in areas where a temperature gradient in the vertical direction still exists is an indication that the flow has become stably stratified with weak or no vertical turbulent velocity components. As can be seen in Fig. 18a, temperature fluctuations are confined to a relatively narrow region at $x = 0.5$ ft. They have very nearly reached the water surface at $x = 1.0$ ft, but do not seem to reach further in depth. At $x = 8.0$ ft the amplitudes of turbulent temperature fluctuations have decreased substantially, and at $x = 32.0$ ft they have disappeared nearly entirely. The x-y-plotter used to make the records had only a very low frequency response, and the temperature probe had a time constant of 0.7 seconds. Therefore the amplitudes shown represent only qualitatively the existence of low-frequency fluctuations. Local amplitudes cannot be expected to be real maxima or minima. The temperature probe was moved at a velocity of approximately 0.02 in. sec^{-1} through the water. These limitations have principal significance near the outlet.

A similar set of temperature profiles at a given distance from the outlet and at various distances from the centerline of the tank is presented in Figs. 19a through 19f. Turbulent temperature fluctuations also disappear with distance from the centerline. It can also be seen that a surface layer of water slightly warmer than the cold water in the bottom of the tank exists over the whole tank due to its limited width. The heated water discharges into an existing warm water layer which is partially controlled by the width of the tank. The same situation exists in other tests, as may be seen in Figs. 10e, 11d, and 12e. Despite its large size the tank cannot be considered a perfect representation of a body of water of infinite extent.

An attempt was also made to plot isotherm patterns at the water surface and in planes parallel to the water surface at distances d_o and $2d_o$ from the surface, d_o being the outlet depth. For the flush outlet, temperatures at depth $z = 2d_o$ were found to be nearly unaffected by the warm water discharge when x was between zero and 10 ft and y was between -3 ft and +3 ft. At depth $z = d_o$ during the same experiments only a small area near

the outlet was affected. Similar results were obtained for the projecting outlet. Consequently, no graphs are presented.

4.22 Flow Patterns -- By adding tracers to the warm water in the outlet channel it was possible to observe the flow pattern in the tank. Food dye, fluoresceine, aluminum powder, and lycopodium powder were used to visualize flow patterns. Dyes were mixed well with the warm water flow in the outlet channel before the point of release into the tank. The dye contour of the warm water plume therefore represented time-lines for the fastest-traveling fluid particles in the plume. Fluoresceine dye was generally preferred to red food dye because it provided better contrast against the black lining of the tank. Aluminum powder and lycopodium powder float on the water and therefore show surface spreading patterns. Lycopodium powder was preferred to aluminum powder because of possible electrostatic effects. Photographs of the plumes were taken from above at a right angle to the water surface. Examples of such photographs are presented in Fig. 20. A time exposure for the same flow is shown in Fig. 21. Time lines from different series of photographs were assembled to show the evolution of a plume. Figures 22 through 26 are examples of such plots. The motion picture referred to in the Preface shows these more dramatically. As was to be expected, contours obtained with powder on the water surface and with dye within the whole warm water layer differed only very little, because maximum velocities are found at the water surface.

Crystals of fluoresceine were also deposited at the bottom of the outlet channel. Dye entrained from these generally showed very little lateral spread. In some cases turbulent mixing or internal gravity waves issuing from the channel bottom, mostly of an unstable nature, were observed. Figures 27 and 28a illustrate qualitatively some flow patterns observed near the outlet. Figure 28b shows photographs of surface spreading patterns near the outlet in which lycopodium powder has accumulated in several regular streaks perpendicular to the general flow direction. These streaks were caused by an interfacial wave pattern which began at the bottom of the outlet channel. The circulation of the water particles associated with the interfacial wave pattern caused particles floating at the water surface to accumulate in the form shown. The waves shown were observed to break after a

few wave lengths. This phenomenon occurred at a reduced outlet Froude number of 1.31 and at an outlet Reynolds number of approximately 3000. The flow patterns shown should not be considered the only ones possible.

4.23 Velocity Distributions -- More precise information on the flow pattern was obtained from the velocity measurements taken with the aid of the buoyant tethered sphere probe. Measurements of the components u and v of the velocity vector in the x- and y-direction, respectively, were made at a large number of points. Examples of the velocity profiles obtained from such measurements are given in Figs. 29 through 32. These profiles were taken along the centerline of the tank.

Measured velocity vectors were also plotted in horizontal planes at 0.01 ft and 0.2 ft below the water surface, and these are shown in Figs. 33 and 34. These figures show the velocity pattern. Positive velocities were found only in a relatively thin layer near the water surface. The thickness of that layer was approximately the same as the thickness of the warm water layer. At a depth of 0.2 ft, which is slightly greater than the depth at the outlet ($d_o \approx 0.16$ ft), velocities were very small. Below the surface layer there was backflow toward the outlet at very low and rather uniform velocity. It is interesting to note that there is no spread of the velocity distribution in depth. The shear which the warm water flow exerted on the cold water underneath did not cause any substantial flow of cold water in the x-direction. This is a somewhat surprising result because experience with two-layered density stratified flow or submerged jets leads one to expect considerable entrainment. The results may be attributed to the temperature gradient which exists over a considerable portion of the depth and which produces stratification of such stability that the return flow of the entrained fluid is very difficult. Since this return flow, or recirculation, is necessary for reasons of continuity, entrainment does not exist to the anticipated degree.

A more complete picture of the entire velocity field near the outlet was obtained in a perspective plot of velocity vectors, as shown in Figs. 35a through 35d. The velocities have magnitudes which are generally difficult to measure. A new device and a fairly complex data reduction procedure were used. The reported results are believed to represent correct magnitudes;

however, these measurements should not be used to obtain velocity gradients or higher order derivatives.

That portion of the cross-section in which the flow had a positive u component of velocity is shown by a heavy dotted pattern. It is apparent that the thickness of the layer having a positive forward flow is relatively small compared to the total water depth in the tank. The thicknesses of the warm water surface layer increased as the flow rates of warm water into the tank were increased. (With the flow rates, reduced Froude numbers and Reynolds numbers also increased.) This result agrees with the findings on two-layered, two-dimensional flow given in Project Report No. 101 (cited in the Preface) and with general concepts of two-dimensional, two-layered stratified flow.

The surface layer is shown in Figs. 36a and 36b for two flows with higher Froude and Reynolds numbers. A lack of symmetry is evident. This has been explained previously by the limited width of the tank.

5. Concluding Remarks

The experimental results provide a basis for the understanding and discussion of the flow and temperature fields which result from the discharge of heated water from a channel into a reservoir, lake, or other type of impoundment. Although such a discharge has some resemblance to a turbulent half jet in homogeneous flow, heated water flow into a colder impoundment is not a homogeneous fluid flow problem. The difference may be measured in terms of the reduced or internal Froude number at the channel outlet, Fr_o'. In homogeneous fluid flow its value is infinite, indicating that dynamic forces govern the flow and buoyancy is absent. At the other end of the scale one finds zero internal Froude number flow, which is a hydrostatic problem. Because of the absence of flow and dynamic forces, buoyancy is the only controlling force. Real fluid flow from heated water outlets is somewhere in between. Reduced outlet Froude numbers are often found in the range from 0.1 to 10.0. Hence, real flow has some features, such as mixing, which must be attributed to dynamic and viscous forces (the relative importance of which is generally characterized by the Reynolds number at the outlet), and other features, such as stratification,

which must be attributed to buoyancy. The present experiments were conducted in the important range of $0.62 \leqslant Fr_o' \leqslant 7.2$, as shown in Table I.

A heated water plume may go through three stages: a jet-type mixing flow near the outlet, then a spreading stratified flow, and finally a homogeneous fluid flow. The second stage very often represents the major part of the plume, as can be seen, for example, in Figs. 11a and 12a in this report or in Figs. 15c, 15d, and 15e of Project Report No. 101 (Ref. [7]) for two-dimensional flow.

If the internal Froude number at the outlet is small enough, stratification may reach all the way into the outlet and suppress the jet-type flow, as is the case for the experiment shown in Fig. 10a and also for that shown in Fig. 15a of Project Report No. 101. If the internal Froude number is larger, so that the jet is present, transition to the stratified regime will inevitably occur. The transition is some form of internal hydraulic jump, as has been discussed in Ref. [7] for two-dimensional, two-layered flow. The experiments described herein show that the discussion of the two-dimensional internal jump also applies in three dimensions.

Isotherm patterns in Fig. 12a, for example, show a transition which occurs within the first two feet beyond the channel outlet. It is essentially of the "submerged internal hydraulic jump" type (see Ref. [7]). The flow in the jet regime is controlled from the outlet and has been called internally supercritical, whereas the stratified flow regime is subcritical and is controlled from downstream.

In an infinitely wide and deep reservoir or lake without currents or wind, stratification must occur at some distance from the outlet, no matter how much initial mixing takes place. If little heat is transferred through the water surface, the stratification is controlled from a point far away from the outlet, such as by an outflow channel or by a weir. By virtue of internal gravity this control will determine the depth of the stratified layers pretty much as water surface profiles are controlled in slowly flowing rivers and will also determine the location and form of the internal jump. The flow condition at the end of the impoundment opposite the heated water outlet projects its influence all the way across the impoundment and even up to the heated water outlet.

It may be noted that in an impoundment without an opposite end a steady flow condition cannot be obtained. This consideration of the "opposite end" can now be seen to be very important in modeling stratified flow, especially where mixing is not very important. In the three-dimensional tank experiments described herein the rate of surface heat loss was very substantial, and because of this, control of the flow from the downstream end was largely through this mechanism, as explained below, rather than by the weir provided at the outlet of the tank. Both the weir and the side walls of the tank did produce some "opposite end" effects, however.

Frequently currents in natural lakes and reservoirs, as well as surface waves, cause the eventual destruction of a stratified flow situation which has been produced by a heated water discharge. The break-up point then functions as the downstream control. No such currents or waves were generated in the present experiments, but it is planned to study this mechanism at a later time.

The effect of heat loss from the water surface to the atmosphere is characterized by an overall Biot modulus and was discussed in Project Report No. 101. The rate of heat loss directly affects density, hence buoyancy, and therefore the flow pattern. Due to heat loss the density of the warm water layer increases. The temperature eventually approaches an equilibrium value at some distance from the heated water outlet. The ultimate fate of the warm water plume or layer will depend on the relationship between the equilibrium temperature E of the water and the ambient water temperature in the impoundment, T_ℓ. Assuming that the impoundment is very large, but has an effluent, a heated water plume will form a continuous surface layer on the impoundment if E is greater than T_ℓ (lake is in heating cycle). If E is less than T_ℓ (lake is in cooling cycle), if the lake is large enough, and if both E and T_ℓ are larger than $39.2^\circ F$, the surface layer will break up at the point where the plume temperature is reduced to the ambient water temperature T_ℓ. Lake water and discharged heated water will become identical, and stratification will terminate at that point. If both E and T_ℓ are less than $39.2^\circ F$ the surface layer will "dive" when it approaches $39.2^\circ F$. It may continue as a bottom density current if it is not fully mixed with the surrounding water on the way down. Relative densities must be considered for other cases, also.

The effect of surface cooling on the isotherm pattern in a longitudinal cross section can be seen most clearly in Fig. 10a. Buoyancy is dominant over the first three feet, even permitting the cold water to form a wedge in the outlet channel. But because of heat transfer through the surface, buoyancy decreases at an increasing rate beyond 3 ft and the warm water layer thickness increases. If the tank were long enough, this process would lead to disappearance of stratification if E were less than T_ℓ.

The farthest point downstream to which stratification can be traced is a very important one. It is believed that analysis of the flow and temperature in a stratified plume of heated water must start from downstream. At the same time, as already observed, given sufficiently large densimetric Froude numbers at the outlet some areas around the outlet can be exempt from this influence. This area has previously been called the mixing jet regime, and it must be analyzed by going from the outlet into the impoundment. The two types of analysis proceeding in opposite directions must produce a joining condition in the form of an internal hydraulic jump. The analysis must of course consider both flow and heat transfer. This concept is believed to be theoretically sound. Whether it is also practical cannot yet be ascertained. A number of difficulties certainly exist in the practical application of the concept.

Another qualitative observation made in the course of this study, in contrast to that illustrated by Fig. 10a, is related to the effect of surface cooling and downstream control on the surface spreading patterns of the heated water. If both these phenomena produce a warm water layer which is much thicker than the outlet depth, the heated water will discharge as a jet into a layer of essentially its own temperature. In horizontal planes a short distance below the water surface, density differences in the flow direction may be minimal and the spreading of the plume in a horizontal plane will resemble that of a homogeneous fluid rather than a stratified fluid. No specific data on this subject are contained in this report, but such matters are important considerations in the modeling of thermal plumes. Modeling of the outlet flow conditions above is clearly insufficient, and full analysis of downstream conditions is required.

In conclusion, the experiments and the collected data partially described in this and the two previous project reports (see Preface) have clarified some of the most important interactions between various flow and heat transfer mechanisms. This information is believed to be of general value.

The data collected during the course of the research and presented in this report contain valuable quantitative information which to date has not been fully utilized. Further analysis of the data is necessary to produce information on, for example, the rate of entrainment and mixing at the outlet and the spreading angle of heated water plumes near the outlet. Determination of the length of the jet regime and the form of the internal hydraulic jump in the three-dimensional plume should also be goals of the data analysis. Such analysis was not possible within the funds provided for this project. Considering the amount of effort that was necessary to procure the data, it is hoped that an opportunity for the analysis will be found in the near future.

6. Acknowledgments

The study was carried out under a grant from the Federal Water Pollution Control Administration awarded to Professor E. Silberman and the senior author. This support is gratefully acknowledged. Mr. James Delker, Mr. Richard Norby, and Mr. Frank Tsai carried out portions of the data-gathering program. Mr. John Frick and Mr. Norio Hayakawa participated in the data processing. The help received from these gentlemen is gratefully acknowledged.

REFERENCES

[1] Silberman, Edward and Stefan, Heinz, Effects of Condenser Cooling Water Discharge from Projected Allen S. King Generating Plant on Water Temperatures in Lake St. Croix, University of Minnesota, St. Anthony Falls Hydraulic Laboratory Project Report No. 76, December 1964.

[2] Water Temperature--Influences, Effects and Controls, Proceedings of the 12th Pacific Northwest Symposium on Water Pollution Research, Pacific Northwest Water Laboratory, U.S. Public Health Service, November 1963, 156 pages.

[3] Jen, Yuan; Wiegel, R.; and Mobarek, I., "Surface Discharge of Horizontal Warm-Water Jet," Proceedings ASCE, Journal of the Power Division, Vol. 92, No. PO2, April 1966.

[4] Hayashi, T. and Shuto, N., "Diffusion of Warm Water Jet Discharged Horizontally at the Water Surface," Proceedings, Twelfth Congress of the International Association for Hydraulic Research, Vol. 4, September 1967, pp. 47-59.

[5] Hayakawa, N. and Schiebe, F. R., The Role of Mixing in Stratified Flows, An Annotated Bibliography, University of Minnesota, St. Anthony Falls Hydraulic Laboratory Internal Memorandum No. IM-93, October 1968.

[6] Stefan, H. and Schiebe, F. R., "The Measurement of Low Fluid Velocities with the Aid of a Tethered Sphere," Water Resources Research, Vol. 4, No. 6, December 1968, pp. 1351-1357.

[7] Stefan, H. and Schiebe, F. R., Experimental Study of Warm Water Flow into Impoundments. Part I: Flow and Heat Exchange near a Surface Outlet in Two-Dimensional Flow, University of Minnesota, St. Anthony Falls Hydraulic Laboratory Project Report No. 101, December 1968.

LIST OF SYMBOLS AND UNITS

A = area (ft^2)

b_o = width of outlet channel (ft)

b_ℓ = width of tank (ft)

Bi_o = $k_s d_o / k$ = Biot number at outlet (-)

c_p = specific heat (BTU $slug^{-1}$ $^oF^{-1}$)

d_o = depth of outlet channel (ft)

d_ℓ = depth of tank (ft)

E = equilibrium water temperature depending on atmospheric conditions (air temperature, radiation, humidity, etc.) (^oF)

$Fr_o' = U_o(\frac{\Delta\rho}{\rho_o} g d_o)^{-1/2}$ (-)

g = acceleration of gravity ($ft\ sec^{-2}$)

k = thermal conductivity (BTU hr^{-1} ft^{-1} $^oF^{-1}$)

k_s = average surface coefficient of heat transfer (BTU hr^{-1} ft^{-2} $^oF^{-1}$)

ℓ_ℓ = length of tank (ft)

Q_o = volumetric flow rate from outlet channel (ft^3 sec^{-1})

$Re_o = U_o d_o \nu_o^{-1}$

T = temperature (^oF)

T_o = heated water temperature at outlet (^oF)

T_ℓ = cold water temperature in tank (^oF)

$U_o = Q_o d_o^{-1} b_o^{-1}$ = average flow velocity in outlet channel ($ft\ sec^{-1}$)

u = component of flow velocity in x-direction ($ft\ sec^{-1}$)

v = component of flow velocity in y-direction ($ft\ sec^{-1}$)

SYMBOLS AND UNITS (Continued)

x = horizontal coordinate (ft)

y = horizontal coordinate (ft)

z = vertical coordinate (ft)

ν_o = kinematic viscosity of heated water in outlet channel ($ft^2\ sec^{-1}$)

ρ_o = density of heated water in outlet channel (slugs ft^{-3})

$\Delta\rho$ = density difference between heated and cold water at outlet (slugs ft^{-3})

LIST OF FIGURES

FIGURE 11b Isotherms for Test 207 in cross section at $x = 0.5$ ft from Upstream End of Tank. Warm Water Outlet at $x = 0.0$ ft, Outlet Temperature $T_o = 76.5^{\circ}F$.

FIGURE 11c Isotherms for Test 207 in cross section at $x = 1.5$ ft from Upstream End of Tank. Warm Water Outlet at $x = 0.0$ ft, Outlet Temperature $T_o = 76.5^{\circ}F$.

FIGURE 11d Isotherms for Test 207 in cross section at $x = 3.0$ ft from Upstream End of Tank. Warm Water Outlet at $x = 0.0$ ft, Outlet Temperature $T_o = 76.5^{\circ}F$.

FIGURE 11e Isotherms for Test 207 in cross section at $x = 6.0$ ft from Upstream End of Tank. Warm Water Outlet at $x = 0.0$ ft, Outlet Temperature $T_o = 76.5^{\circ}F$.

FIGURE 12a Isotherms for Test 216 in cross section at $y = 0$ (longitudinal cross section). Outlet depth $d_o = 0.162$ ft, Outlet Temperature $T_o = 92.0^{\circ}F$.

FIGURE 12b Isotherms for Test 216 in cross section at $x = 0.5$ ft from Upstream End of Tank. Warm Water Outlet at $x = 0.0$ ft, Outlet Temperature $T_o = 92.0^{\circ}F$.

FIGURE 12c Isotherms for Test 216 in cross section at $x = 1.5$ ft from Upstream End of Tank. Warm Water Outlet at $x = 0.0$ ft, Outlet Temperature $T_o = 92.0^{\circ}F$.

FIGURE 12d Isotherms for Test 216 in cross section at $x = 3.0$ ft from Upstream End of Tank. Warm Water Outlet at $x = 0.0$ ft, Outlet Temperature $T_o = 92.0^{\circ}F$.

FIGURE 12e Isotherms for Test 216 in cross section at $x = 5.0$ ft from Upstream End of Tank. Warm Water Outlet at $x = 0.0$ ft, Outlet Temperature $T_o = 92.0^{\circ}F$.

FIGURE 12f Isotherms for Test 216 in cross section at $x = 8.0$ ft from Upstream End of Tank. Warm Water Outlet at $x = 0.0$ ft, Outlet Temperature $T_o = 92.0^{\circ}F$.

FIGURE 13a Isotherms for Test 214 in cross section at $y = 0$ (longitudinal cross section). Outlet depth $d_o = 0.155$ ft, Outlet Temperature $T_o = 87.0^{\circ}F$.

FIGURE 13b Isotherms for Test 214 in cross section at $x = 5.5$ ft from Upstream End of Tank. Warm Water Outlet at $x = 4.86$ ft, Outlet Temperature $T_o = 87.0^{\circ}F$.

FIGURE 13c Isotherms for Test 214 in cross section at $x = 6.5$ ft from Upstream End of Tank. Warm Water Outlet at $x = 4.86$ ft, Outlet Temperature $T_o = 87.0^{\circ}F$.

FIGURE 13d Isotherms for Test 214 in cross section at $x = 7.5$ ft from Upstream End of Tank. Warm Water Outlet at $x = 4.86$ ft, Outlet Temperature $T_o = 87.0^{\circ}F$.

FIGURE 13e Isotherms for Test 214 in cross section at $x = 9.5$ ft from Upstream End of Tank. Warm Water Outlet at $x = 4.86$ ft, Outlet Temperature $T_o = 87.0^{\circ}F$.

FIGURE 14a Isotherms for Test 211 in cross section at $y = 0$ (longitudinal cross section). Outlet Depth $d_o = 0.158$ ft, Outlet Temperature $T_o = 84.0^{\circ}F$.

FIGURE 14b Isotherms for Test 211 in cross section at $x = 5.5$ ft from Upstream End of Tank. Warm Water Outlet at $x = 4.86$ ft, Outlet Temperature $T_o = 84.0^{\circ}F$.

FIGURE 14c Isotherms for Test 211 in cross section at $x = 6.5$ ft from Upstream End of Tank. Warm Water Outlet at $x = 4.86$ ft, Outlet Temperature $T_o = 84.0^{\circ}F$.

FIGURE 14d Isotherms for Test 211 in cross section at $x = 8.0$ ft from Upstream End of Tank. Warm Water Outlet at $x = 4.86$ ft, Outlet Temperature $T_o = 84.0^{\circ}F$.

FIGURE 14e Isotherms for Test 211 in cross section at $x = 10.0$ ft from Upstream End of Tank. Warm Water Outlet at $x = 4.86$ ft, Outlet Temperature $T_o = 84.0^{\circ}F$.

FIGURE 15a Isotherms for Test 217 in cross section at $y = 0$ (longitudinal cross section). Outlet Depth $d_o = 0.155$ ft, Outlet Temperature $T_o = 92.5^{\circ}F$.

FIGURE 15b Isotherms for Test 217 in cross section at $x = 5.0$ ft from Upstream End of Tank. Warm Water Outlet at $x = 4.86$ ft, Outlet Temperature $T_o = 92.5^{\circ}F$.

FIGURE 15c Isotherms for Test 217 in cross section at $x = 6.0$ ft from Upstream End of Tank. Warm Water Outlet at $x = 4.86$ ft, Outlet Temperature $T_o = 92.5^{\circ}F$.

FIGURE 15d Isotherms for Test 217 in cross section at $x = 7.0$ ft from Upstream End of Tank. Warm Water Outlet at $x = 4.86$ ft, Outlet Temperature $T_o = 92.5^{\circ}F$.

FIGURE 15e Isotherms for Test 217 in cross section at $x = 9.0$ ft from Upstream End of Tank. Warm Water Outlet at $x = 4.86$ ft, Outlet Temperature $T_o = 92.5^{\circ}F$.

FIGURE 16 Examples of Temperatures at Water Surface

FIGURE 17 Dimensionless Values of Temperature Excess above Equilibrium Temperature

FIGURE 30a Velocity Component in x-direction for Test 207 at $y = 0$

FIGURE 30b Velocity Component in x-direction for Test 207 at $y = 0$

FIGURE 30c Velocity Component in x-direction for Test 207 at $y = 0$

FIGURE 30d Velocity Component in x-direction for Test 207 at $y = 0$

FIGURE 31a Velocity Component in x-direction for Test 214 at $y = 0$

FIGURE 31b Velocity Component in x-direction for Test 214 at $y = 0$

FIGURE 31c Velocity Component in x-direction for Test 214 at $y = 0$

FIGURE 31d Velocity Component in x-direction for Test 214 at $y = 0$

FIGURE 32a Velocity Component in x-direction for Test 211 at $y = 0$

FIGURE 32b Velocity Component in x-direction for Test 211 at $y = 0$

FIGURE 32c Velocity Component in x-direction for Test 211 at $y = 0$

FIGURE 32d Velocity Component in x-direction for Test 211 at $y = 0$

FIGURE 32e Velocity Component in x-direction for Test 211 at $y = 0$

FIGURE 33a Velocity Vectors for Test 215 at Water Surface

FIGURE 33b Velocity Vectors for Test 215 at $z = 0.2$ ft

FIGURE 34a Velocity Vectors for Test 207 at Water Surface

FIGURE 34b Velocity Vectors for Test 207 at $z = 0.2$ ft

FIGURE 35a Velocity Field near the Outlet for Test 215. Lengths of bars are proportional to velocity magnitudes. Heavy dotted areas refer to velocity components $u > 0$.

FIGURE 35b Velocity Field near the Outlet for Test 207. Lengths of bars are proportional to velocity magnitudes. Heavy dotted areas refer to velocity components $u > 0$.

FIGURE 35c Velocity Field near the Outlet for Test 211. Lengths of bars are proportional to velocity magnitudes. Heavy dotted areas refer to velocity components $u > 0$.

FIGURE 35d Velocity Field near the Outlet for Test 214. Lengths of bars are proportional to velocity magnitudes. Heavy dotted areas refer to velocity components $u > 0$.

FIGURE 36a Surface Layer near Outlet for Test 216. Heavy dotted areas refer to velocity components $u > 0$.

FIGURE 36b Surface Layer near Outlet for Test 217. Heavy dotted areas refer to velocity components $u > 0$.

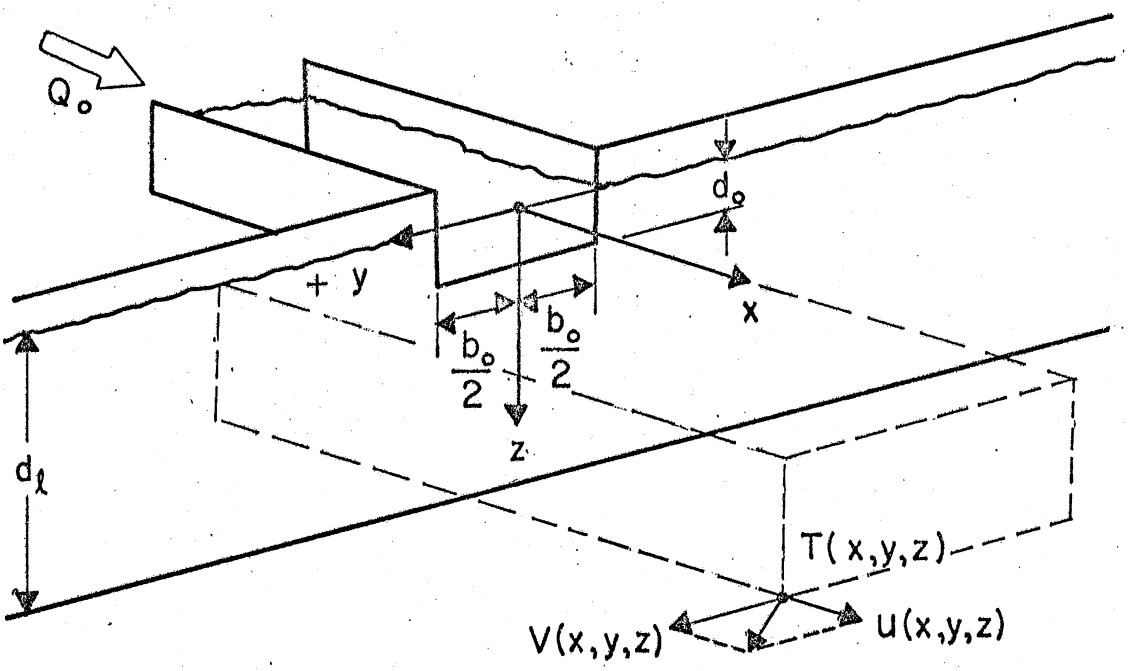

Fig. 1 - Outlet Coordinates and Dimensions

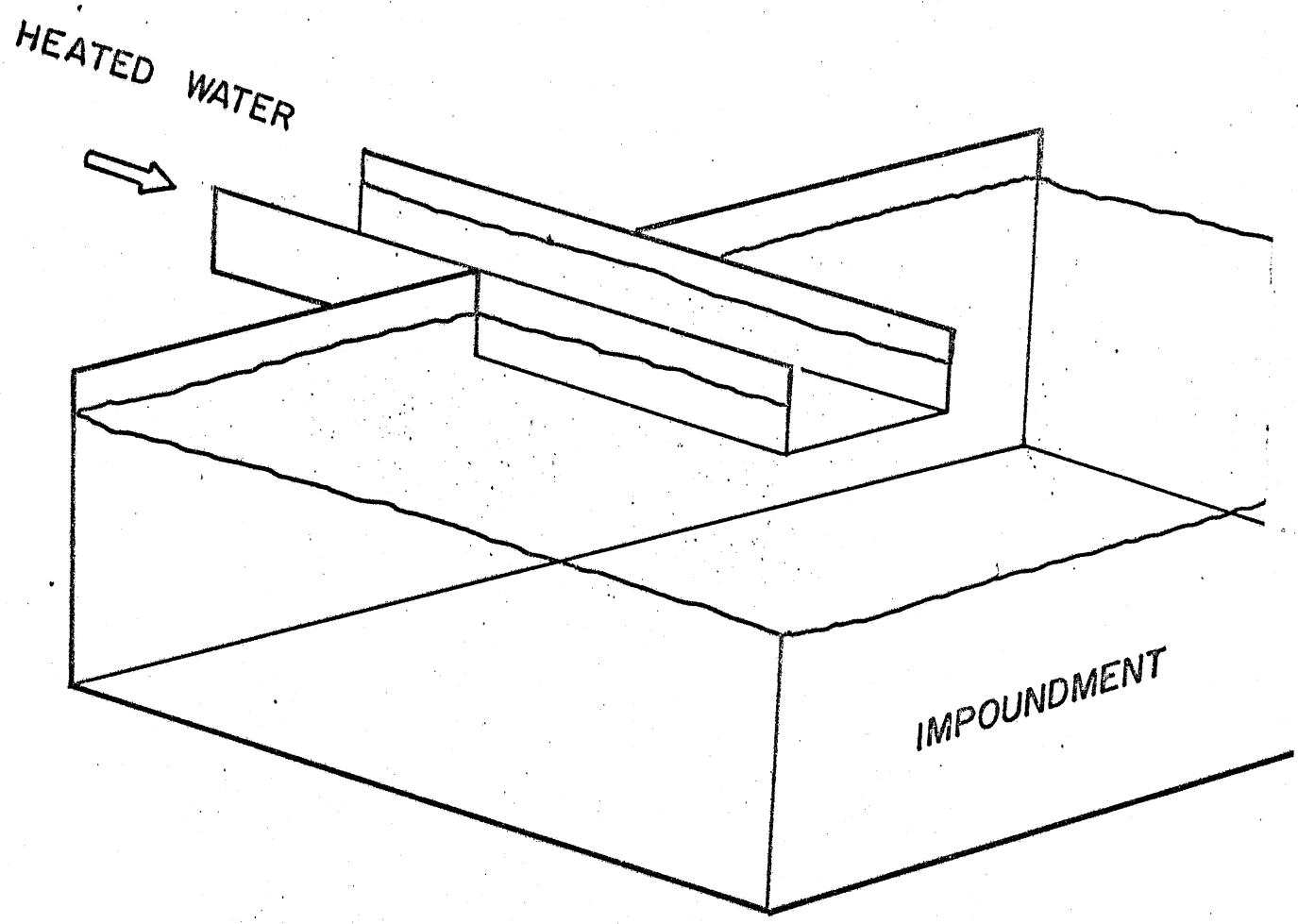

Fig. 2 - Projecting Outlet

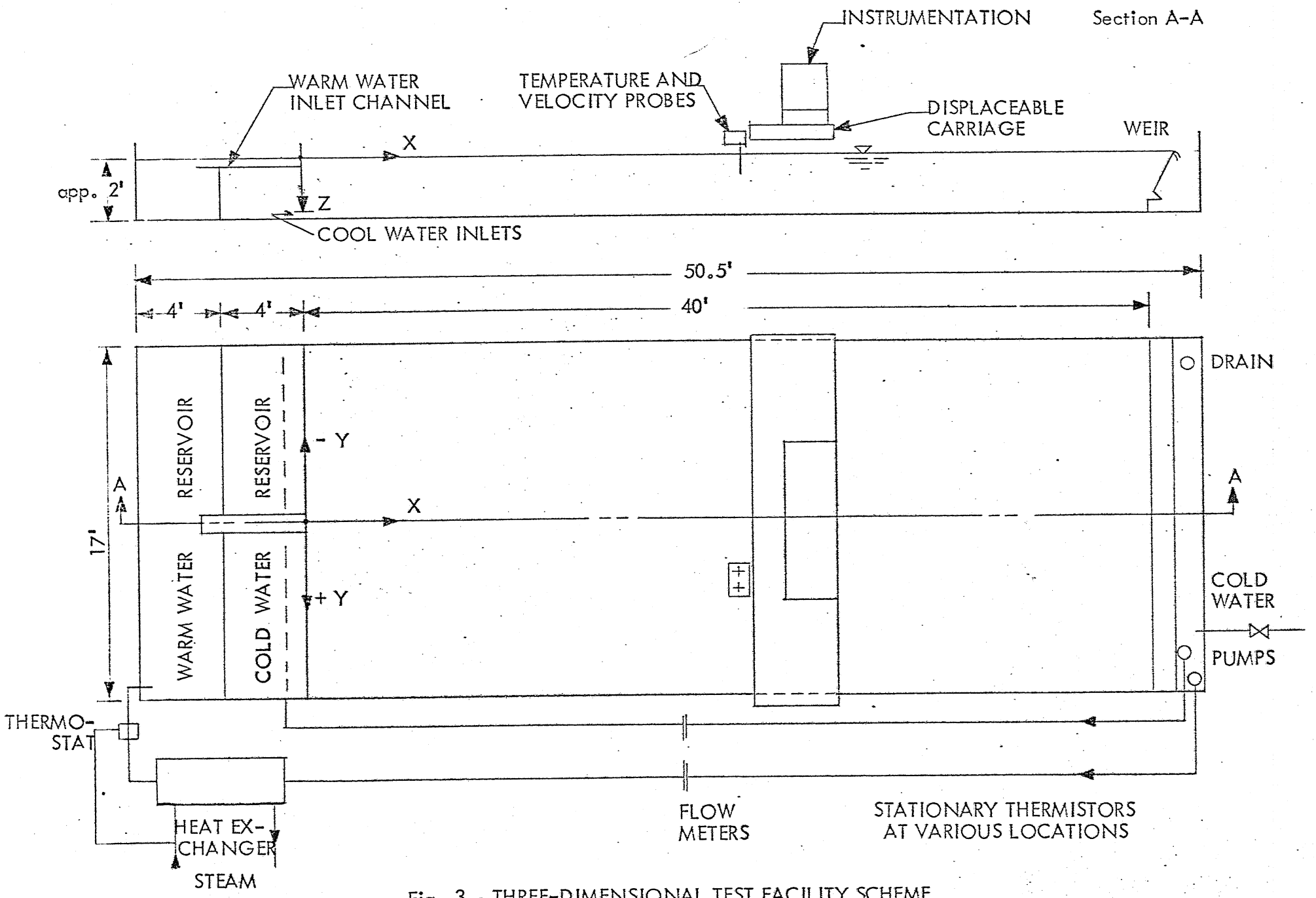

Fig. 3 - THREE-DIMENSIONAL TEST FACILITY SCHEME

Fig. 4 - View of Three-Dimensional Tank

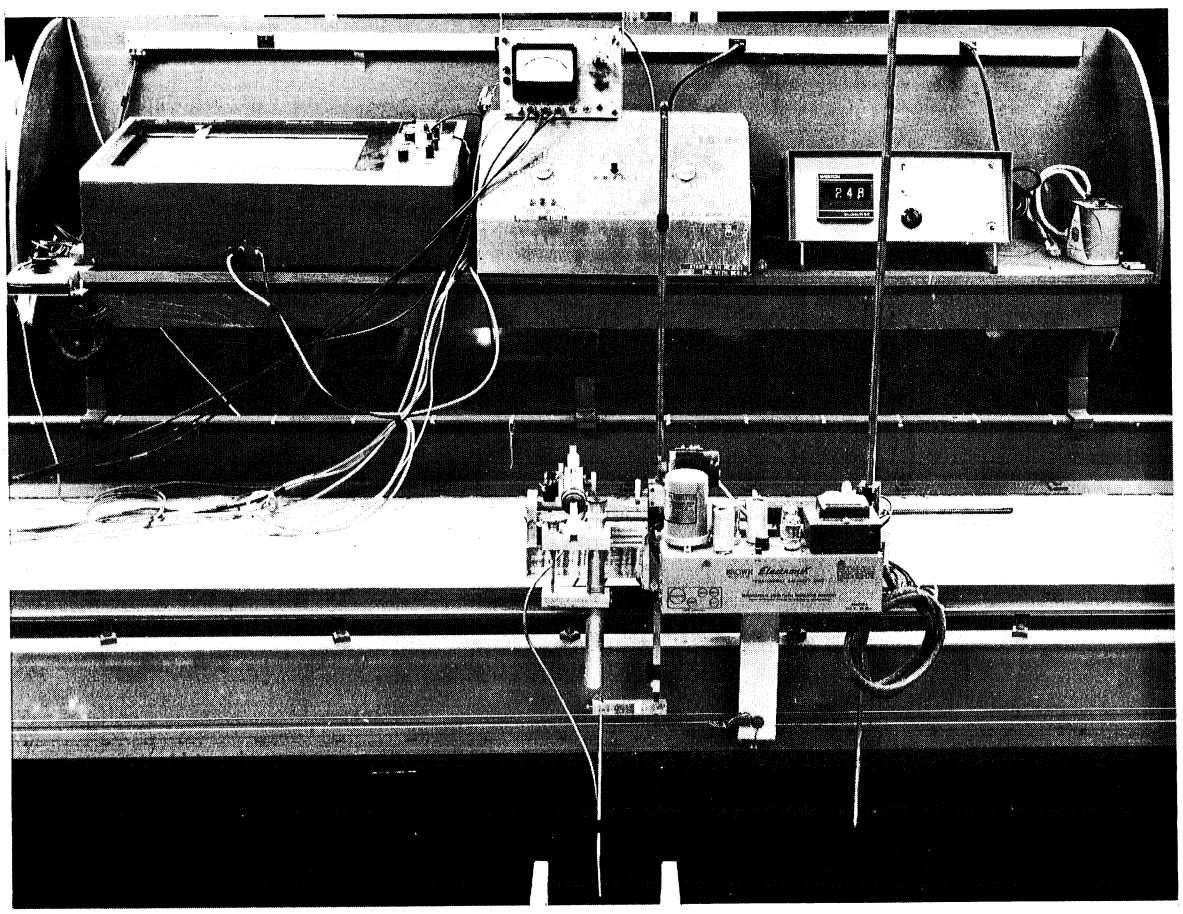

Fig. 5 - Details of Probe Assembly and Associated Equipment Used to Measure Temperature and Velocity Field in Tank

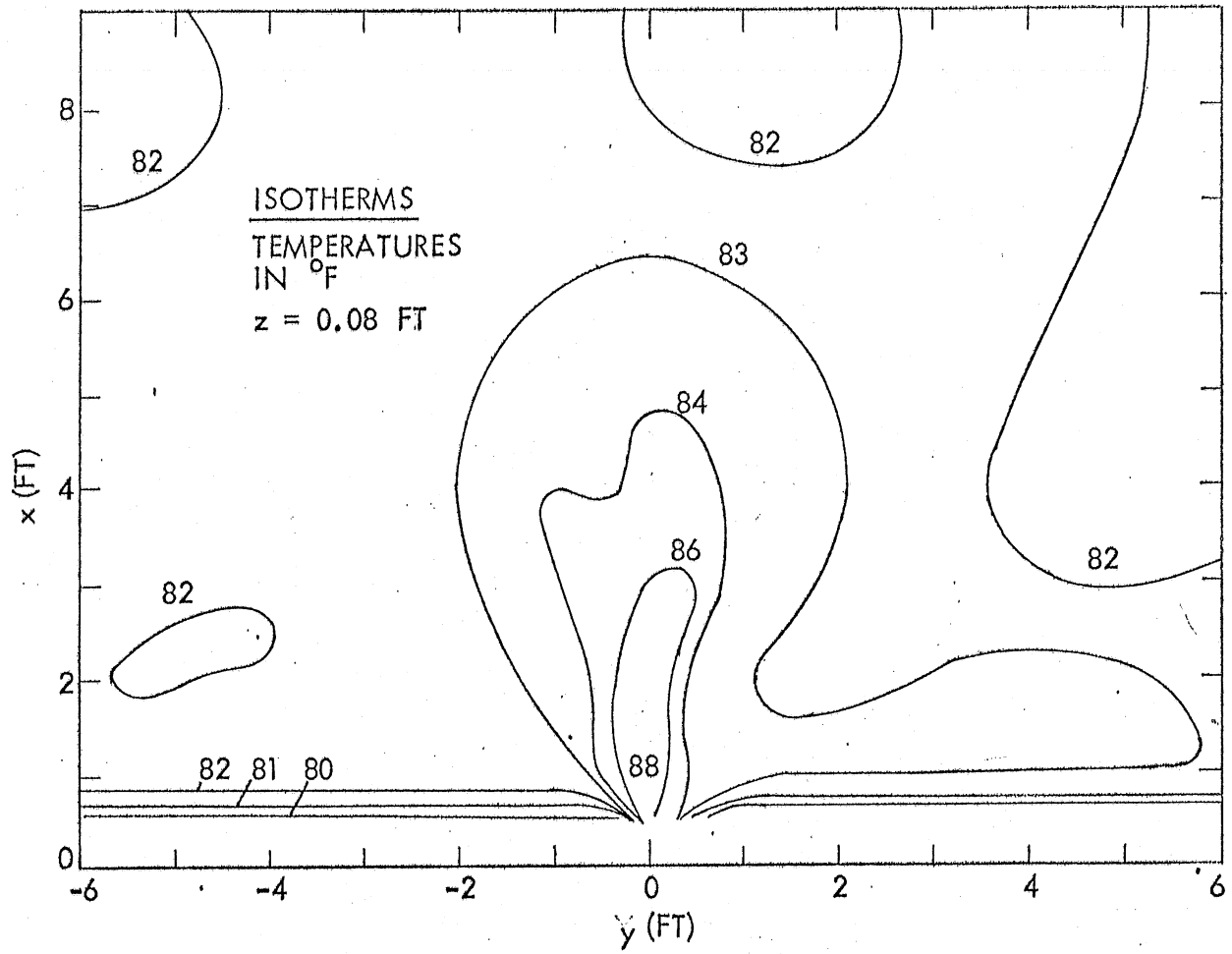

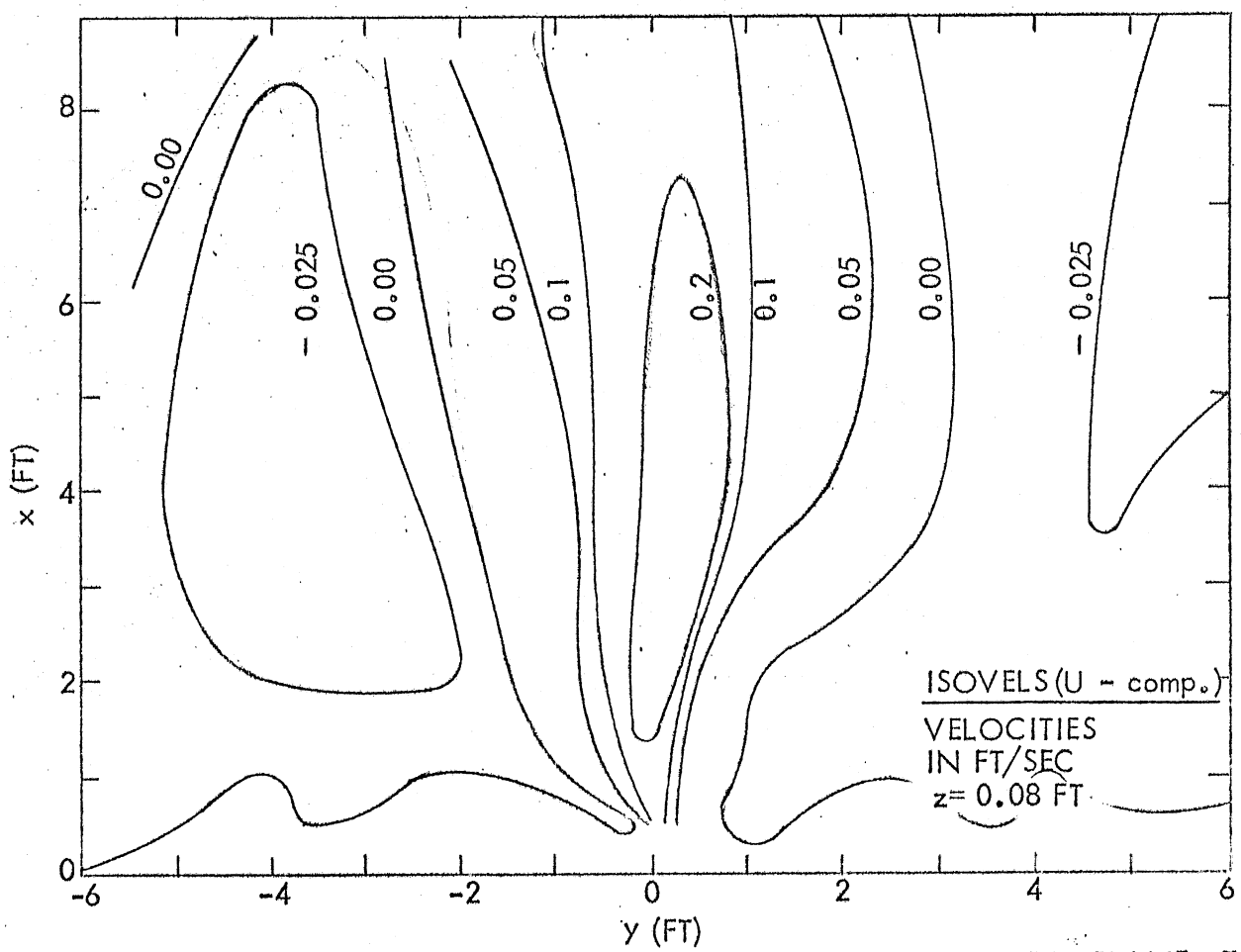

Fig. 6 - EXAMPLE OF ISOTHERMS AND ISOVELS IN A HORIZONTAL PLANE- TEST 101

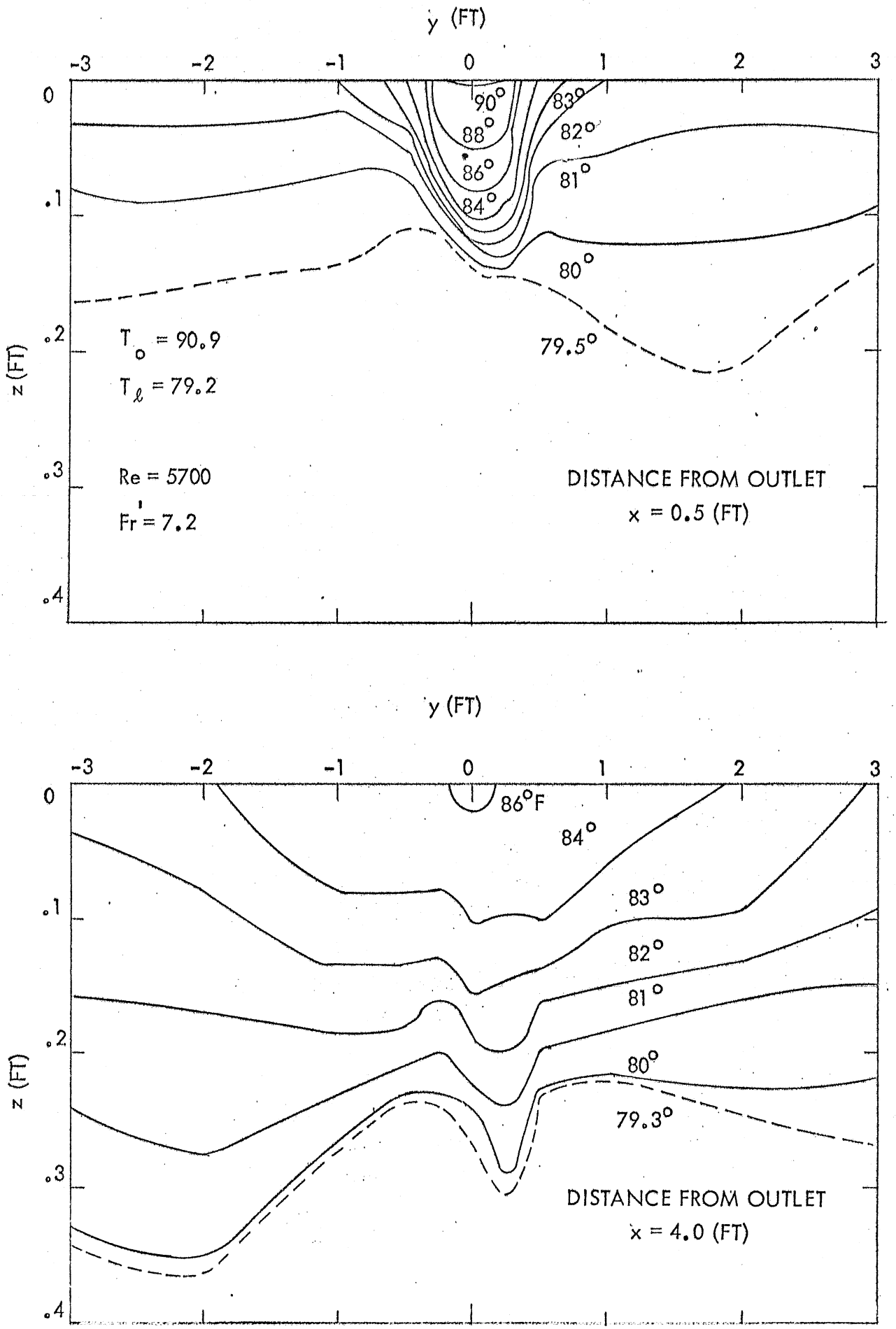

Fig. 7 - EXAMPLE OF TEMPERATURE DISTRIBUTION IN CROSS SECTIONS PERPENDICULAR TO THE OUTLET CHANNEL - TEST 101

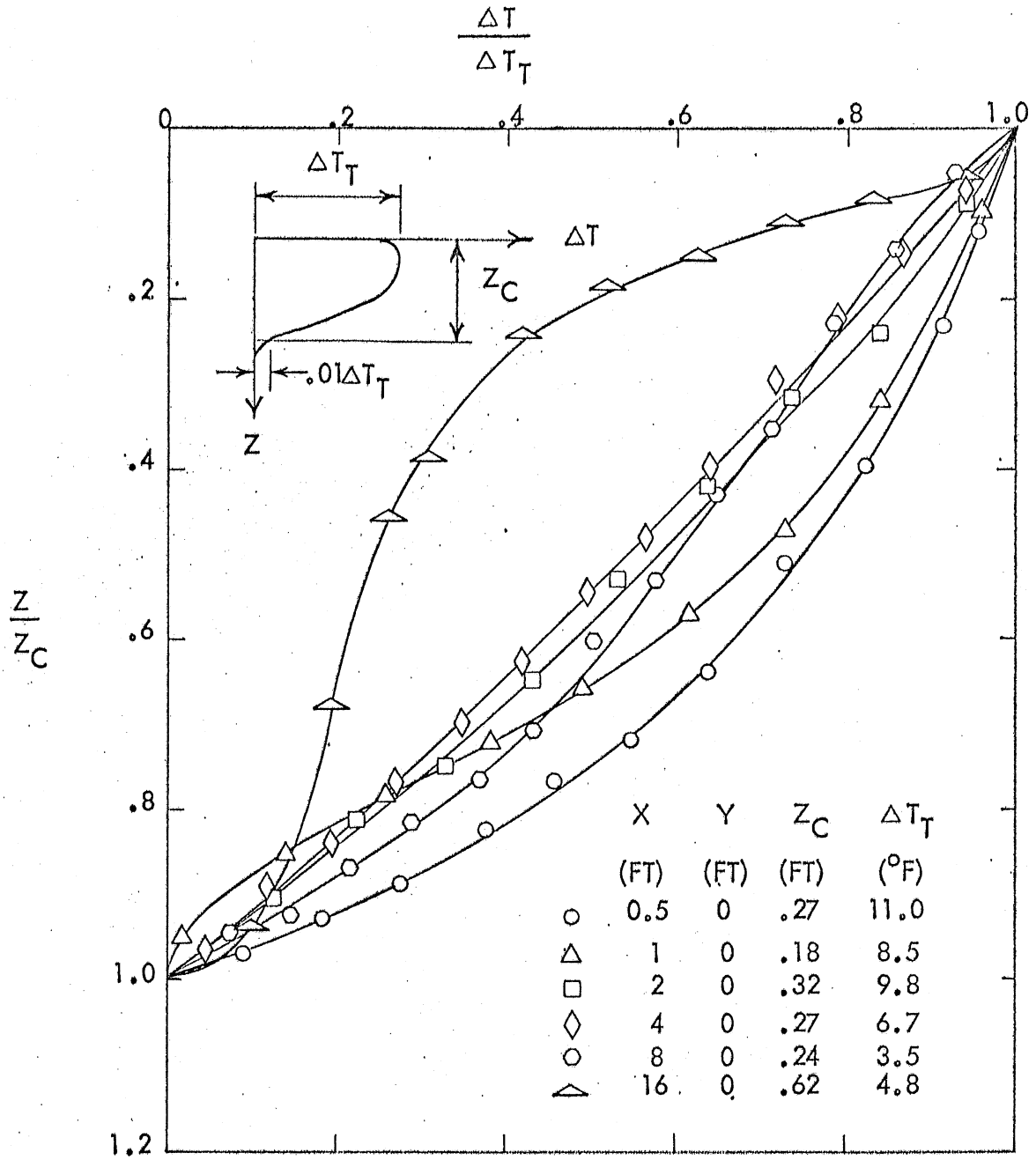

Fig. 8 - DIMENSIONLESS TEMPERATURE DISTRIBUTION IN THE THREE-DIMENSIONAL WARM WATER SURFACE LAYER - TEST 101

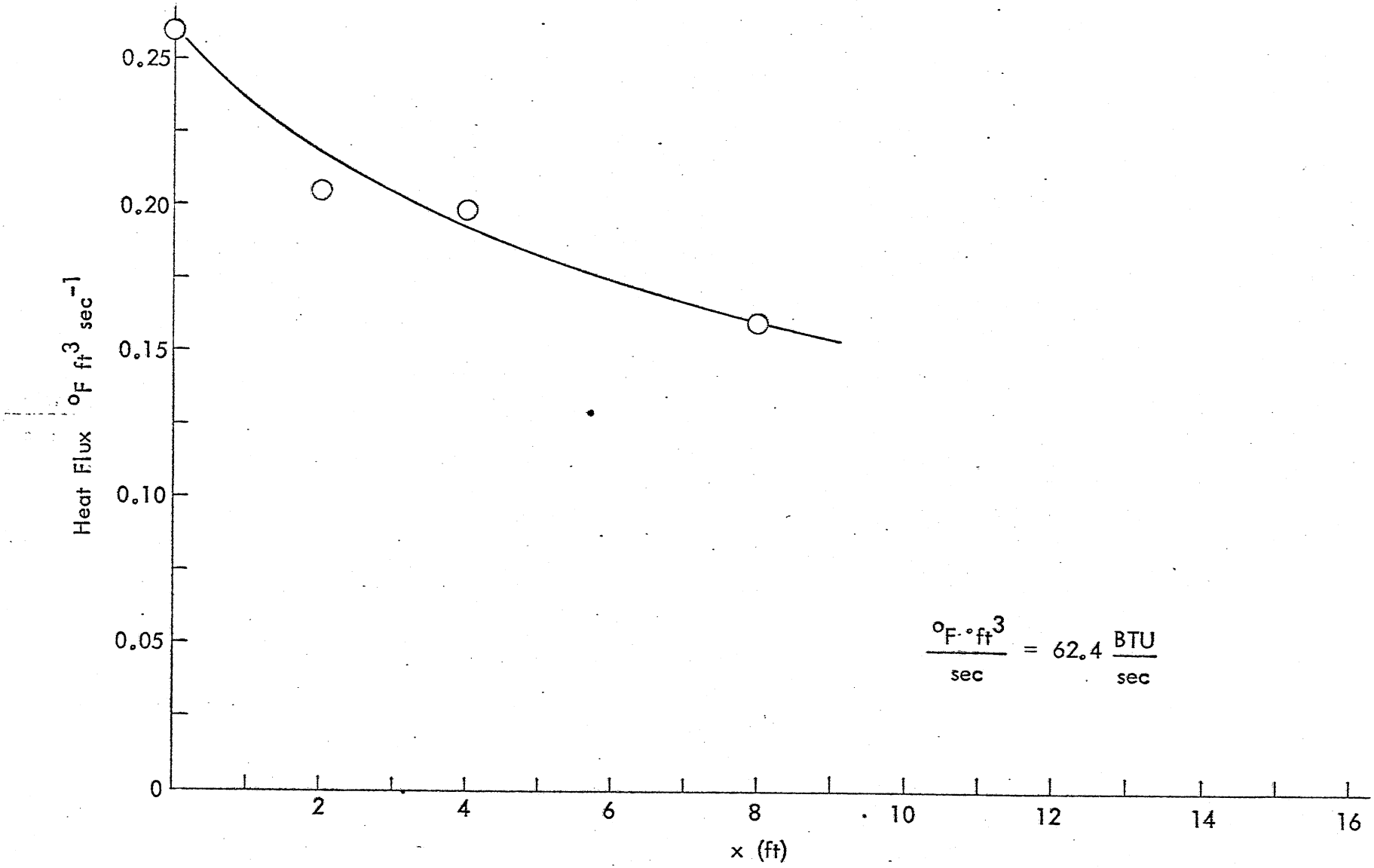

Fig. 9 - Excess Heat Flux in x-direction in the Receiving Reservoir - Test 101

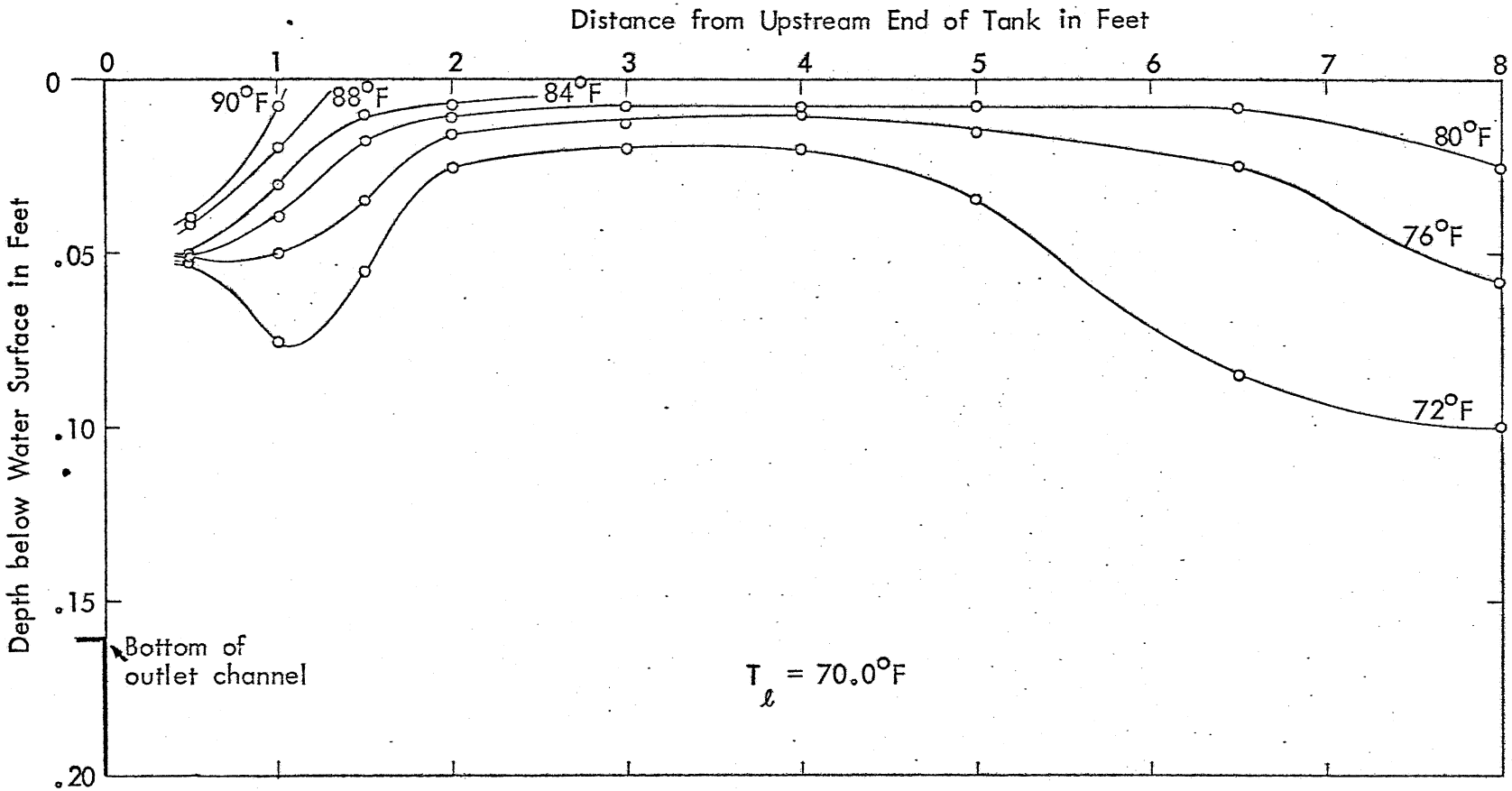

Fig. 10a - Isotherms for Test 215 in cross section at $y = 0$ (longitudinal cross section)
Outlet Depth d_o = 0.162 ft, Outlet Temperature T_o = 91.0°F

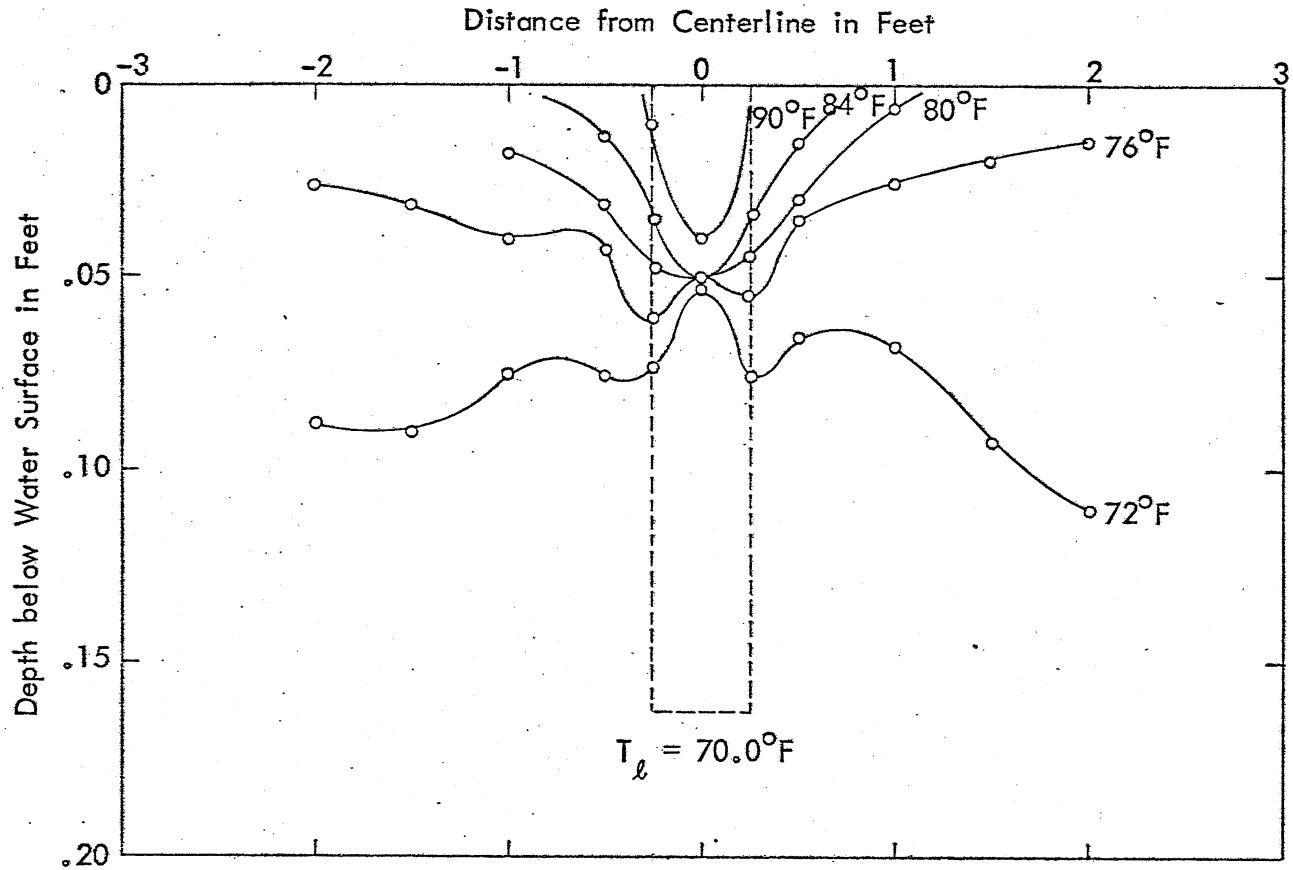

Fig. 10b - Isotherms for Test 215 in cross section at x = 0.5 ft from Upstream End of Tank. Warm Water Outlet at x = 0.0 ft, Outlet Temperature T_o = 91.0°F.

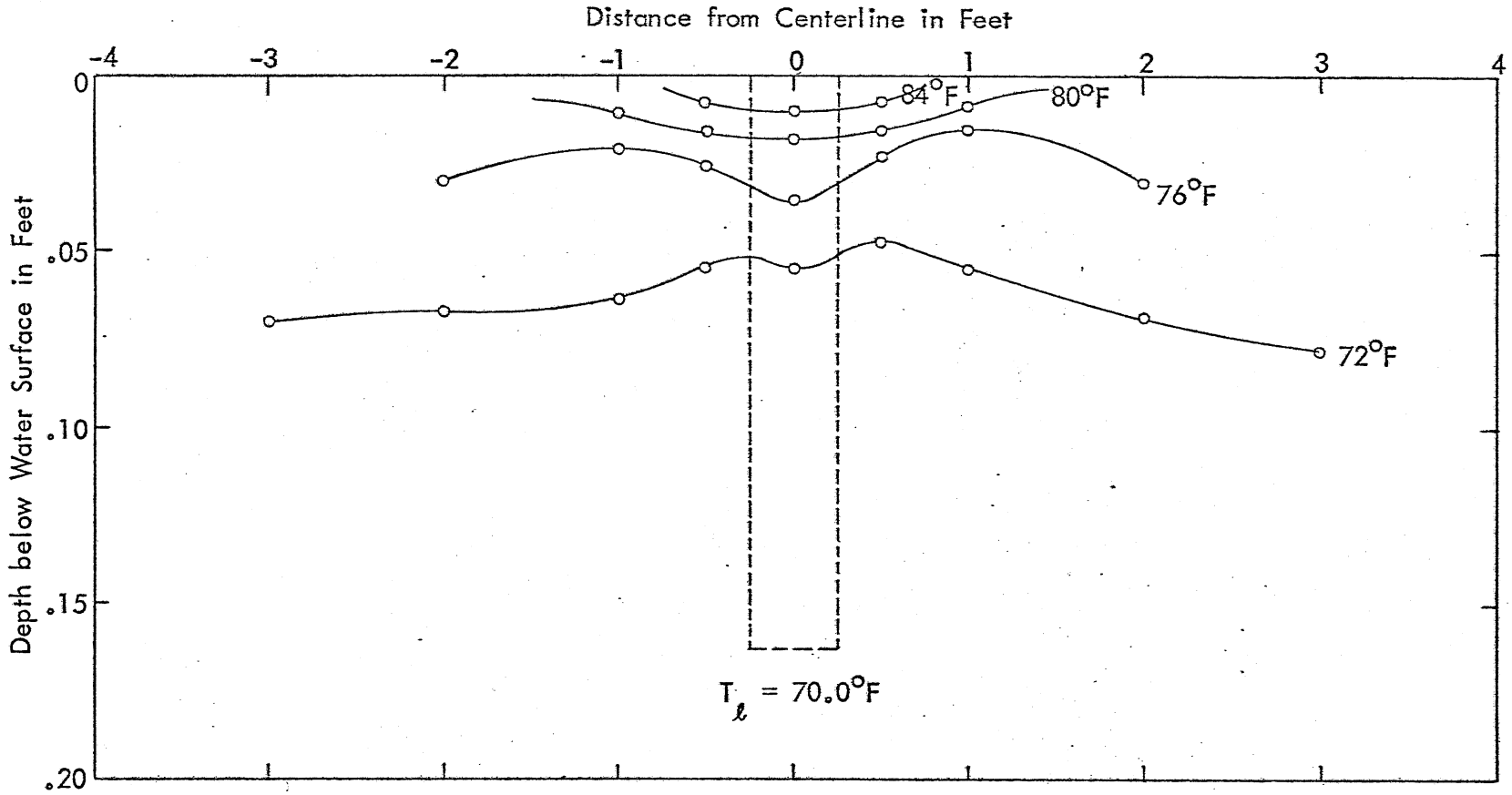

Fig. 10c - Isotherms for Test 215 in cross section at x = 1.5 ft from Upstream End of Tank. Warm Water Outlet at x = 0.0 ft, Outlet Temperature T_o = 91.0°F.

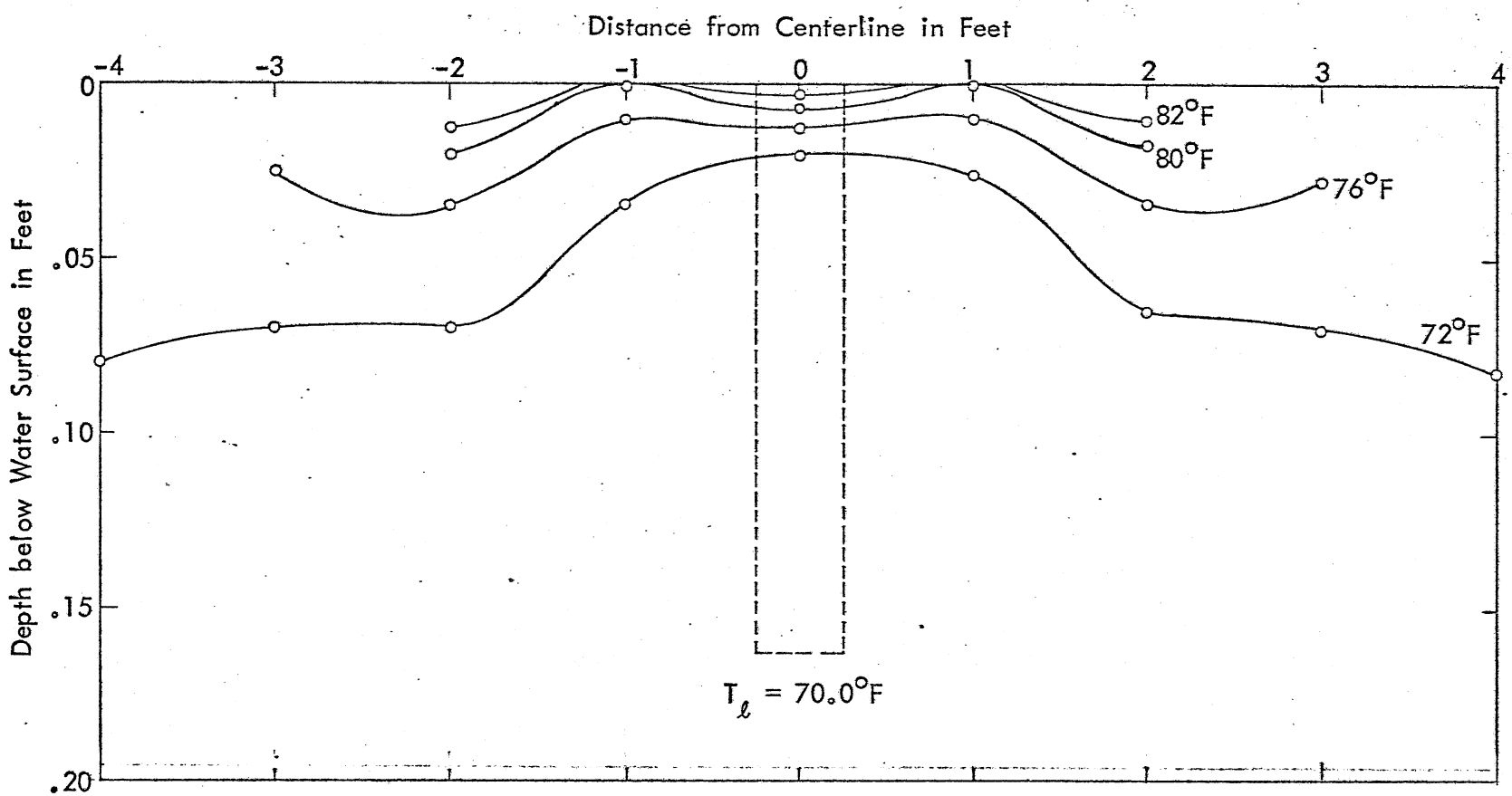

Fig. 10d - Isotherms for Test 215 in cross section at x = 3.0 ft from Upstream End of Tank. Warm Water Outlet at x = 0.0 ft, Outlet Temperature T_o = 91.0°F.

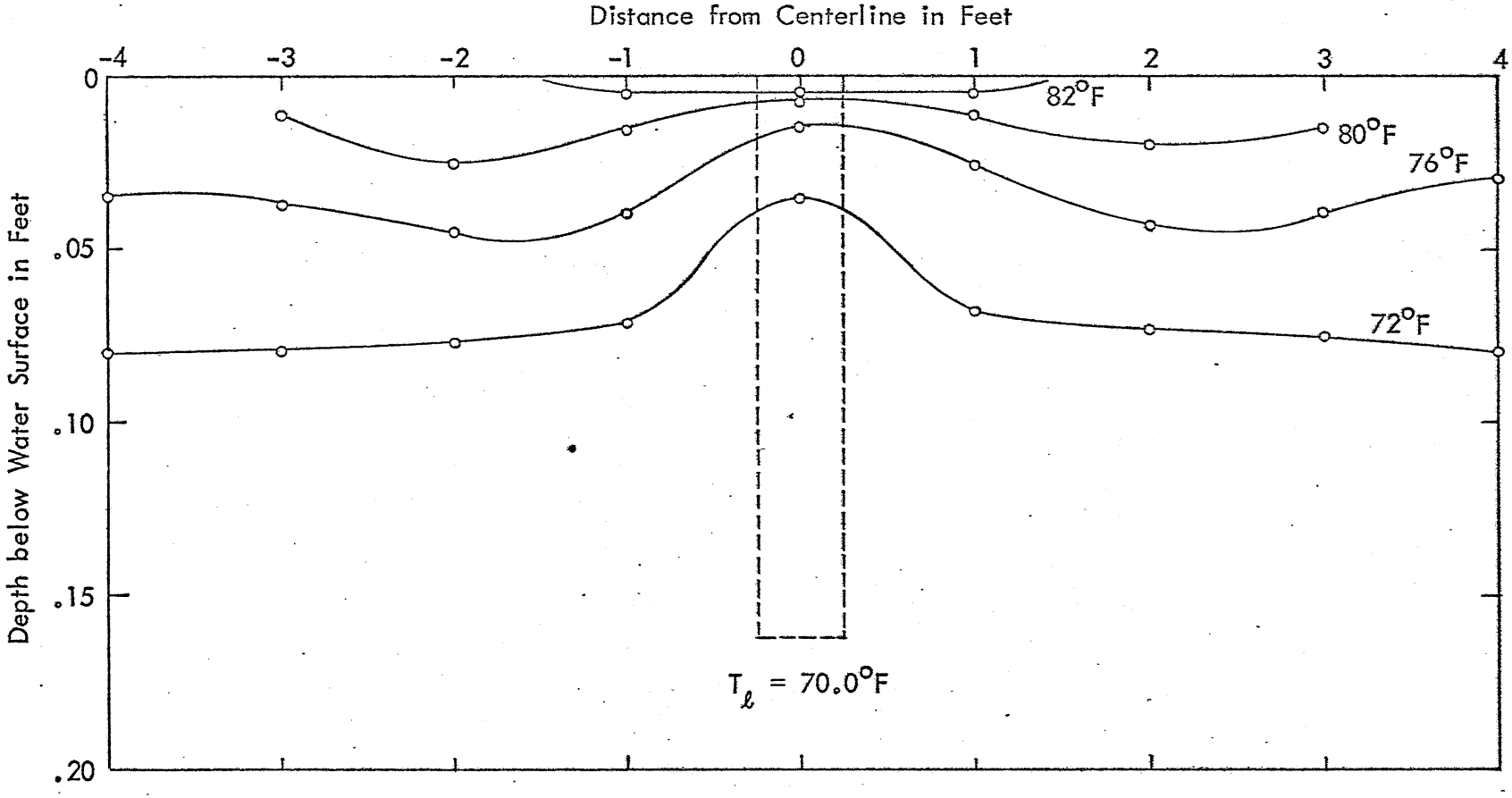

Fig. 10e - Isotherms for Test 215 in cross section at x = 5.0 ft from Upstream End of Tank. Warm Water Outlet at x = 0.0 ft, Outlet Temperature T_o = 91.0°F.

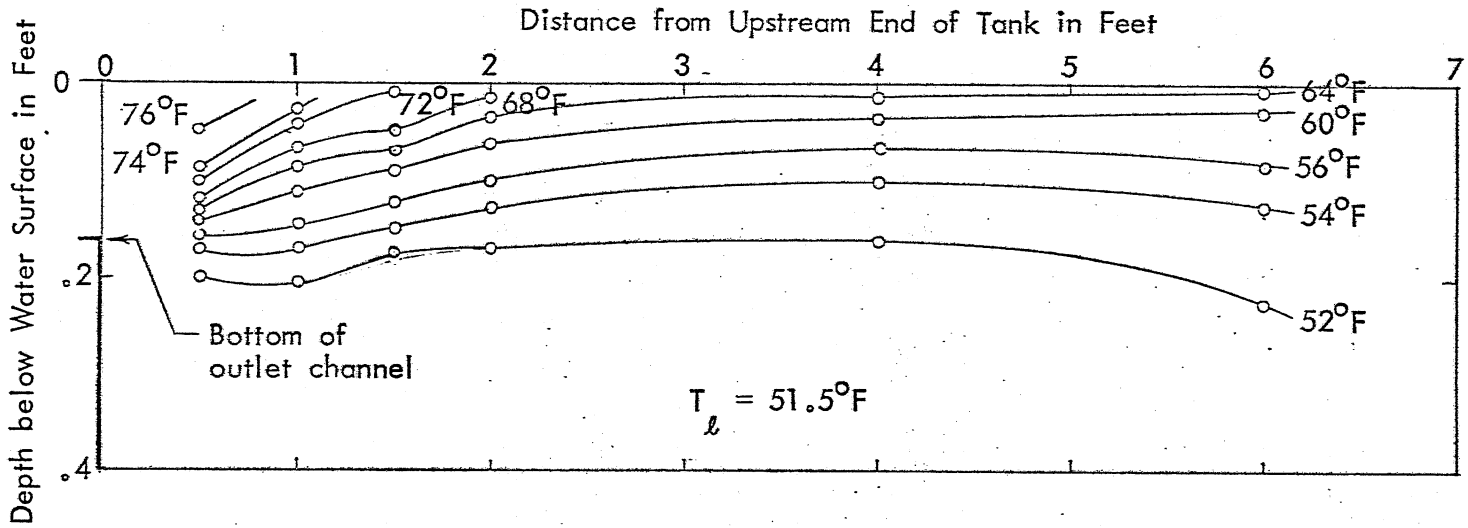

Fig. 11a - Isotherms for Test 207 in cross section at $y = 0$ (longitudinal cross section)
Outlet Depth d_o = 0.164 ft, Outlet Temperature T_o = 76.5°F

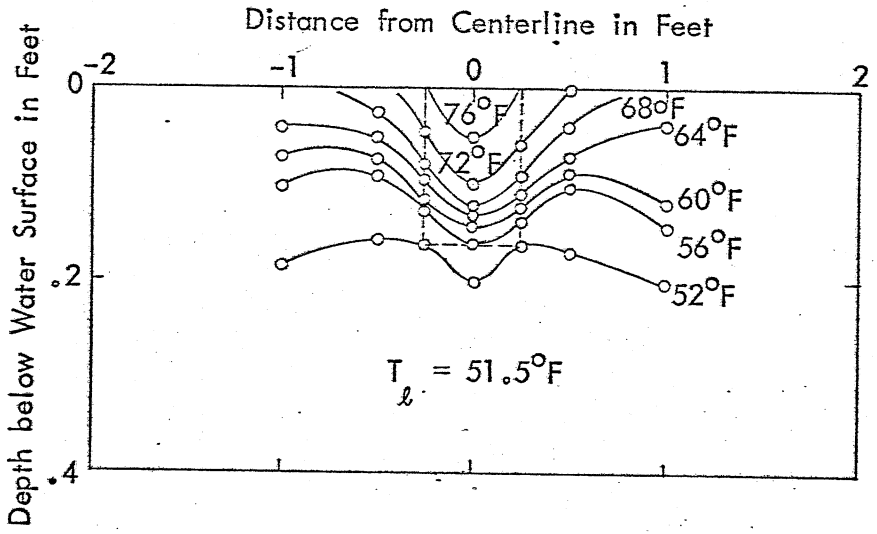

Fig. 11b - Isotherms for Test 207 in cross section at x = 0.5 ft from Upstream End of Tank. Warm Water Outlet at x = 0.0 ft, Outlet Temperature T_o = 76.5°F.

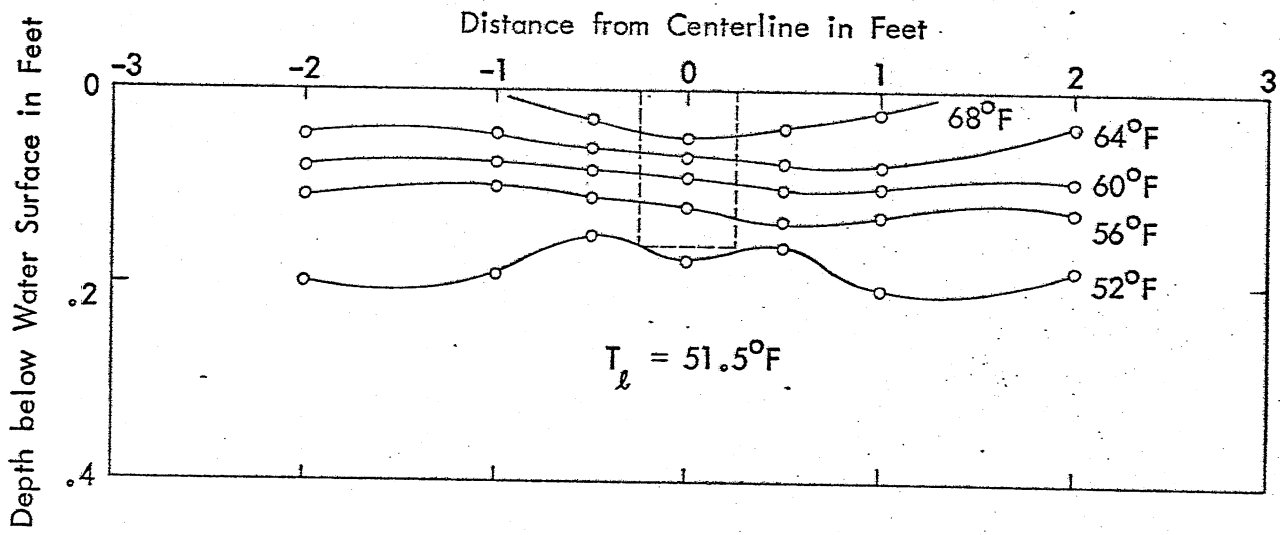

Fig. 11c - Isotherms for Test 207 in cross section at x = 1.5 ft from Upstream End of Tank. Warm Water Outlet at x = 0.0 ft, Outlet Temperature T_o = 76.5°F.

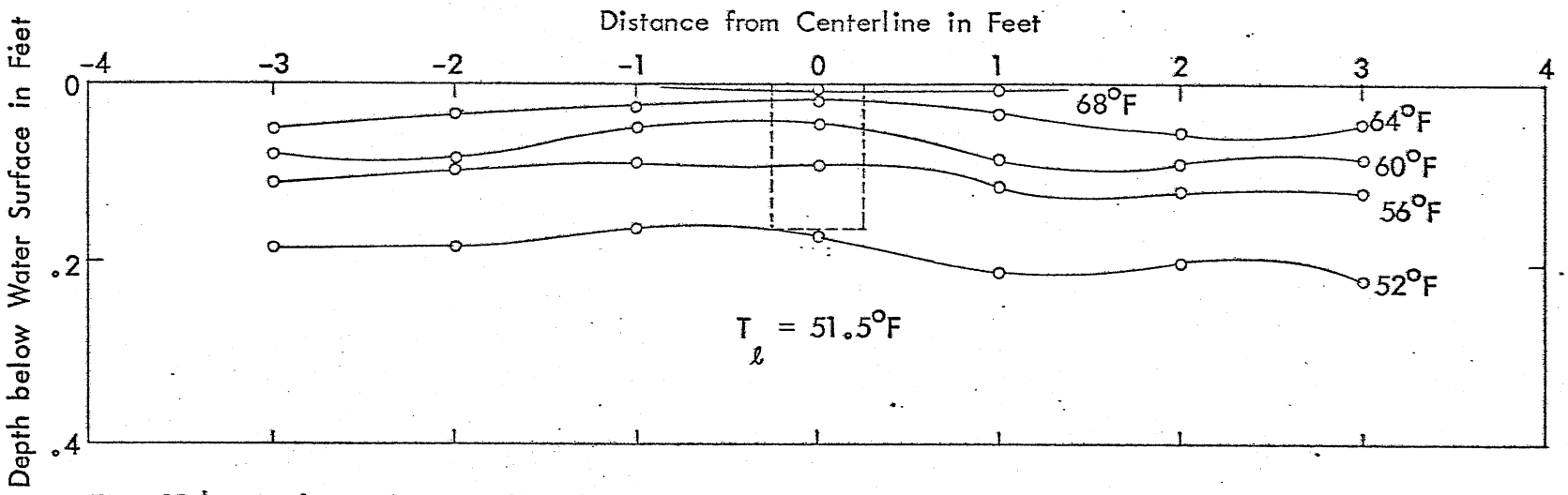

Fig. 11d – Isotherms for Test 207 in cross section at x = 3.0 ft from Upstream End of Tank. Warm Water Outlet at x = 0.0 ft, Outlet Temperature T_o = 76.5°F.

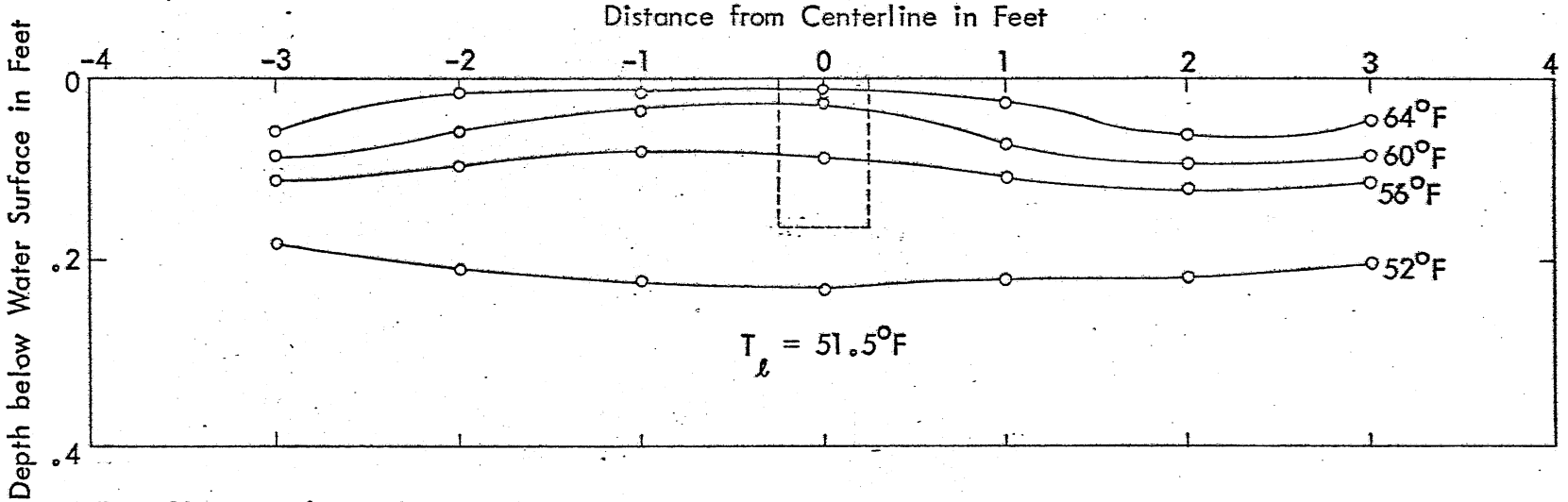

Fig. 11e – Isotherms for Test 207 in cross section at x = 6.0 ft from Upstream End of Tank. Warm Water Outlet at x = 0.0 ft, Outlet Temperature T_o = 76.5°F.

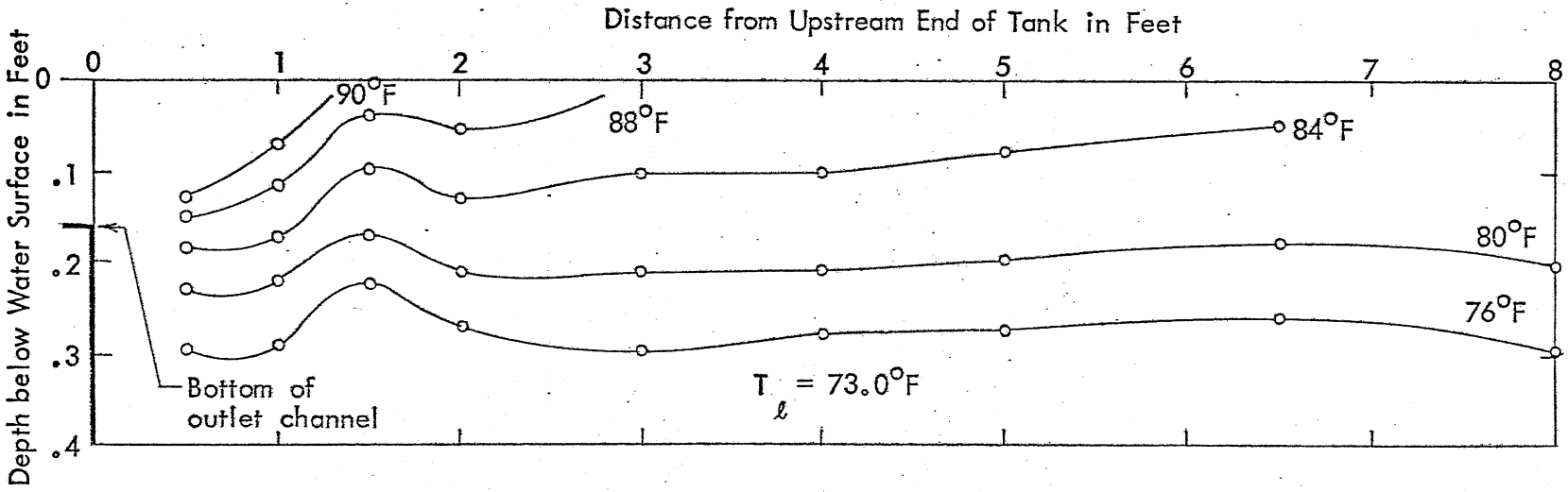

Fig. 12a – Isotherms for Test 216 in cross section at $y = 0$ (longitudinal cross section). Outlet depth $d_o = 0.162$ ft, Outlet Temperature $T_o = 92.0°F$.

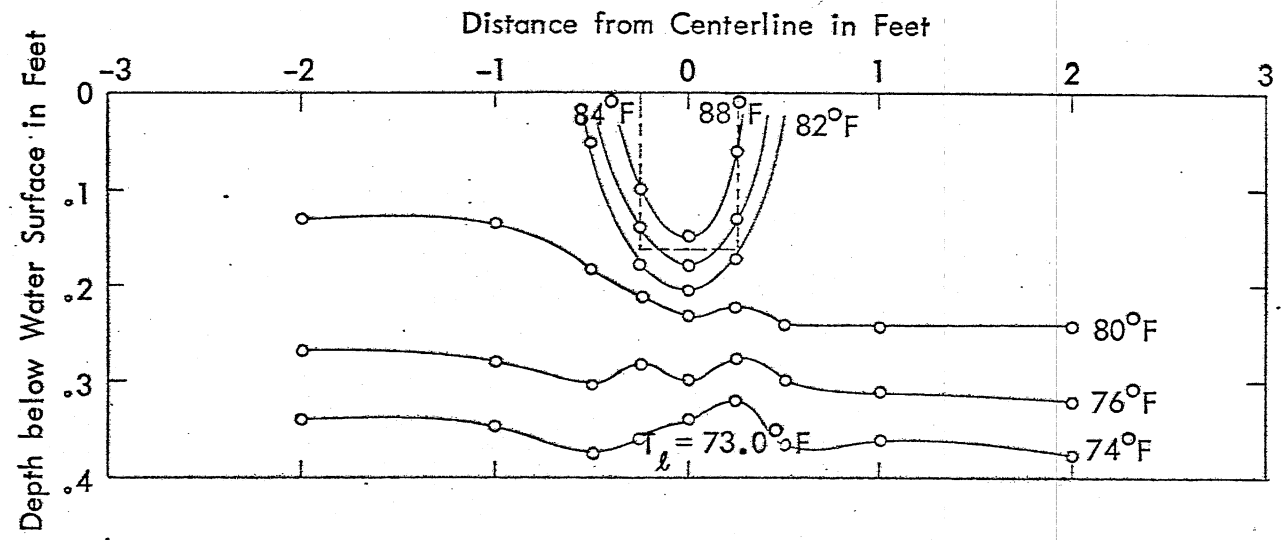

Fig. 12b - Isotherms for Test 216 in cross section at x = 0.5 ft from Upstream End of Tank. Warm Water Outlet at x = 0.0 ft, Outlet Temperature T_o = 92.0°F.

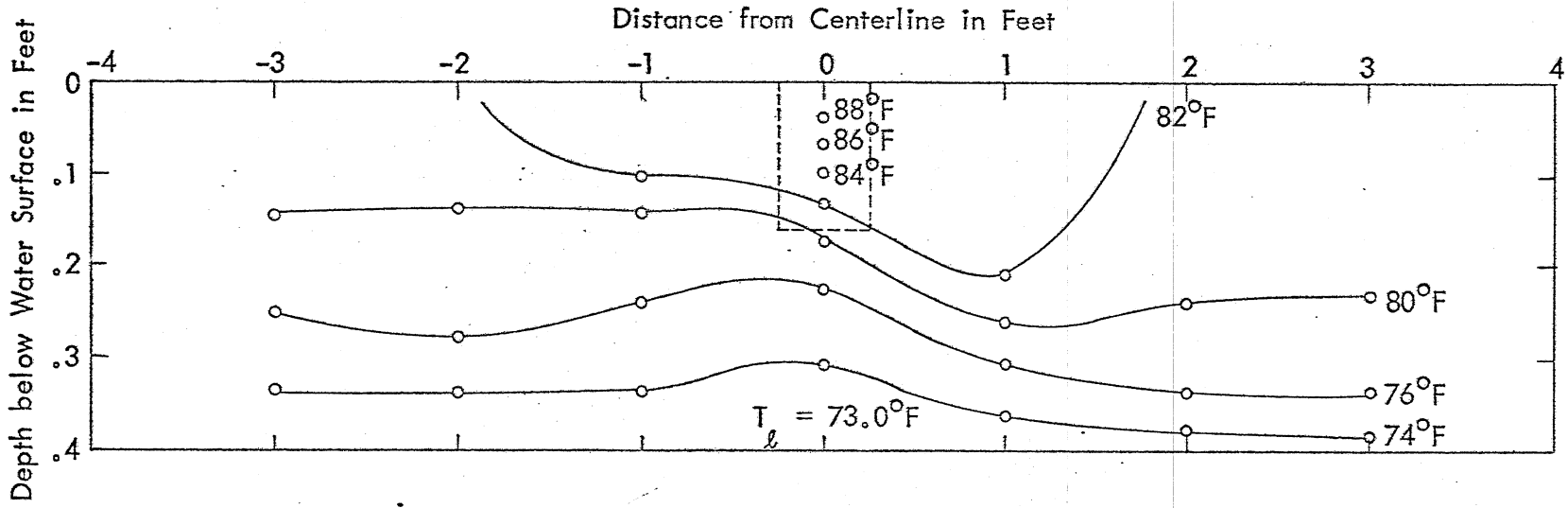

Fig. 12c - Isotherms for Test 216 in cross section at x = 1.5 ft from Upstream End of Tank. Warm Water Outlet at x = 0.0 ft, Outlet Temperature T_o = 92.0°F.

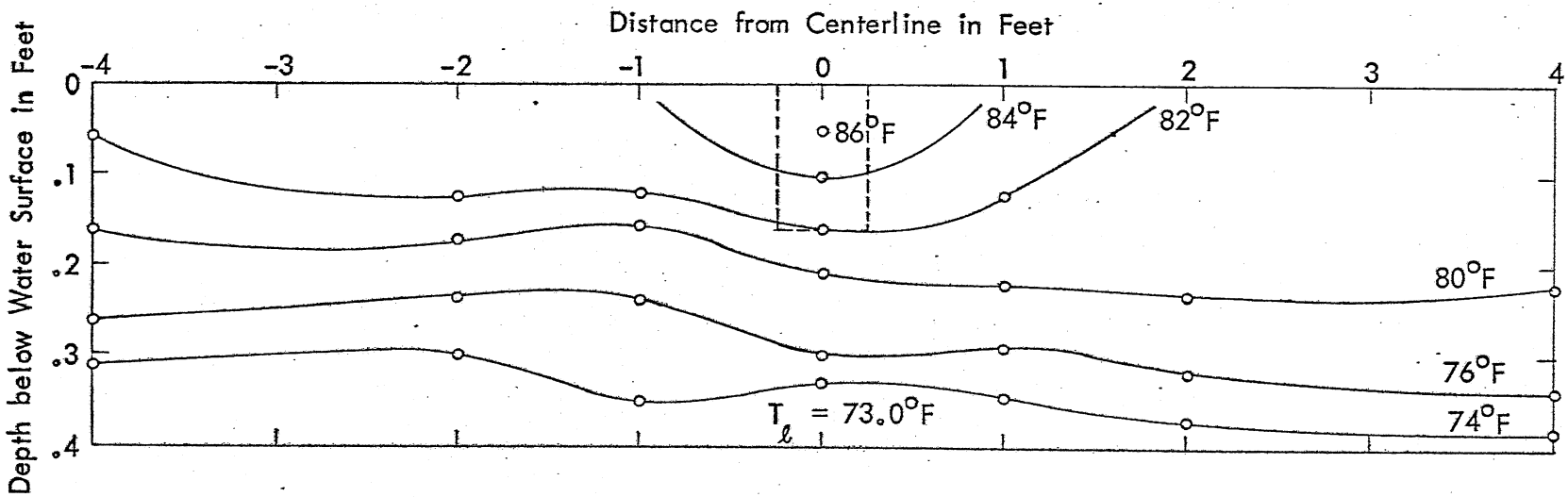

Fig. 12d - Isotherms for Test 216 in cross section at x = 3.0 ft from Upstream End of Tank. Warm Water Outlet at x = 0.0 ft, Outlet Temperature T_o = 92.0°F.

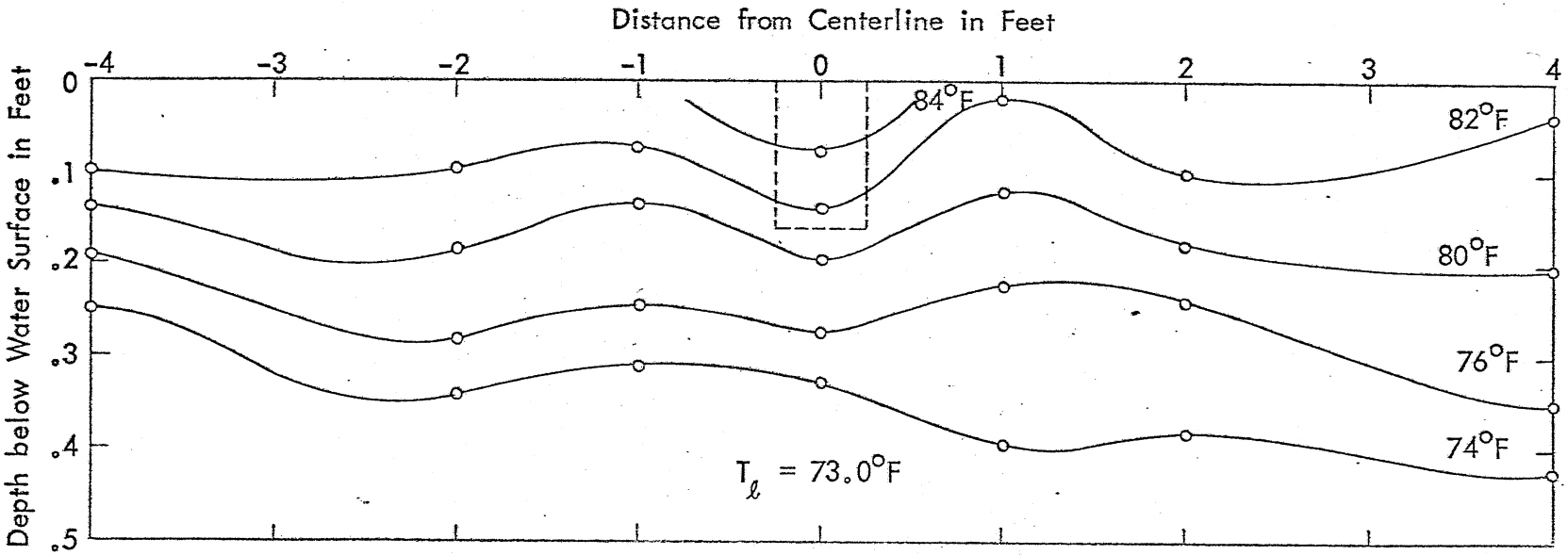

Fig. 12e - Isotherms for Test 216 in cross section at x = 5.0 ft from Upstream End of Tank. Warm Water Outlet at x = 0.0 ft, Outlet Temperature T_o = 92.0°F.

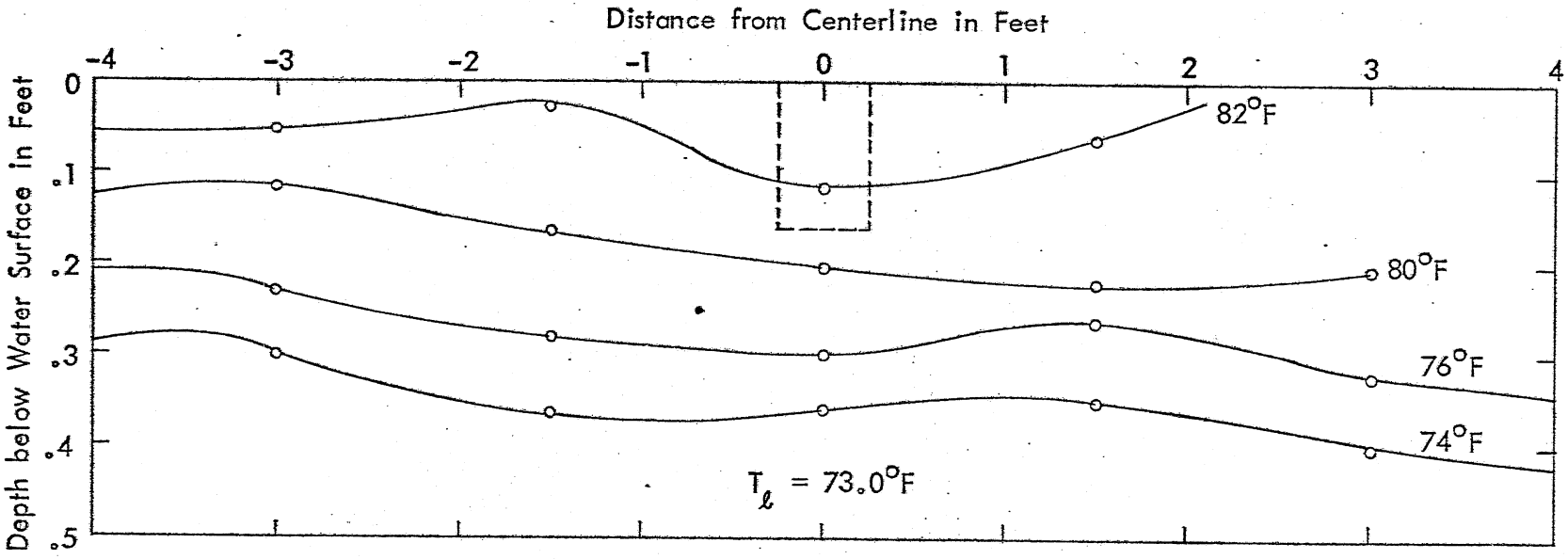

Fig. 12f - Isotherms for Test 216 in cross section at x = 8.0 ft from Upstream End of Tank. Warm Water Outlet at x = 0.0 ft, Outlet Temperature T_o = 92.0°F.

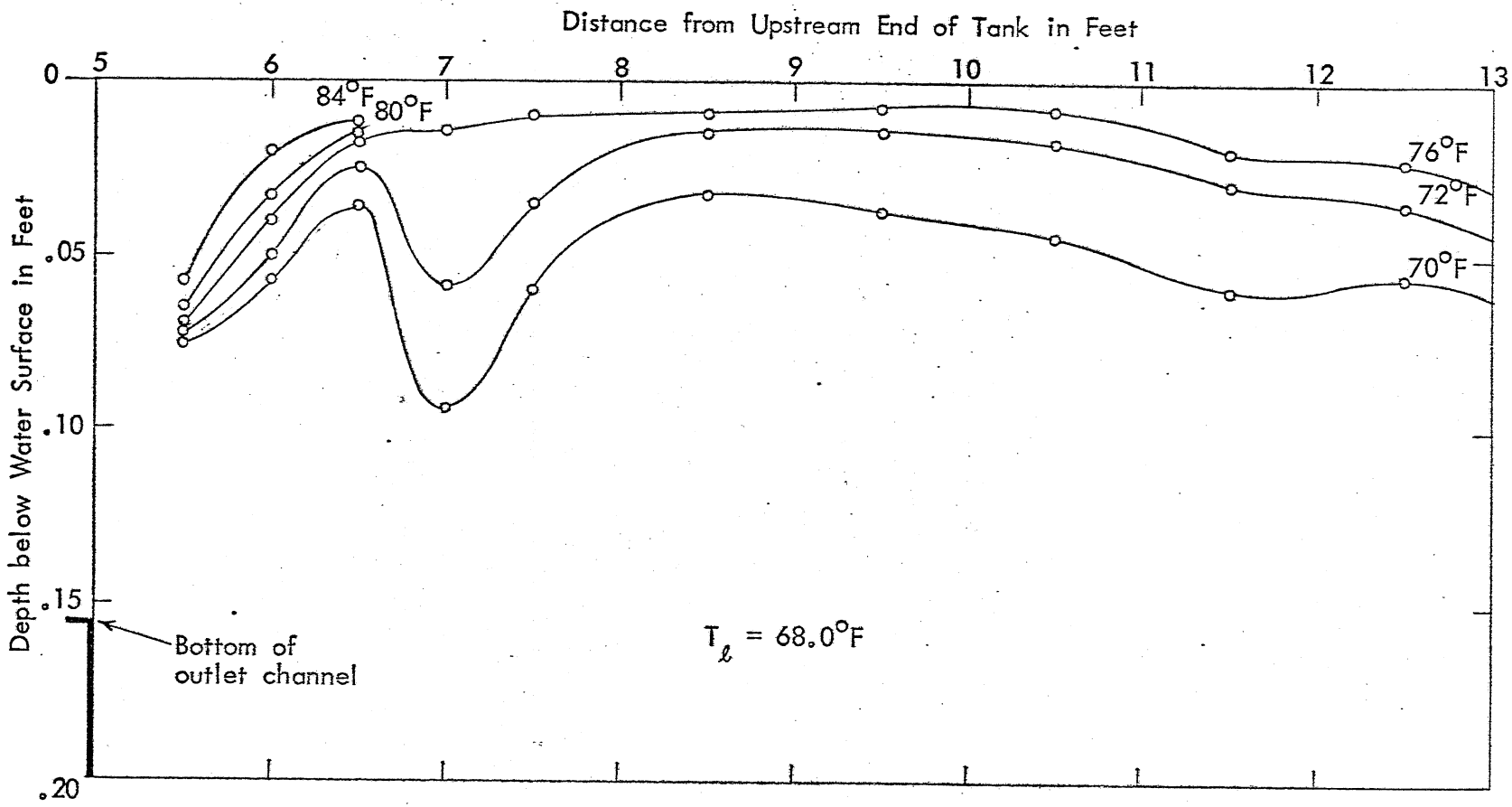

Fig. 13a - Isotherms for Test 214 in cross section at $y = 0$ (longitudinal cross section).
Outlet Depth d_o = 0.155 ft, Outlet Temperature T_o = 87.0°F.

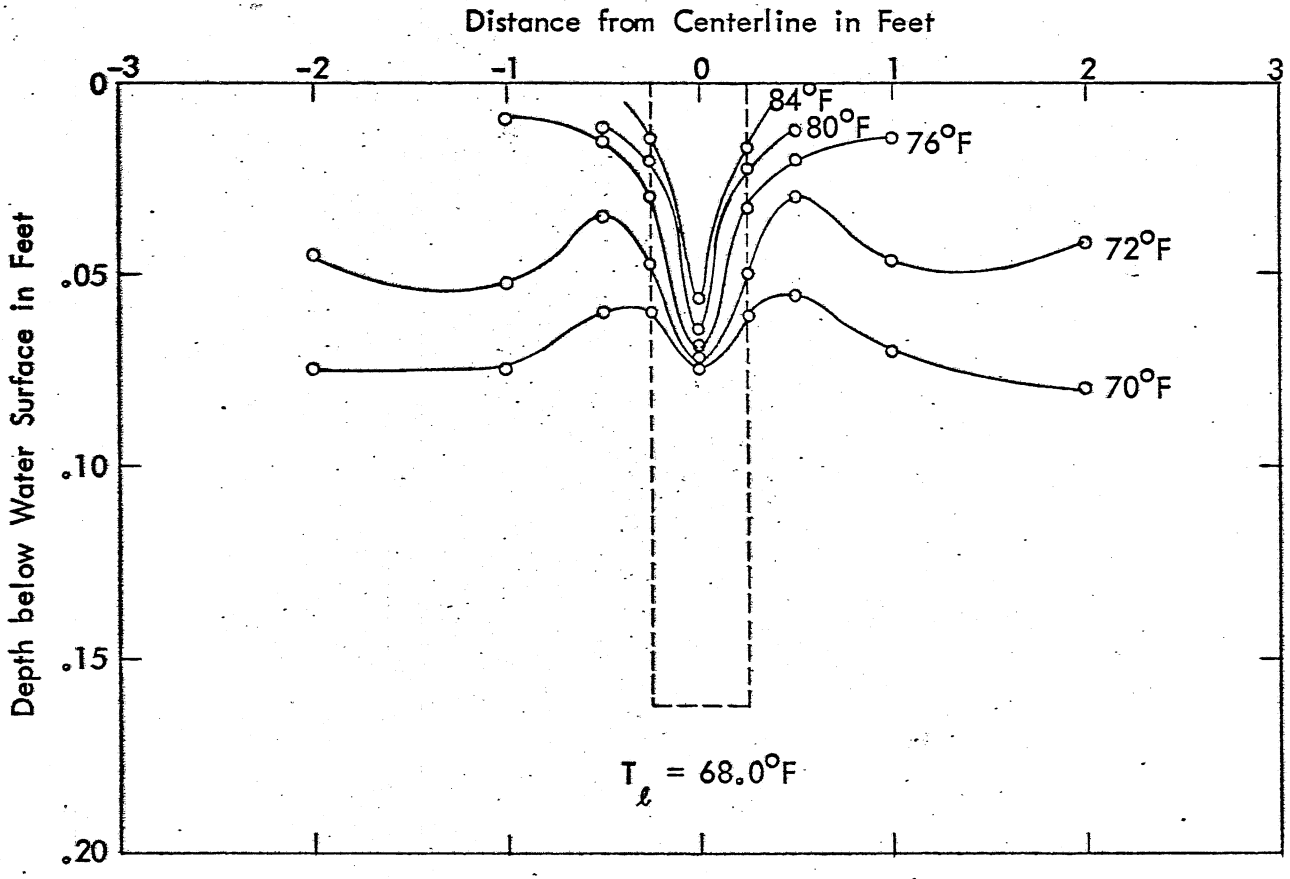

Fig. 13b - Isotherms for Test 214 in cross section at x = 5.5 ft from Upstream End of Tank. Warm Water Outlet at x = 4.86 ft, Outlet Temperature T_o = 87.0°F.

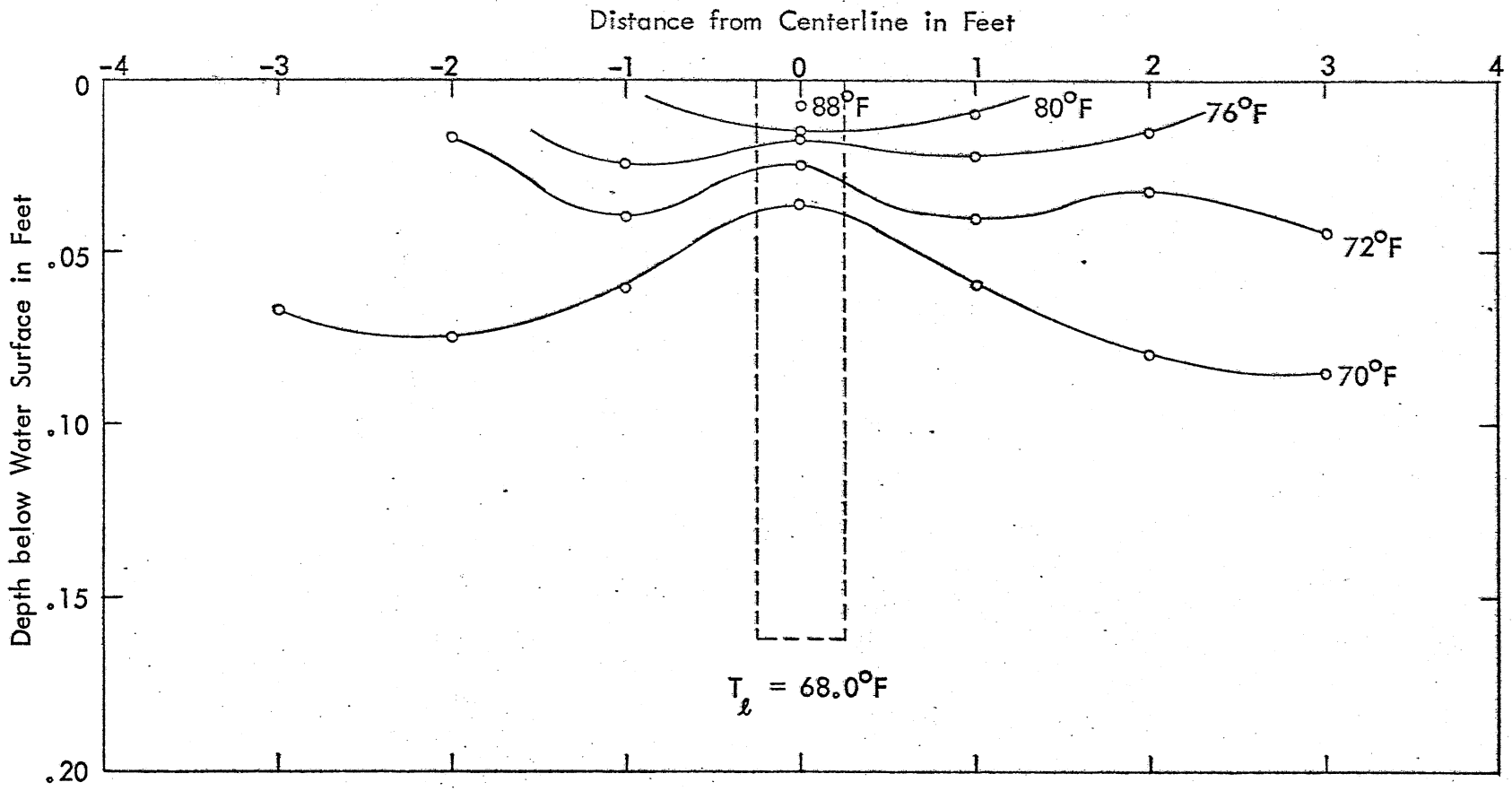

Fig. 13c - Isotherms for Test 214 in cross section at x = 6.5 ft from Upstream End of Tank. Warm Water Outlet at x = 4.86 ft, Outlet Temperature T_o = 87.0°F.

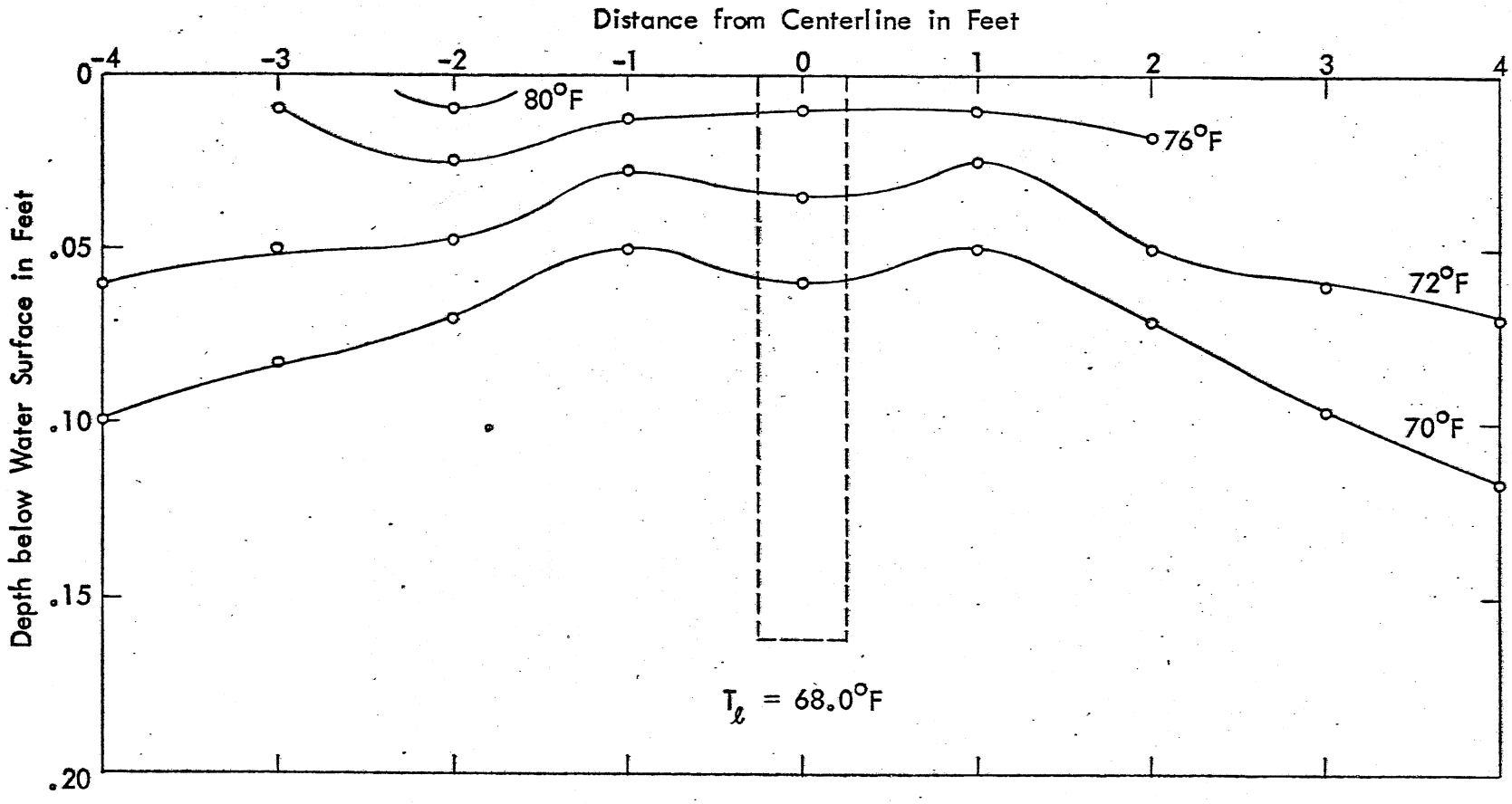

Fig. 13d - Isotherms for Test 214 in cross section at x = 7.5 ft from Upstream End of Tank. Warm Water Outlet at x = 4.86 ft, Outlet Temperature T_o = 87.0°F.

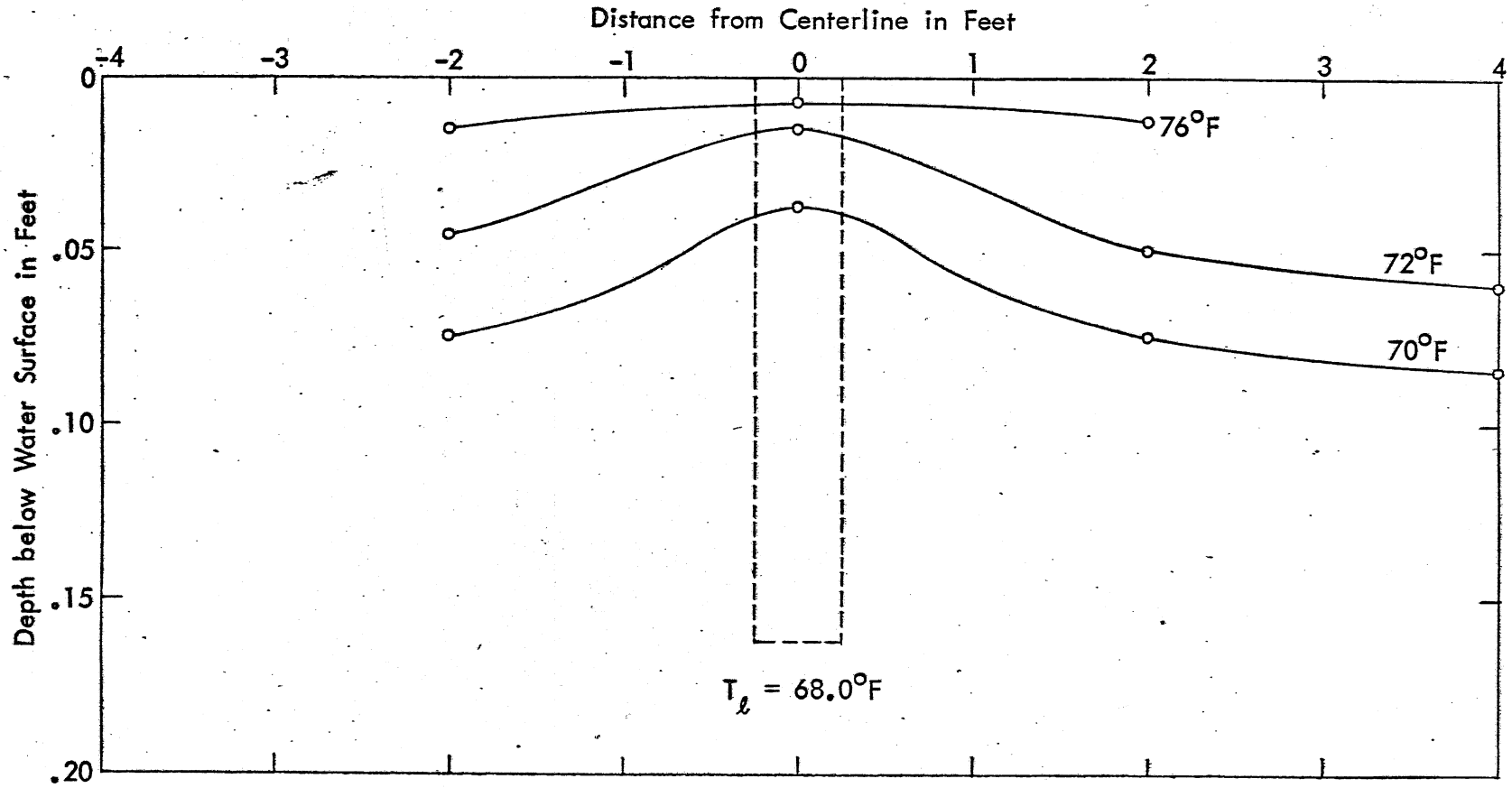

Fig. 13e - Isotherms for Test 214 in cross section at x = 9.5 ft from Upstream End of Tank. Warm Water Outlet at x = 4.86 ft, Outlet Temperature T_o = 87.0°F.

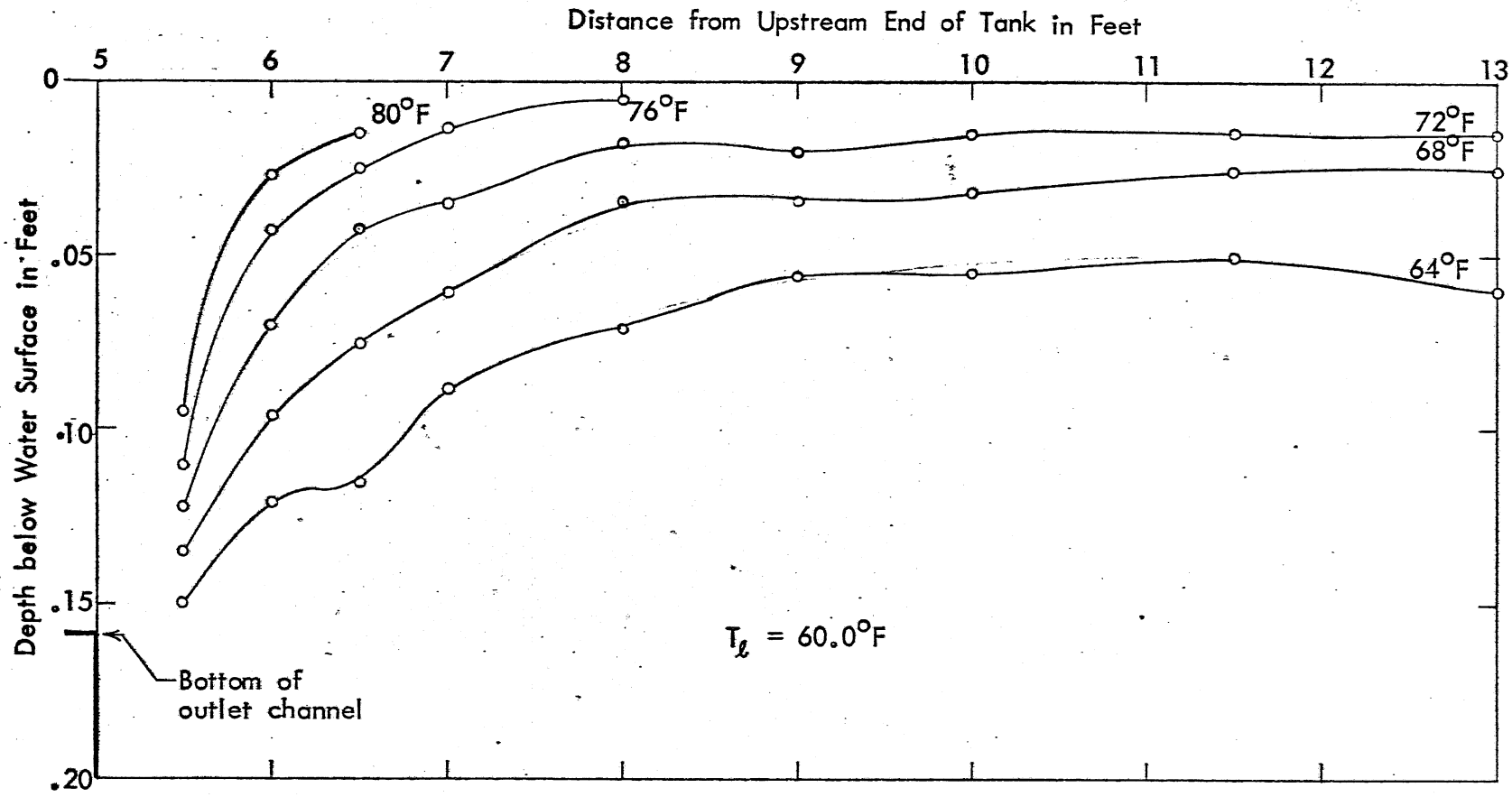

Fig. 14a - Isotherms for Test 211 in cross section at $y = 0$ (longitudinal cross section).
Outlet Depth $d_o = 0.158$ ft, Outlet Temperature $T_o = 84.0°F$.

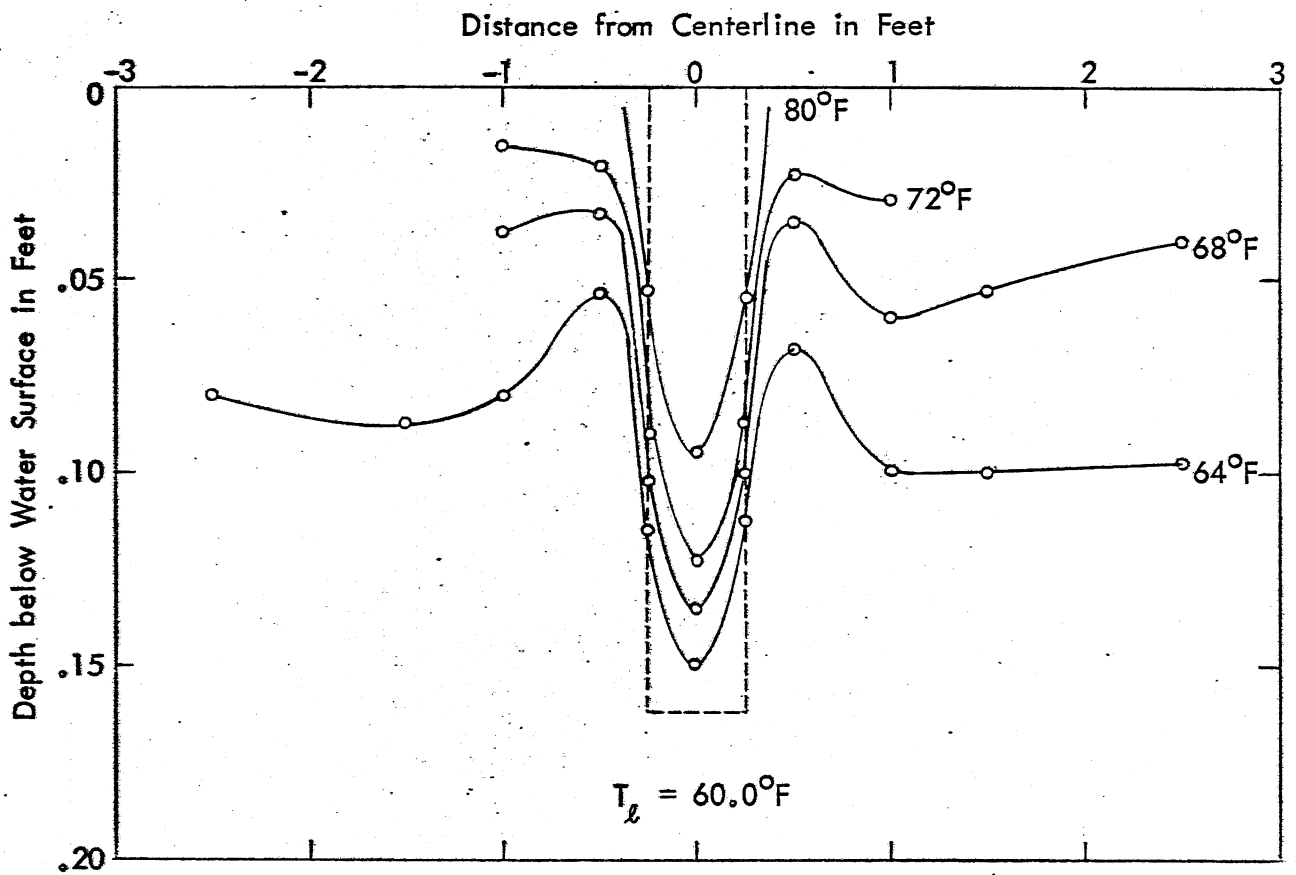

Fig. 14b - Isotherms for Test 211 in cross section at x = 5.5 ft from Upstream End of Tank. Warm Water Outlet at x = 4.86 ft, Outlet Temperature T_o = 84.0°F.

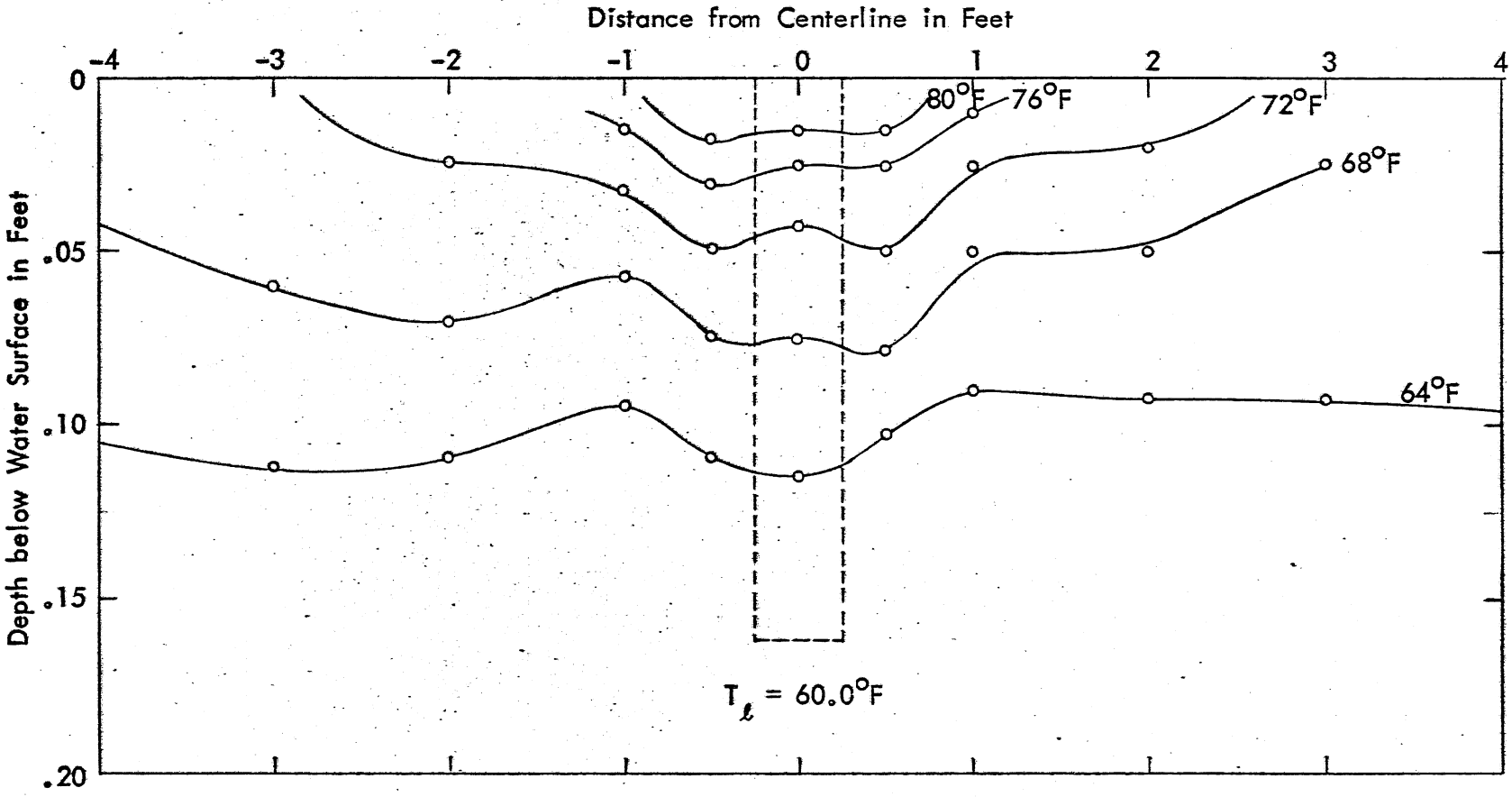

Fig. 14c - Isotherms for Test 211 in cross section at x = 6.5 ft from Upstream End of Tank. Warm Water Outlet at x = 4.86 ft, Outlet Temperature T_o = 84.0°F.

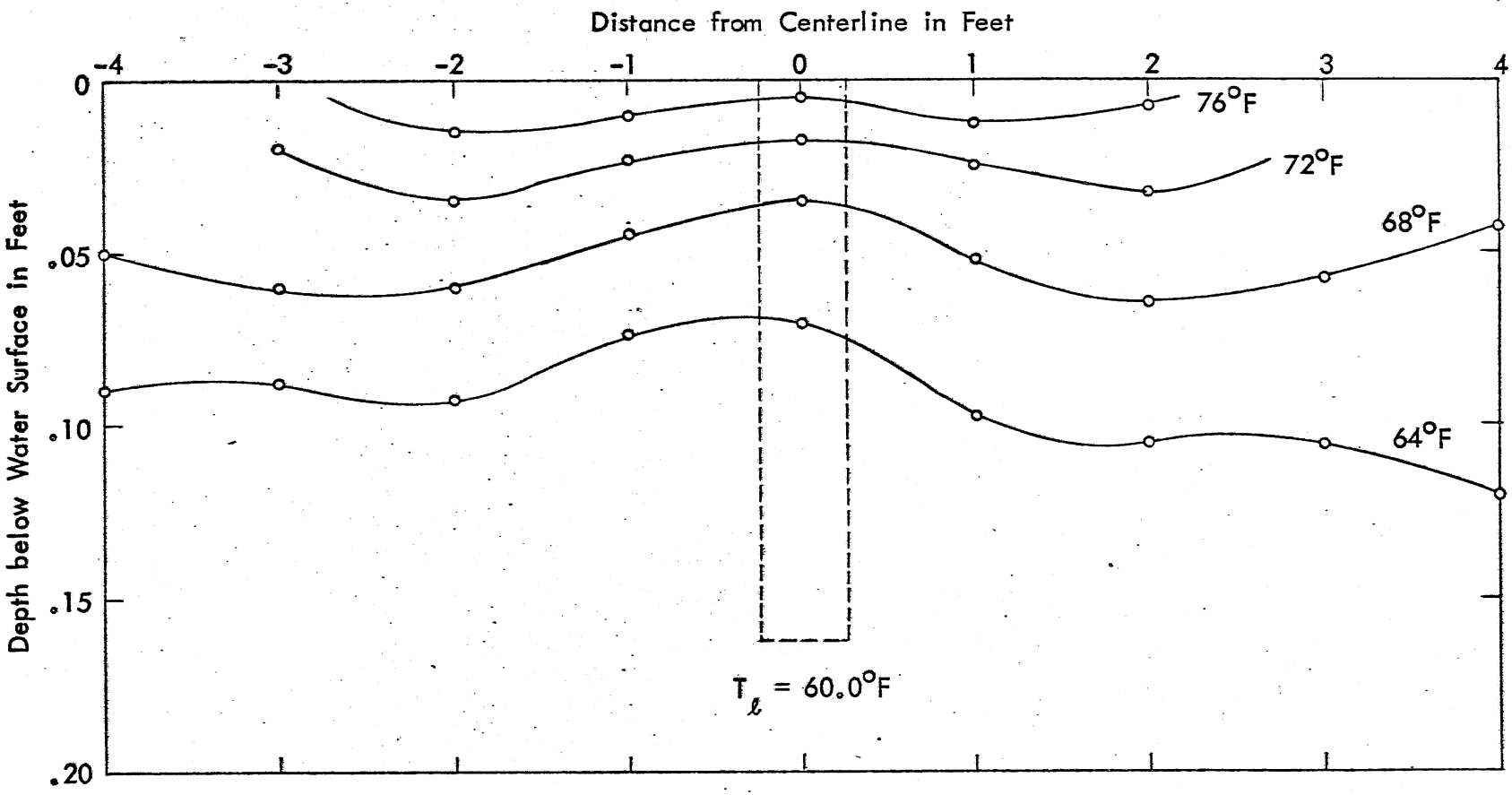

Fig. 14d – Isotherms for Test 211 in cross section at x = 8.0 ft from Upstream End of Tank. Warm Water Outlet at x = 4.86 ft, Outlet Temperature T_o = 84.0°F.

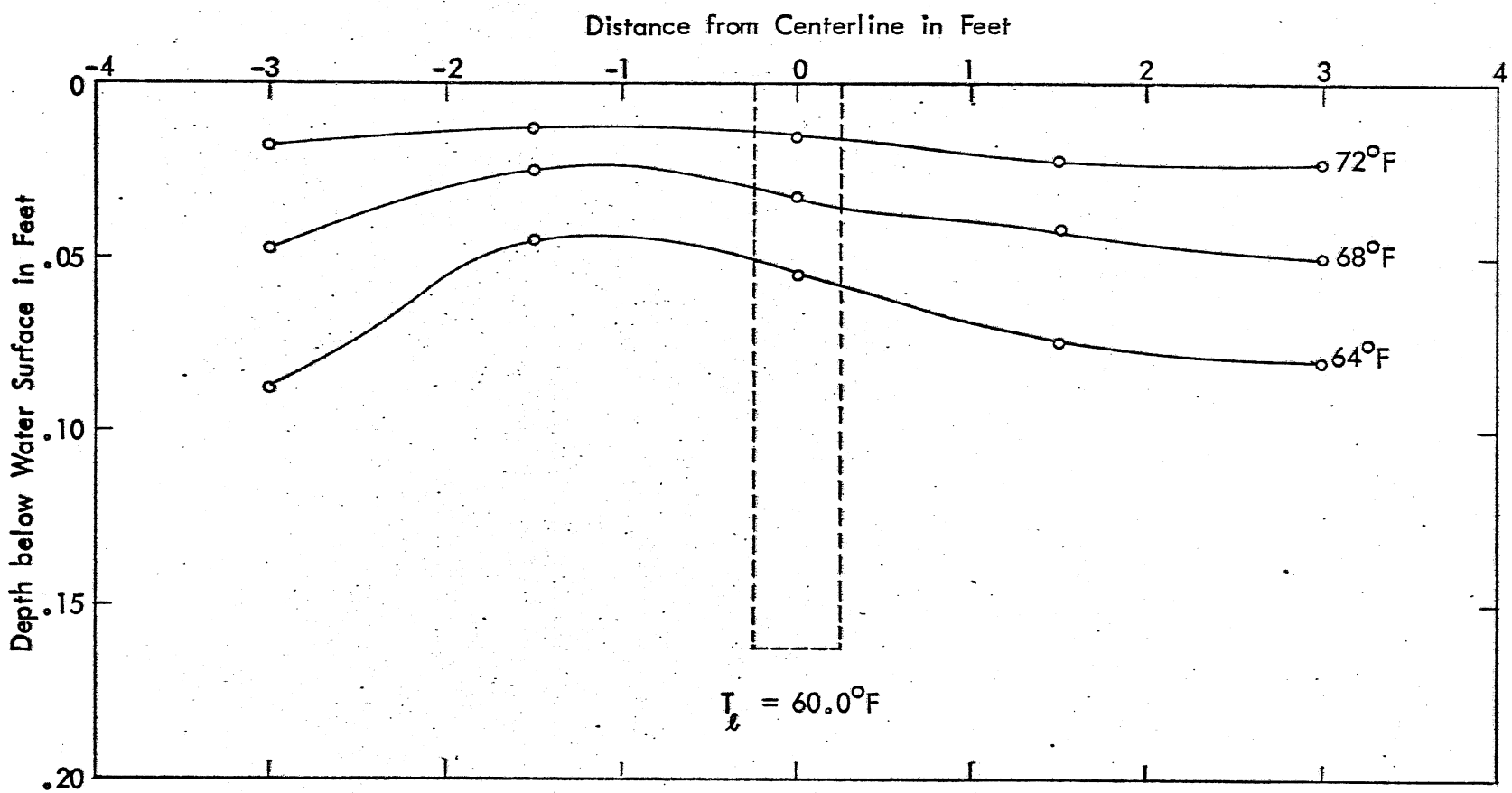

Fig. 14e - Isotherms for Test 211 in cross section at x = 10.0 ft from Upstream End of Tank. Warm Water Outlet at x = 4.86 ft, Outlet Temperature T_o = 84.0°F.

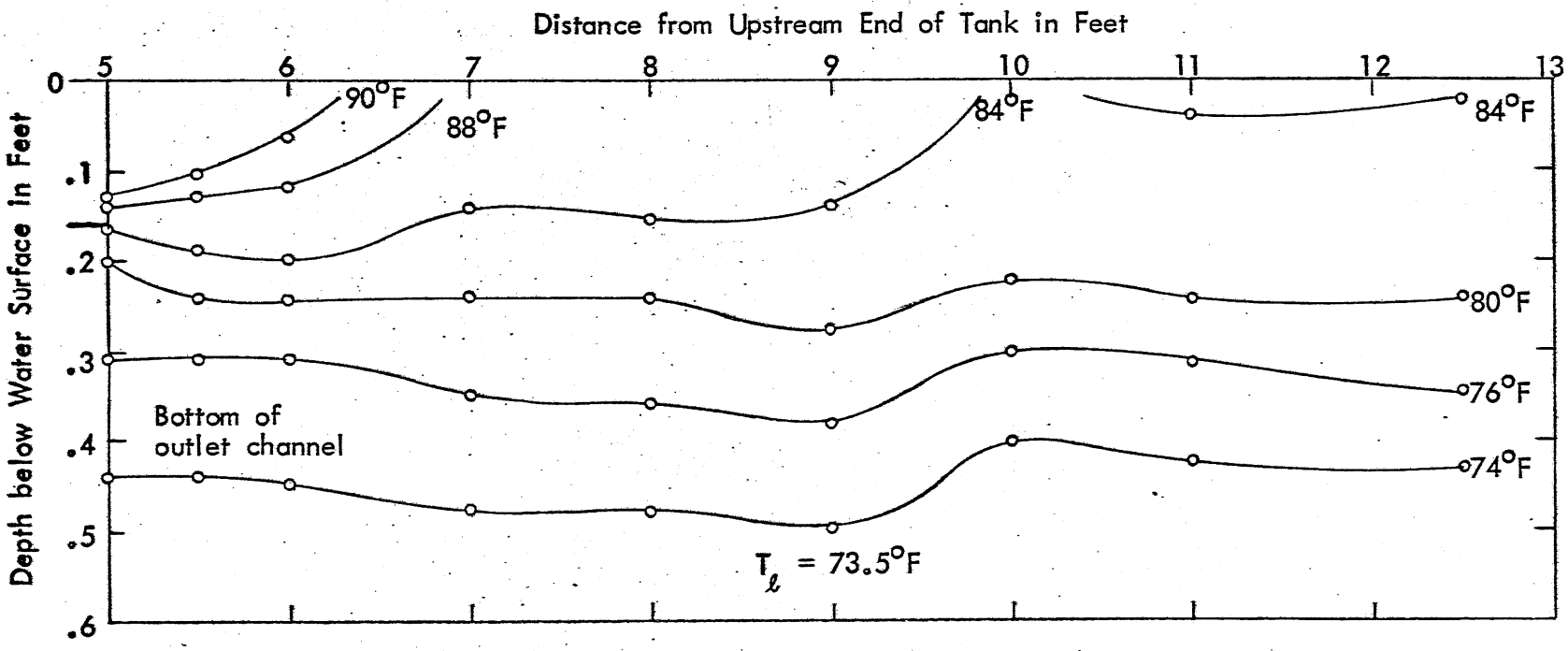

Fig. 15a - Isotherms for Test 217 in cross section at $y = 0$ (longitudinal cross section).
Outlet Depth d_o = 0.155 ft, Outlet Temperature T_o = 92.5°F.

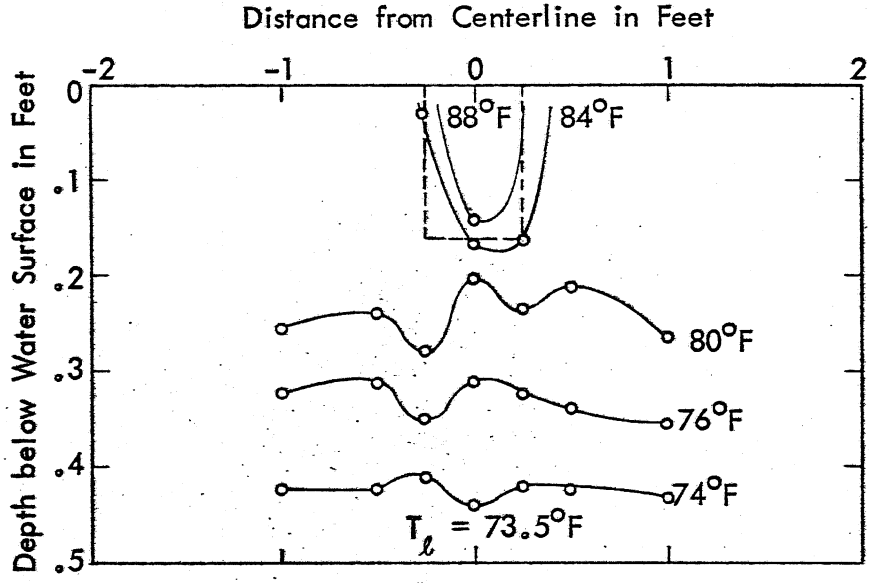

Fig. 15b - Isotherms for Test 217 in cross section at x = 5.0 ft from Upstream End of Tank. Warm Water Outlet at x = 4.86 ft, Outlet Temperature T_o = 92.5°F.

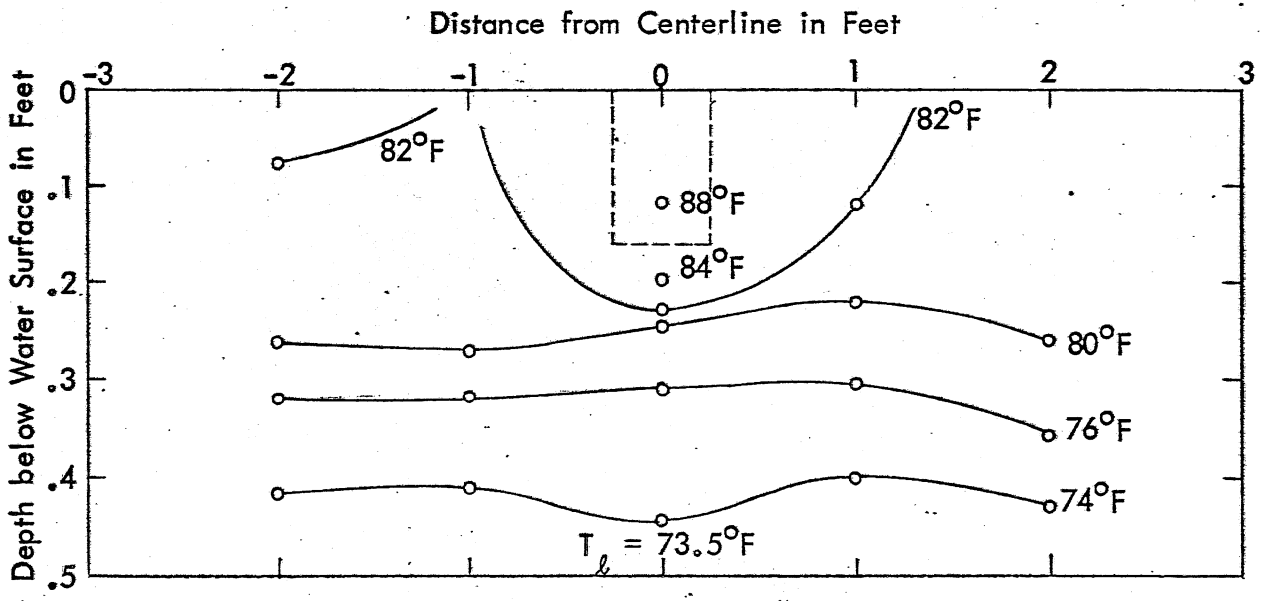

Fig. 15c - Isotherms for Test 217 in cross section at x = 6.0 ft from Upstream End of Tank. Warm Water Outlet at x = 4.86 ft, Outlet Temperature T_o = 92.5°F.

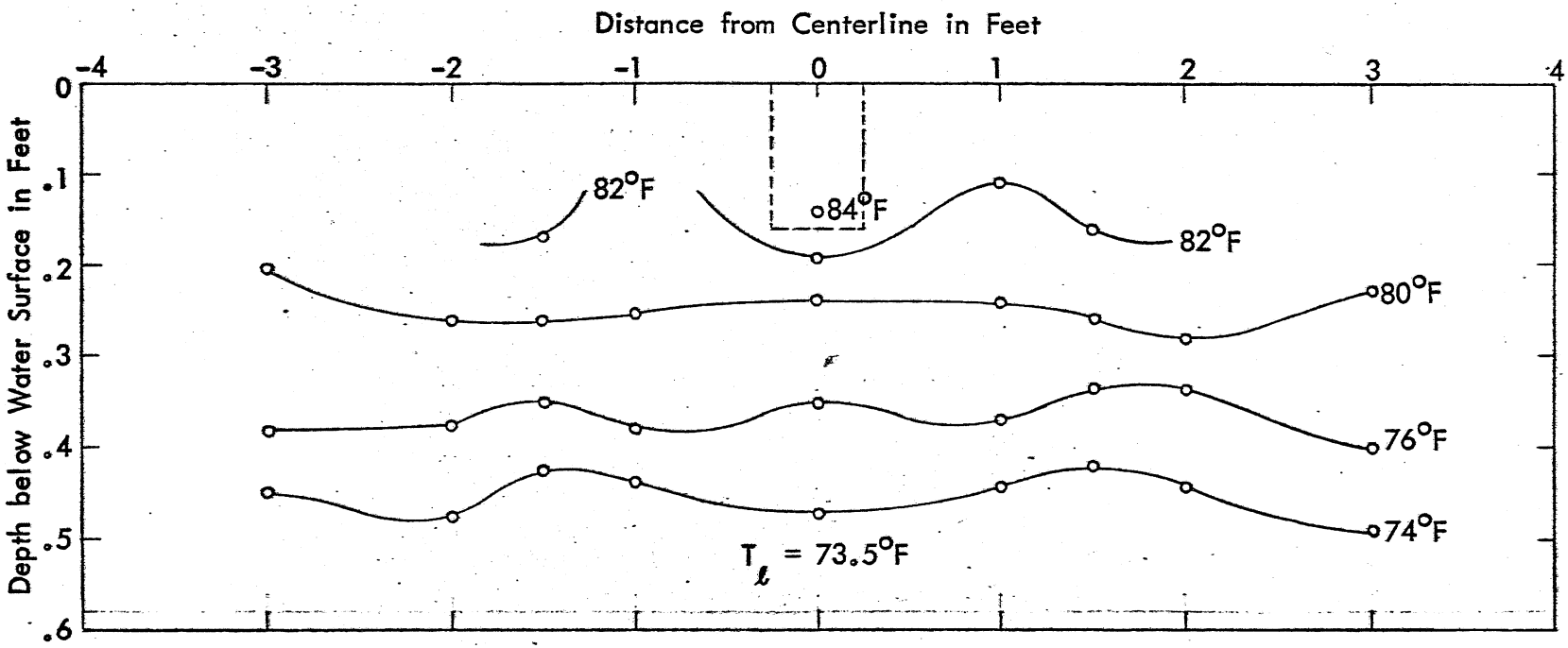

Fig. 15d – Isotherms for Test 217 in cross section at x = 7.0 ft from Upstream End of Tank. Warm Water Outlet at x = 4.86 ft, Outlet Temperature T_o = 92.5°F.

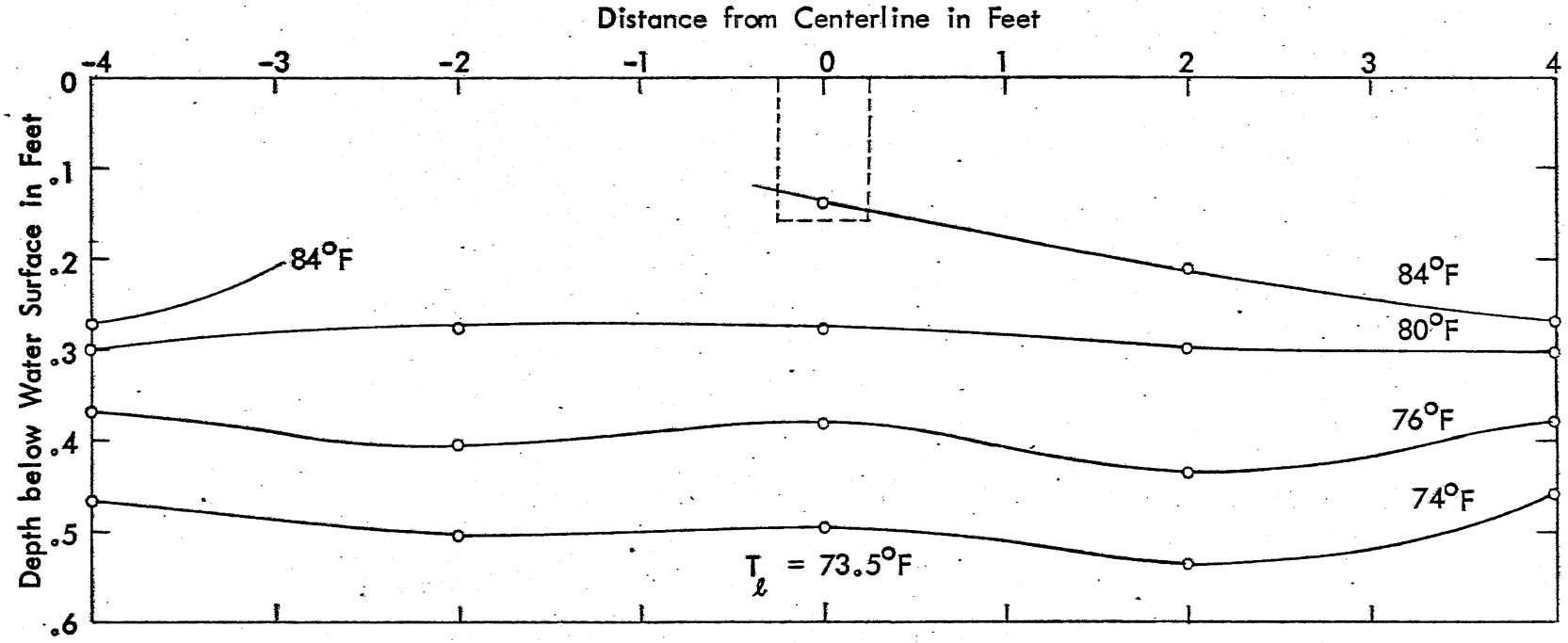

Fig. 15e - Isotherms for Test 217 in cross section at x = 9.0 ft from Upstream End of Tank. Warm Water Outlet at x = 4.86 ft, Outlet Temperature T_o = 92.5°F.

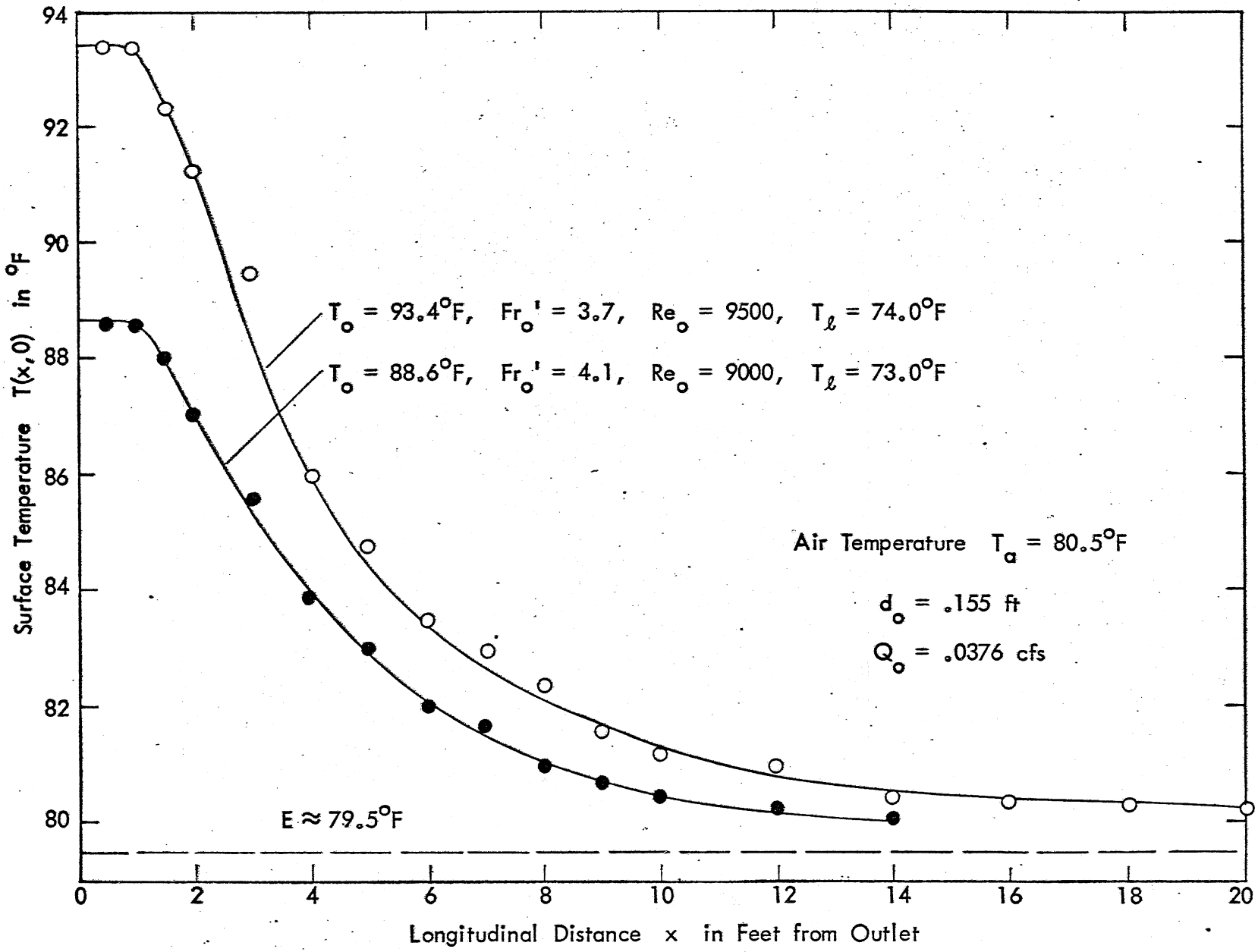

Fig. 16 - Examples of Temperatures at Water Surface

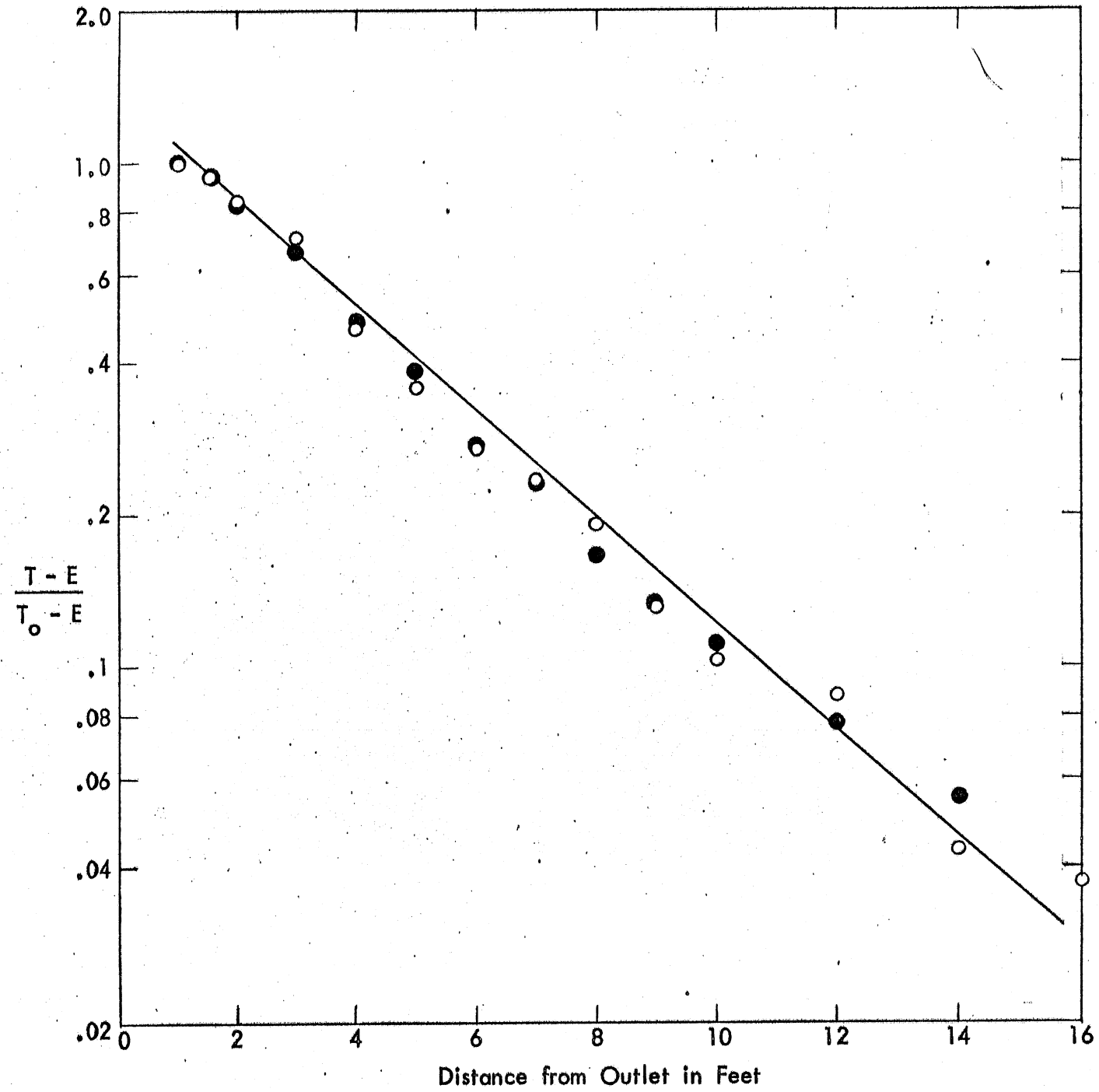

Fig. 17 - Dimensionless Values of Temperature Excess above Equilibrium Temperature

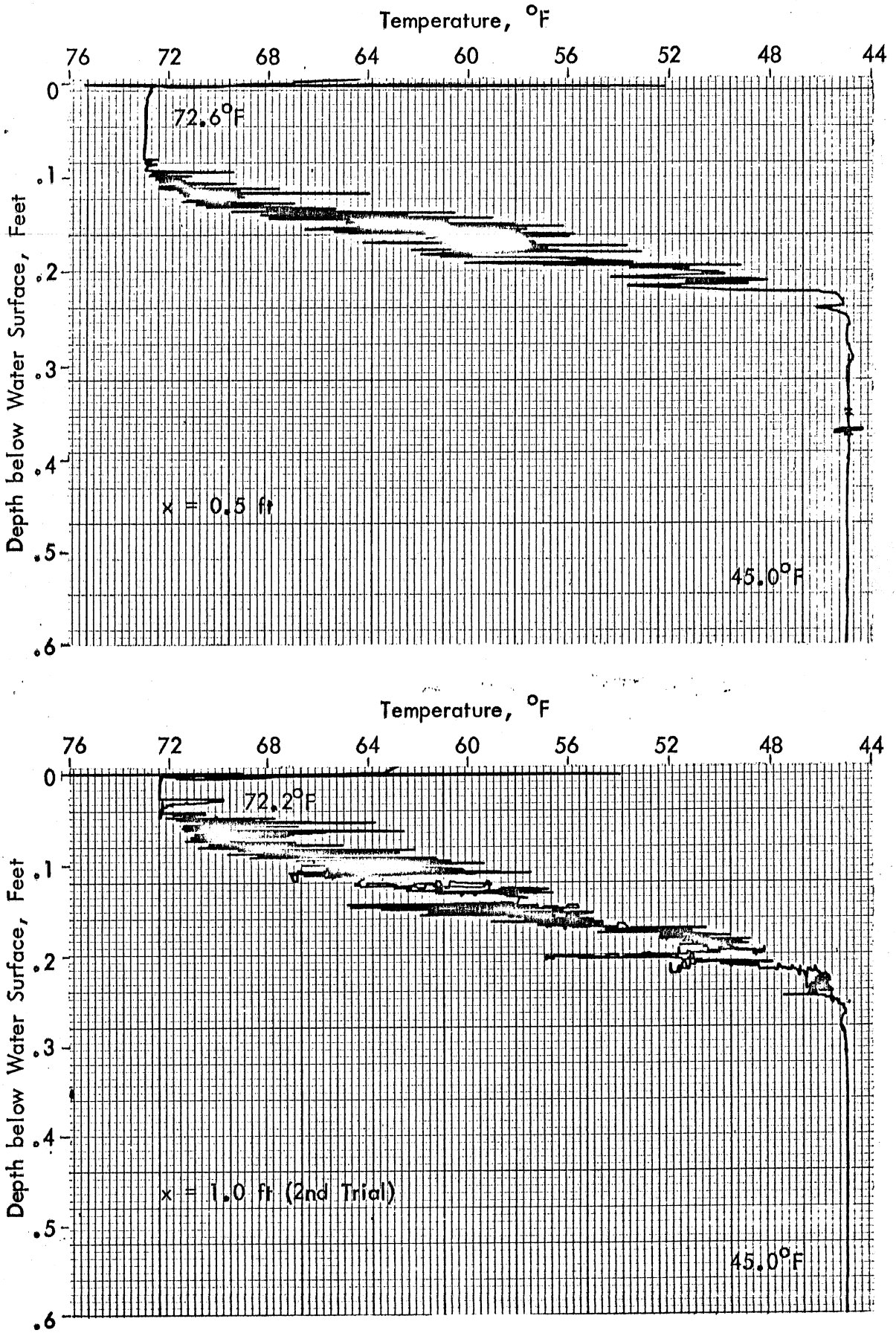

Fig. 18a - Temperatures for Test 201 at y = 0

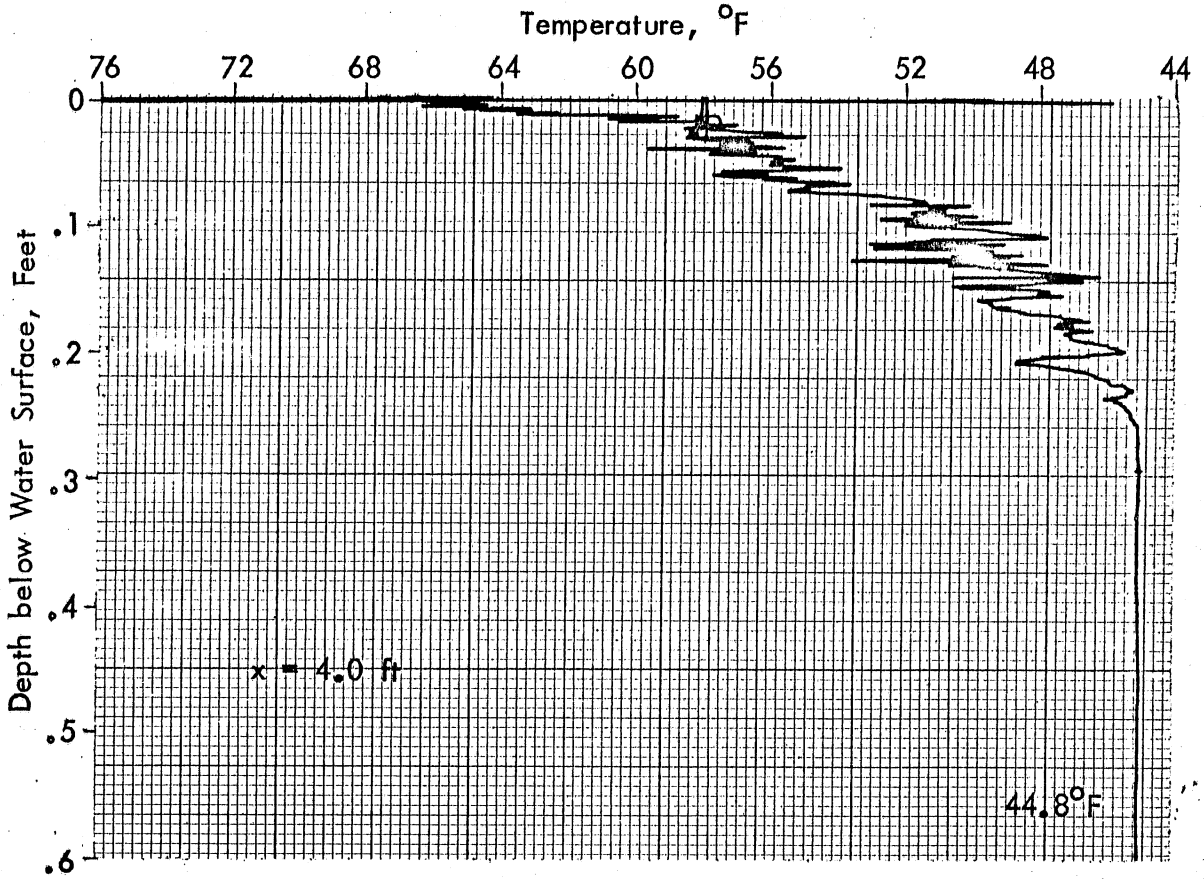

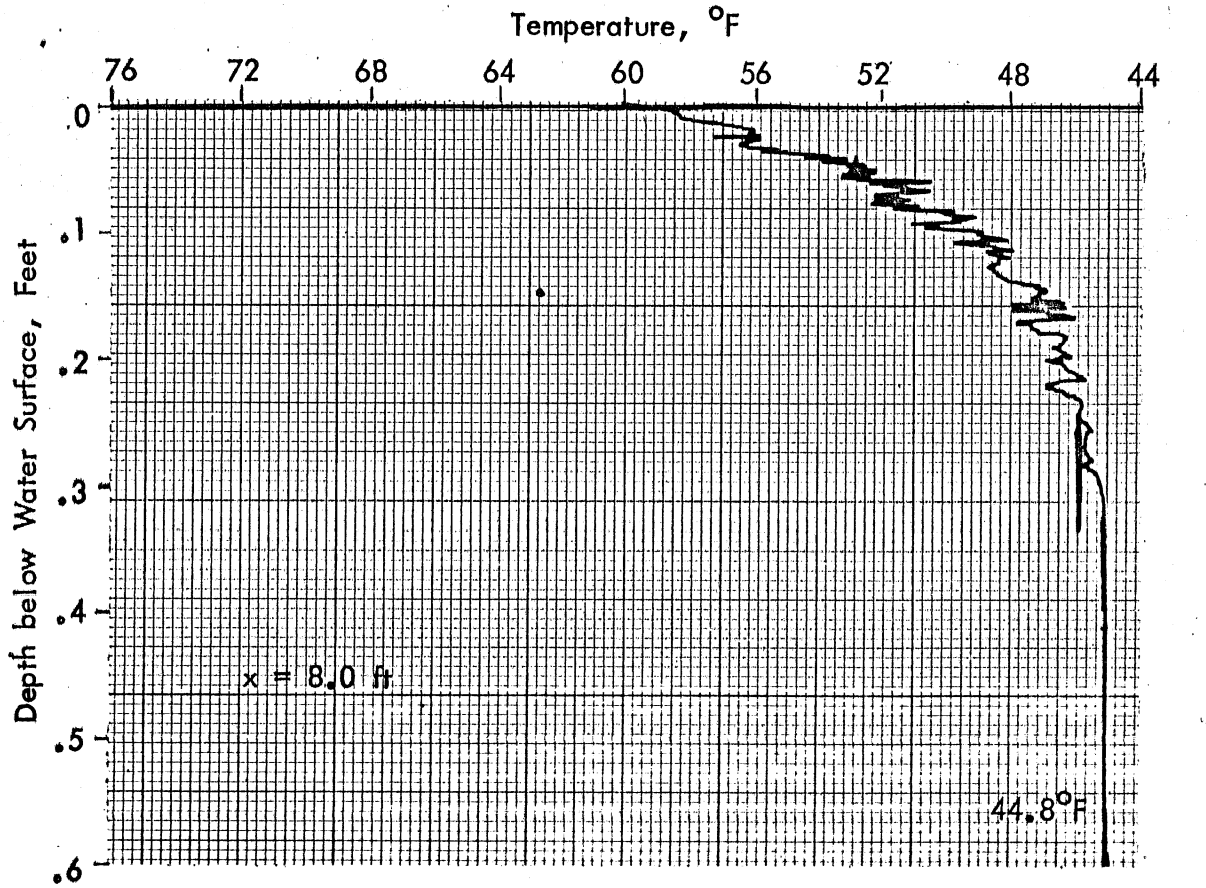

Fig. 18b - Temperatures for Test 201 at y = 0

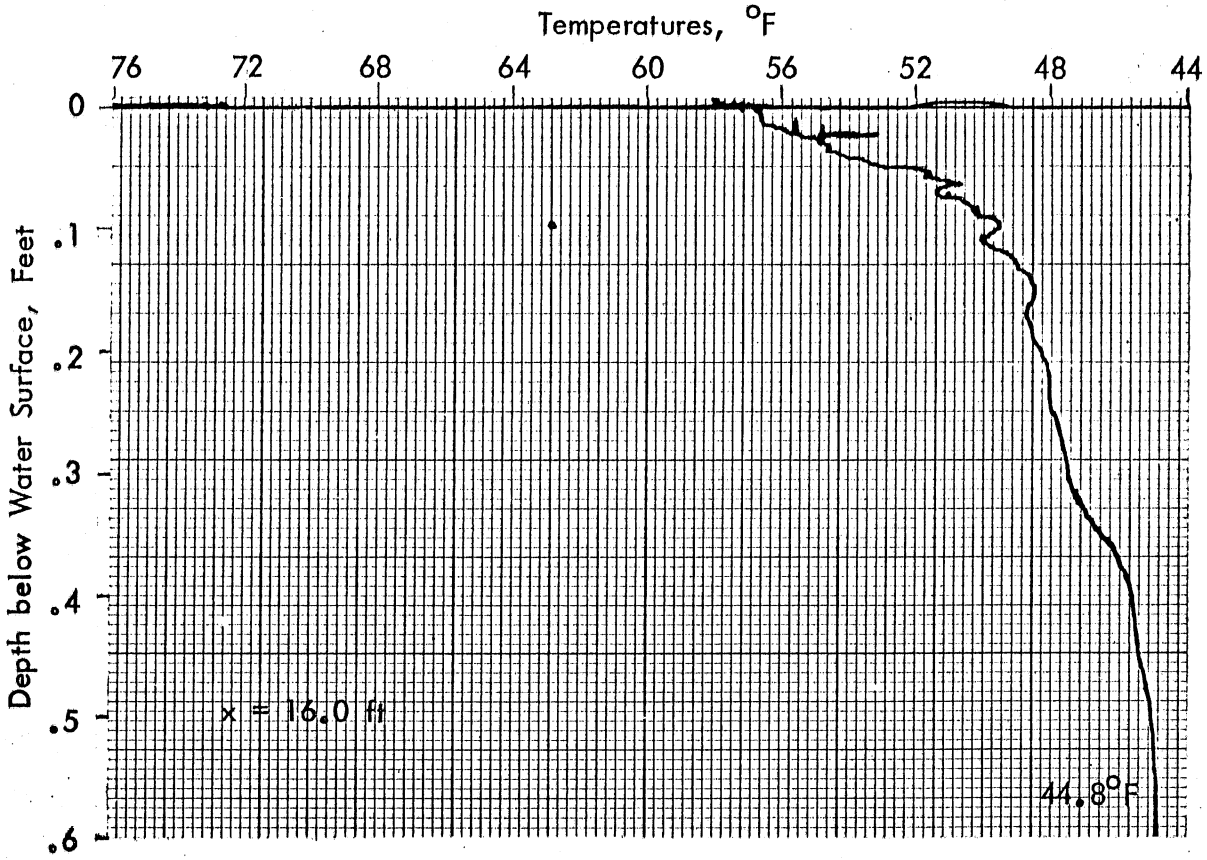

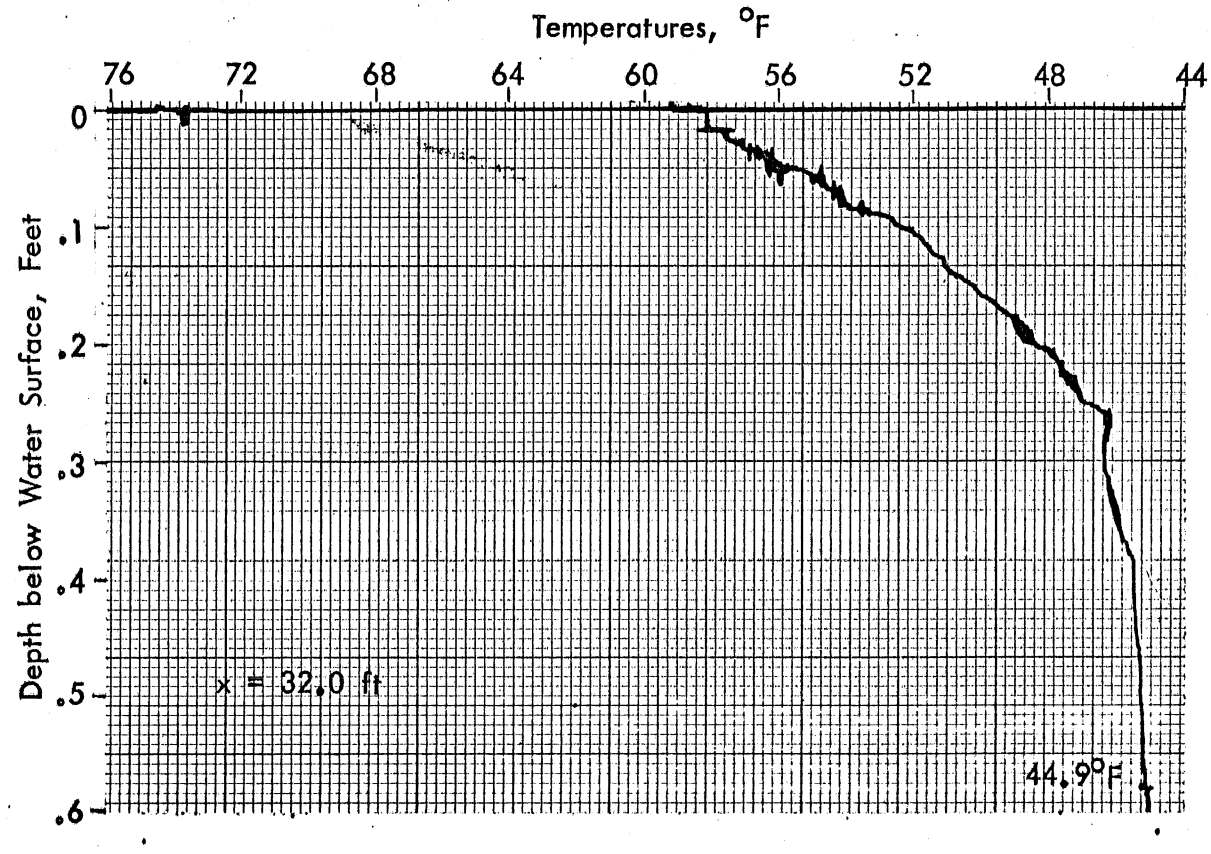

Fig. 18c - Temperatures for Test 201 at y = 0

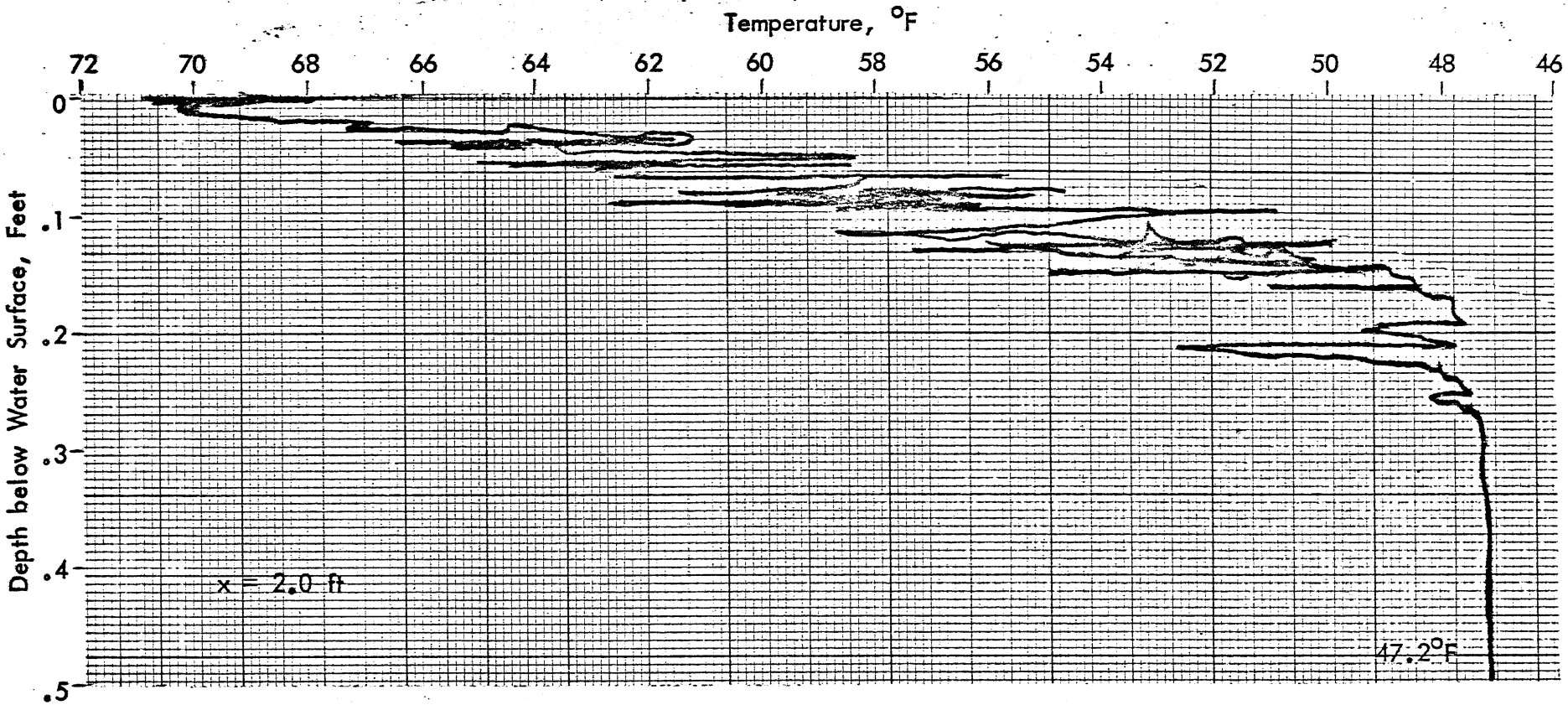

Fig. 19a - Temperatures for Test 203 at y = 0

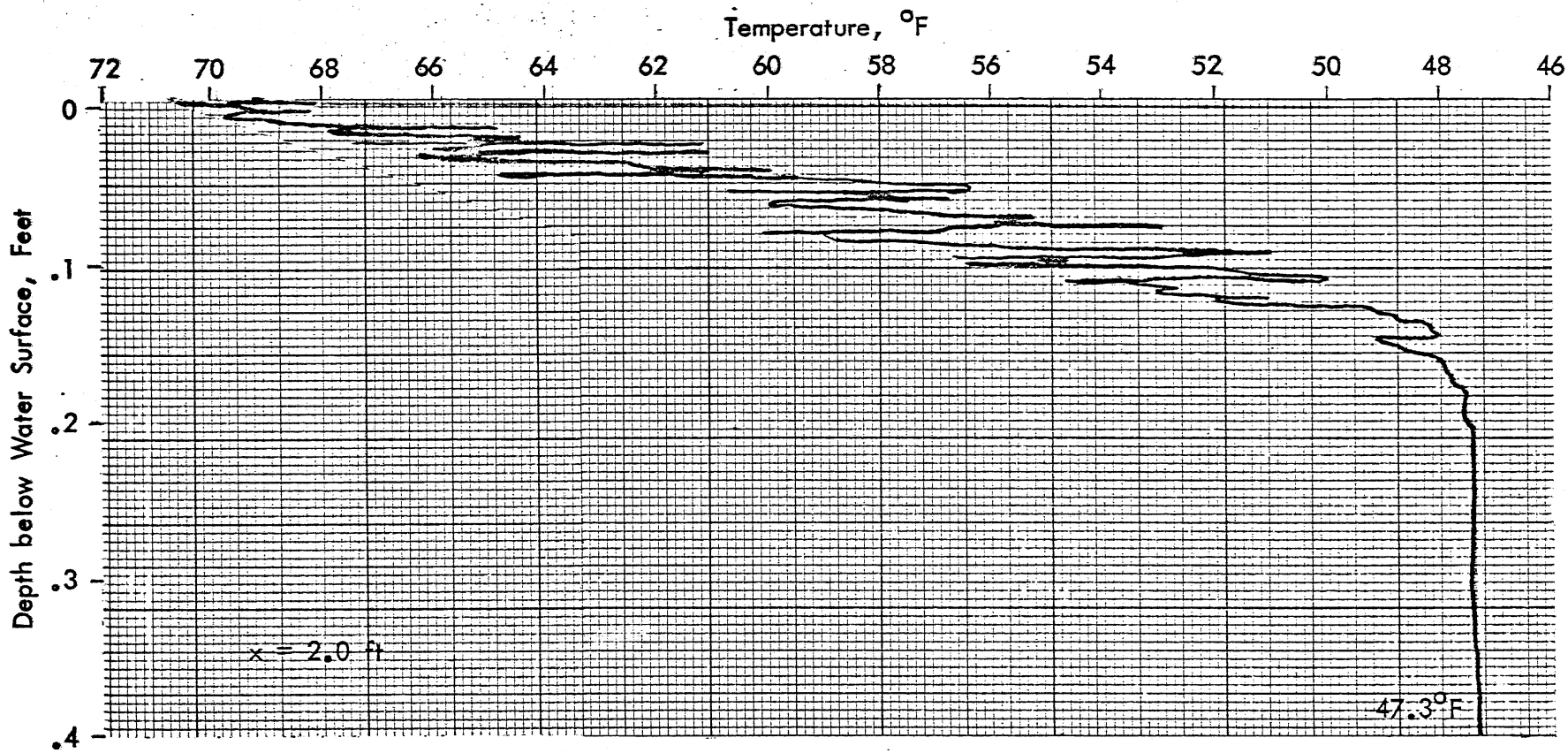

Fig. 19b - Temperatures for Test 203 at y = -0.5

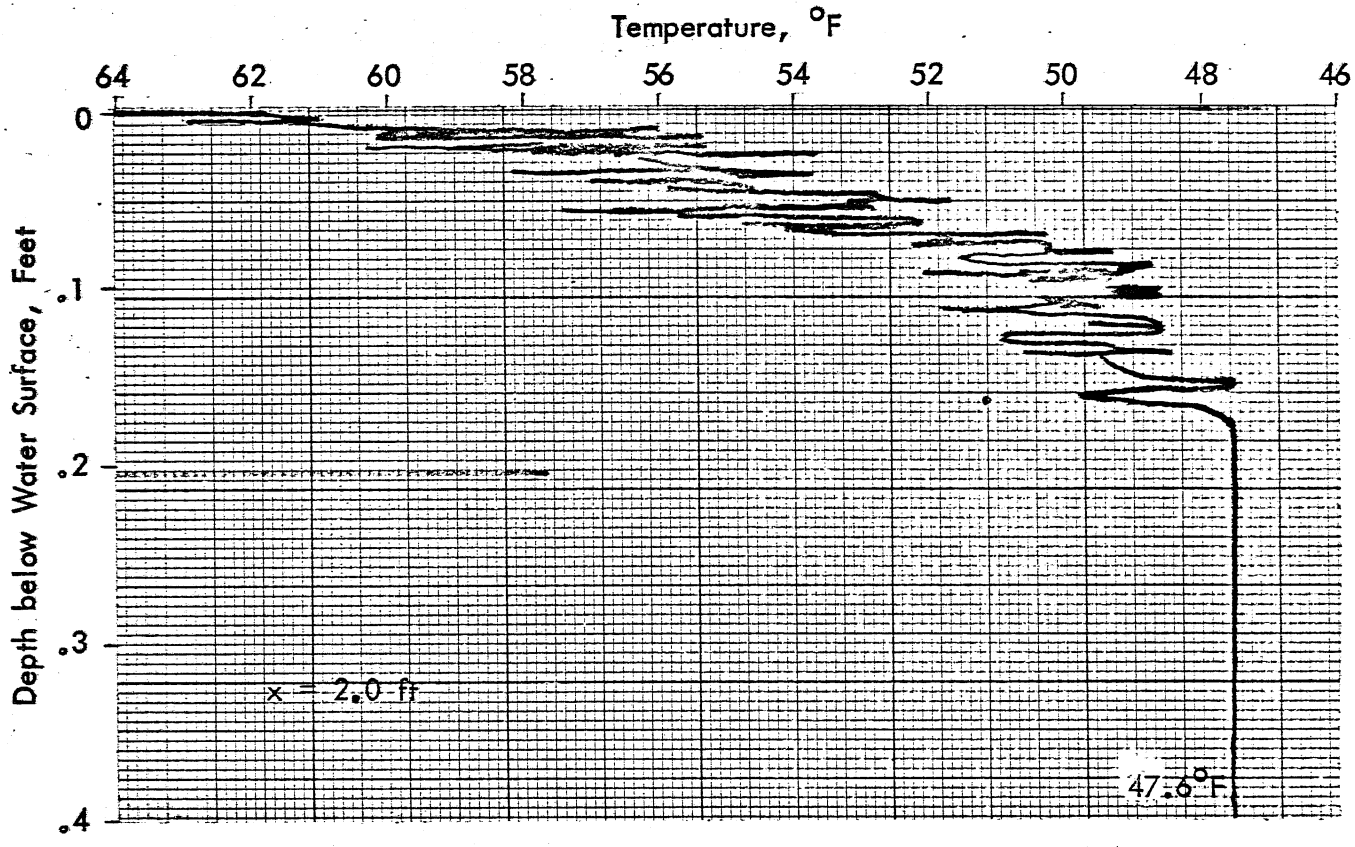

Fig. 19c - Temperatures for Test 203 at y = -1.0

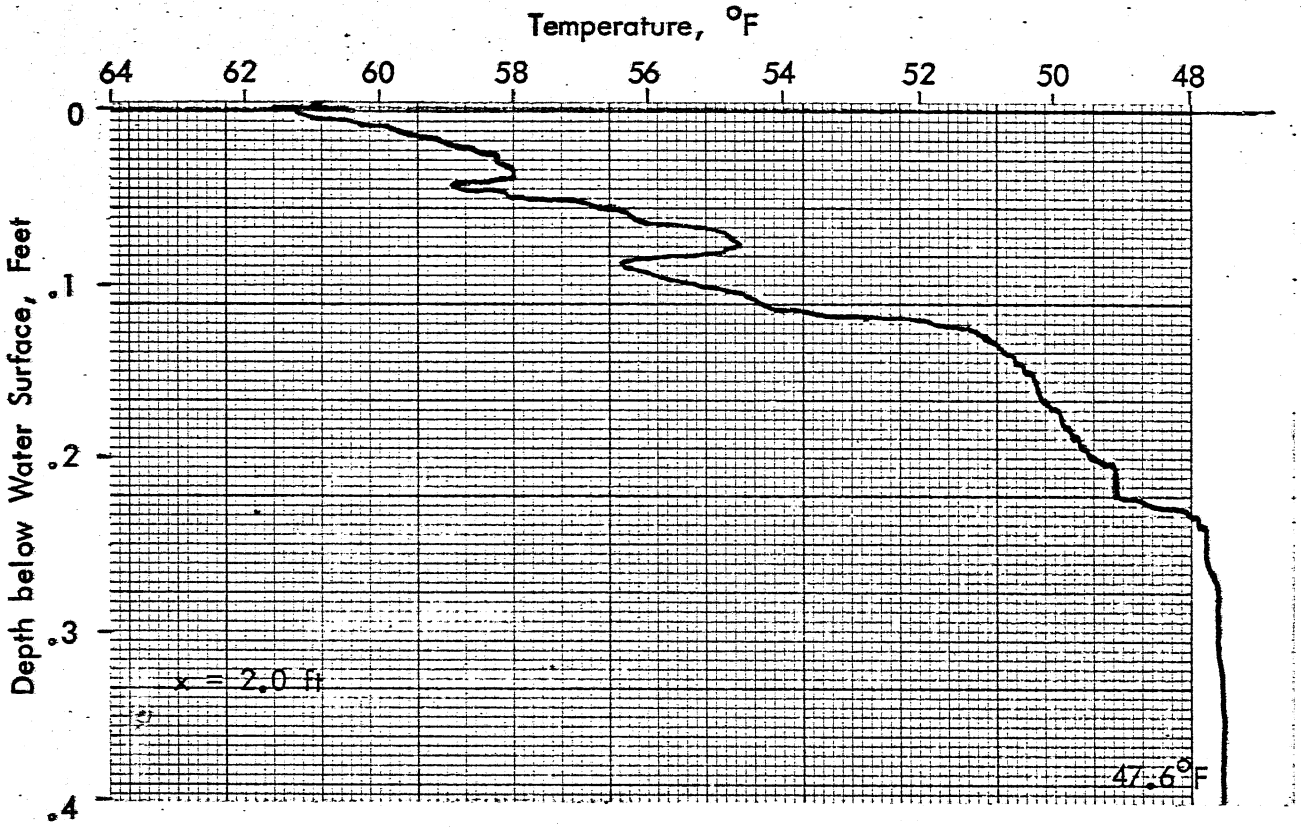

Fig. 19d - Temperatures for Test 203 at $y = -2.0$

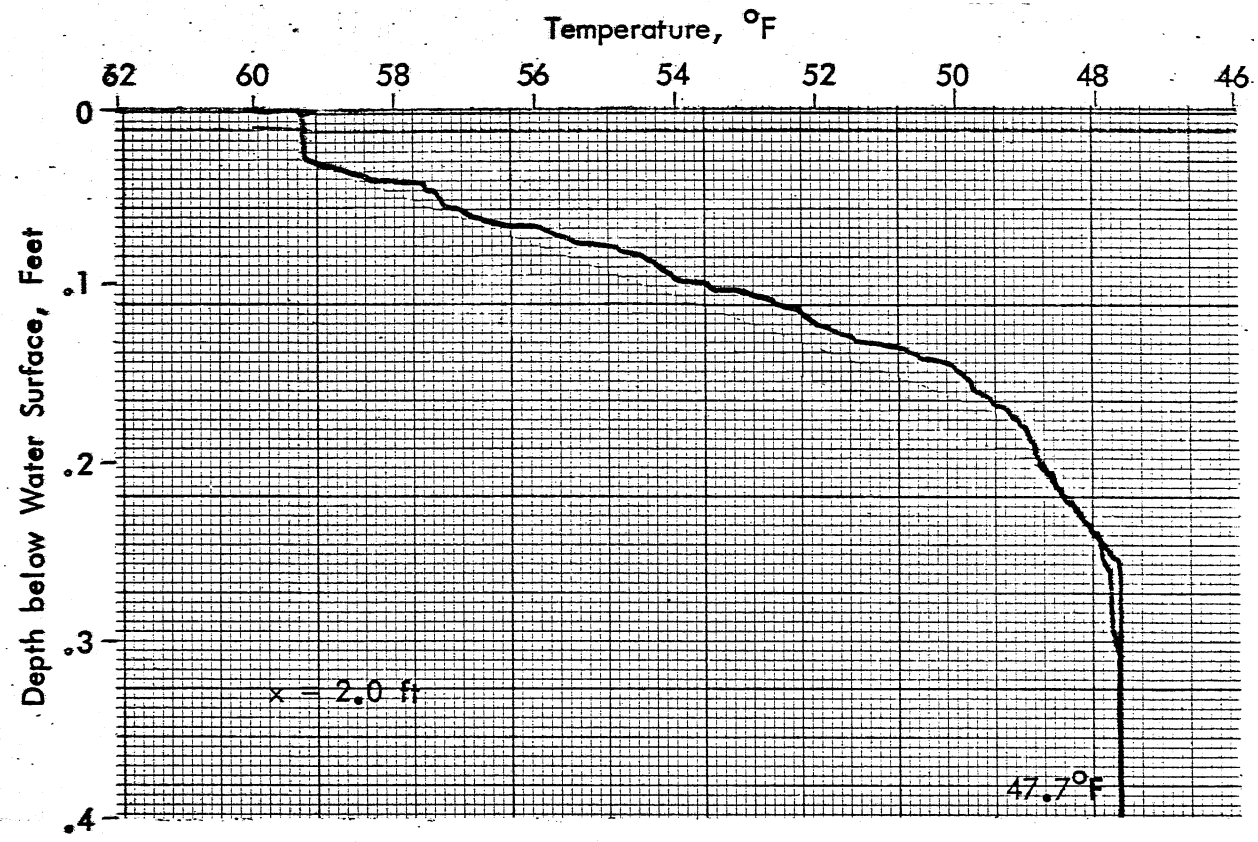

Fig. 19e - Temperatures for Test 203 at y = -3.0

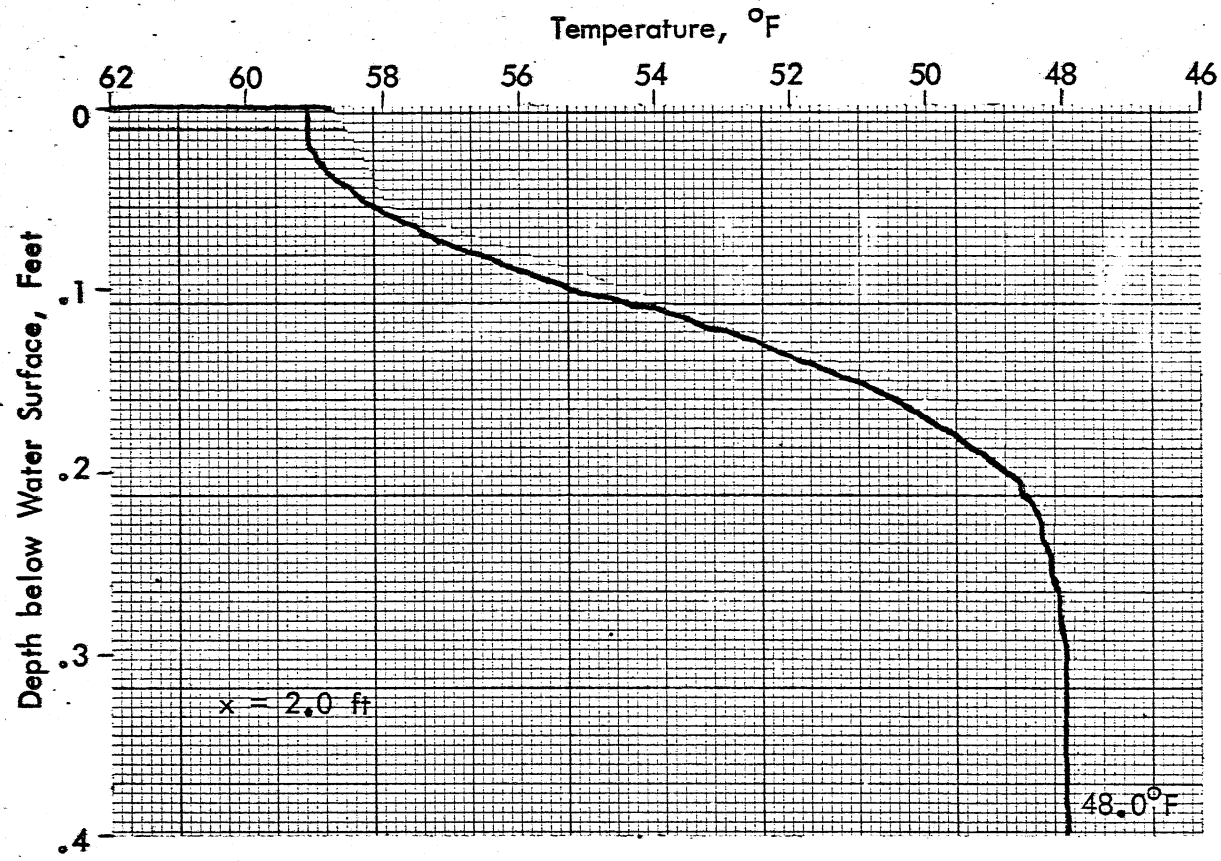

Fig. 19f - Temperatures for Test 203 at y = -4.0

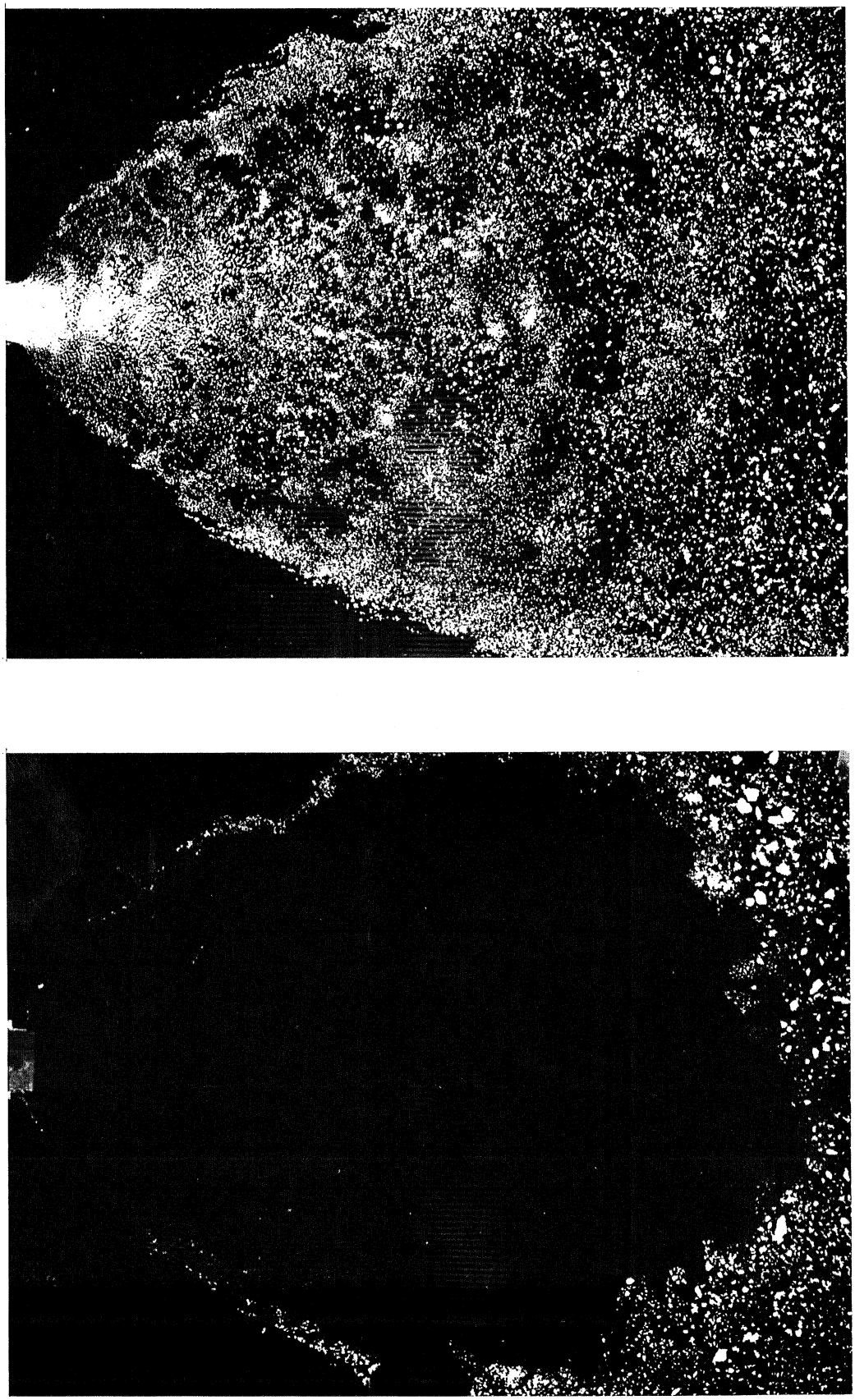

Fig. 20 - Examples of Surface Spreading Patterns Obtained with Lycopodium Powder (Test 210)

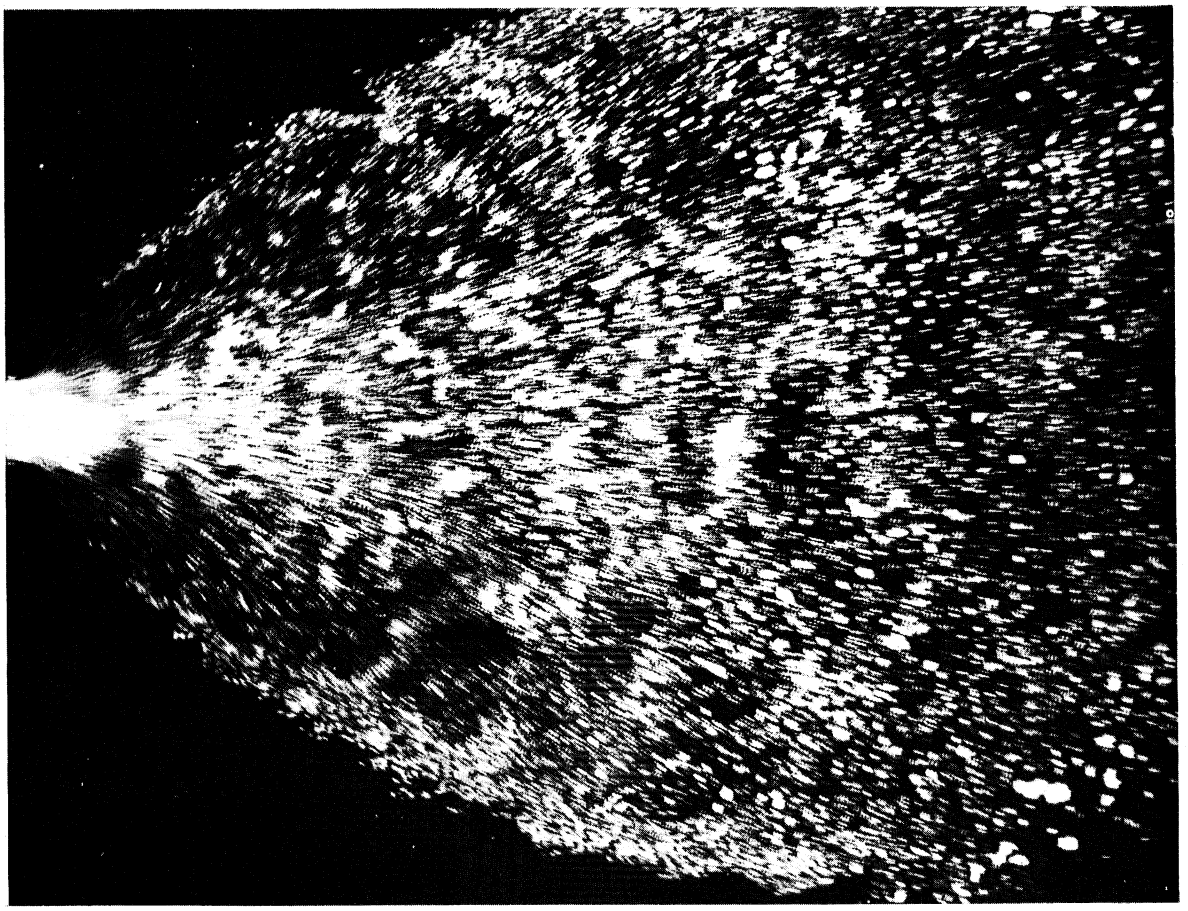

Fig. 21 - Time Exposure of Spreading Pattern (Test. 210)

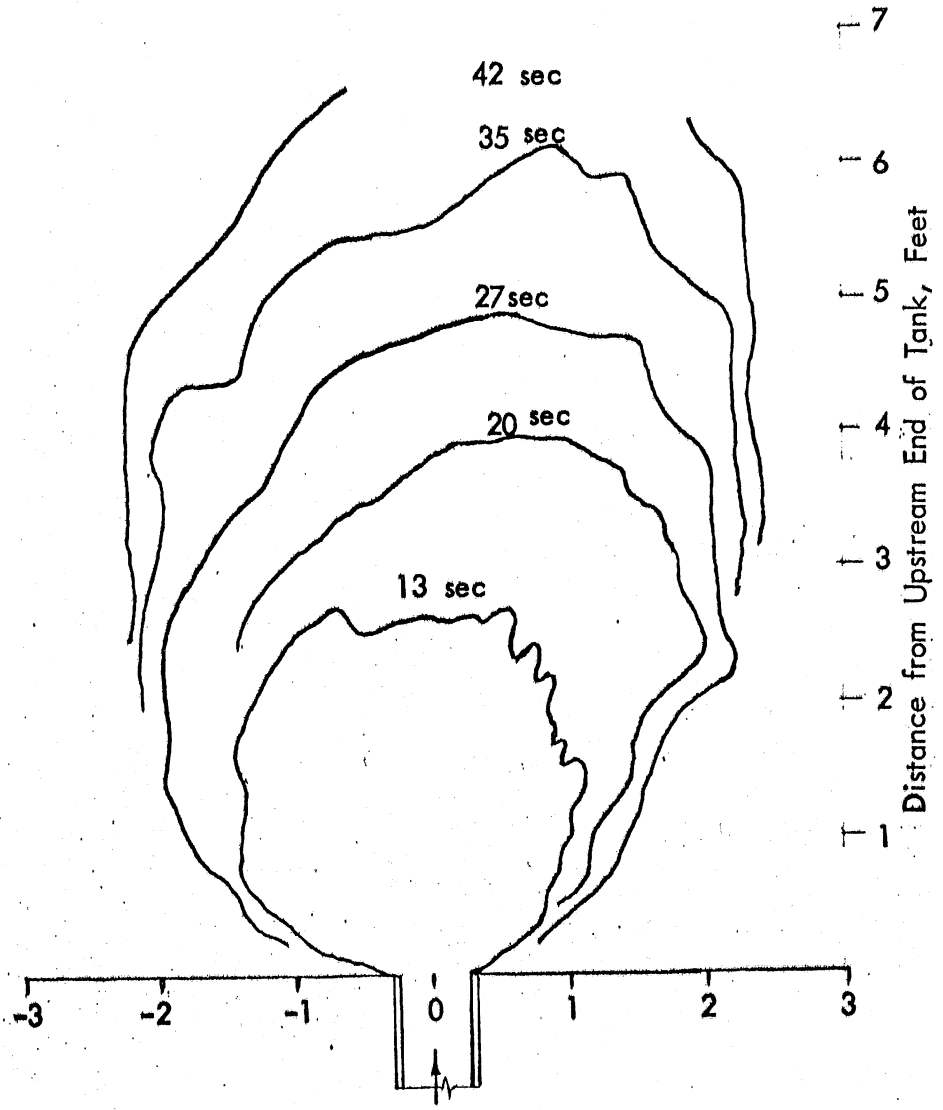

Fig. 22 - Surface Spreading Pattern for Test 207.
Timelines obtained with Fluoresceine Dye.

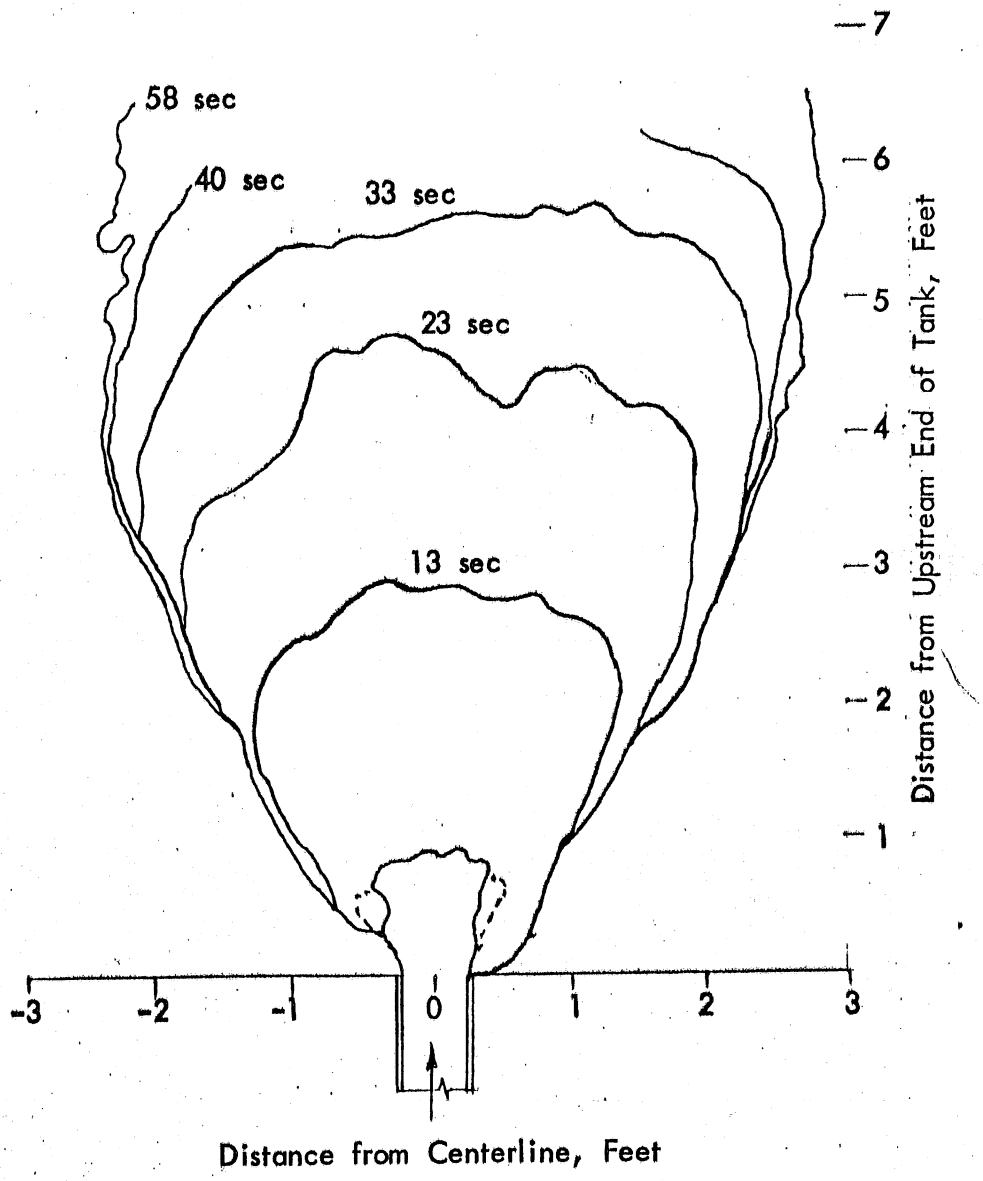

Fig. 23 - Surface Spreading Pattern for Test 208.
Timelines obtained with Aluminum Powder.

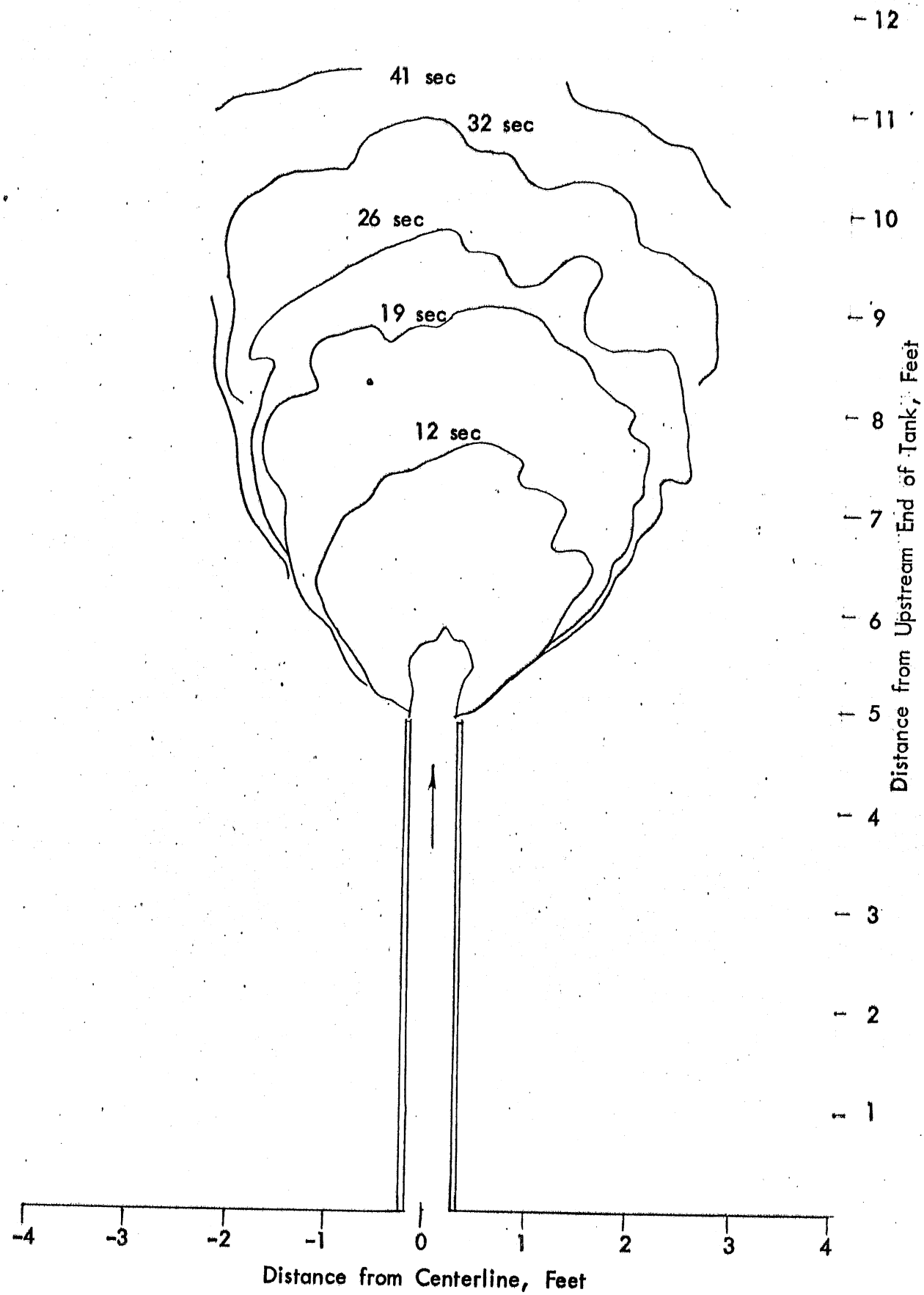

Fig. 24 - Surface Spreading Pattern for Test 209. Timelines obtained with Aluminum Powder.

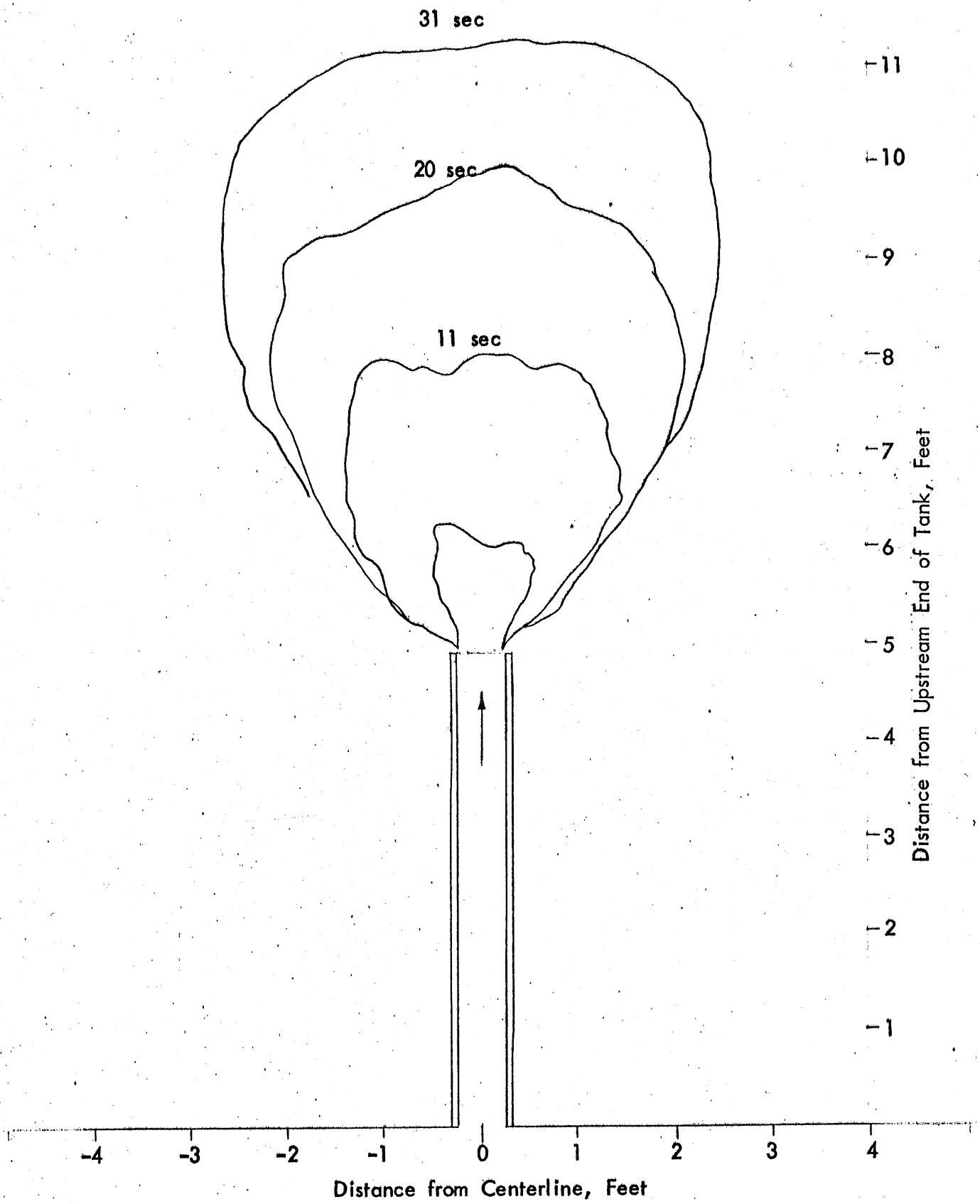

Fig. 26 - Surface Spreading Pattern for Test 212. Timelines obtained with Lycopodium Powder and Fluorescent Dye.

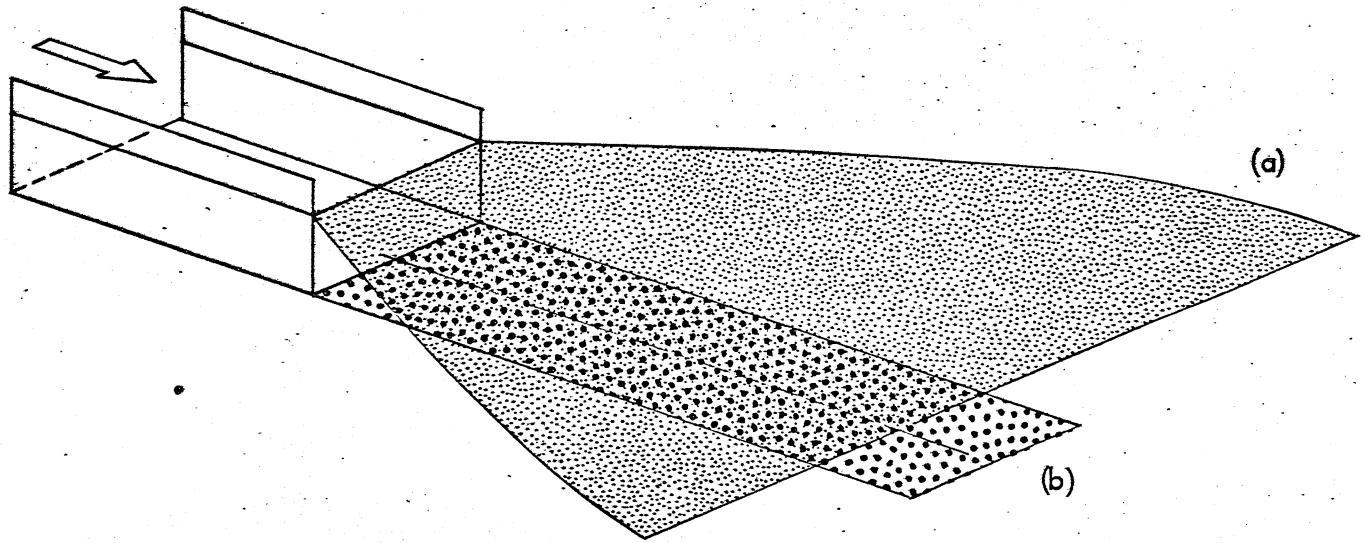

Fig. 27 - Spreading of Dye released at
(a) Water Surface
(b) Bottom of Outlet Channel

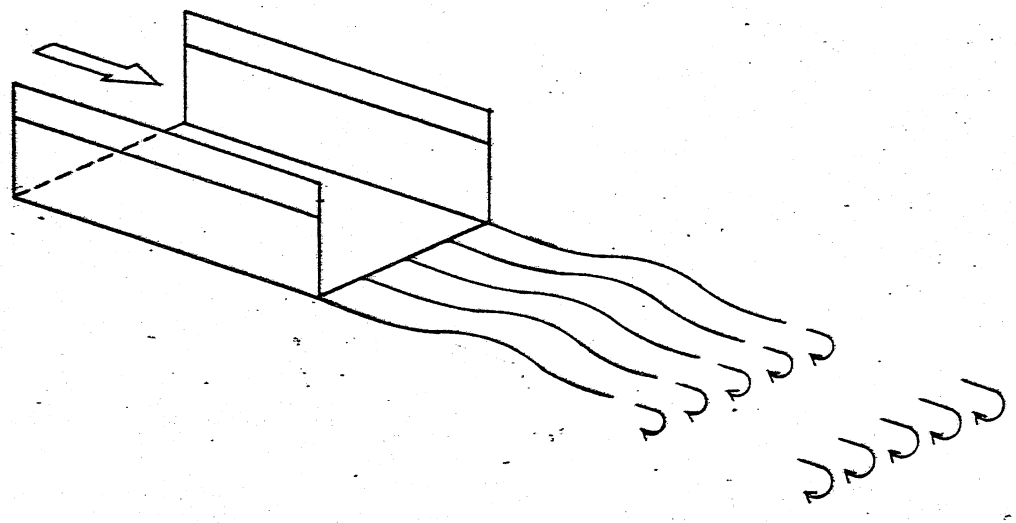

Fig. 28a - Formation of Internal Gravity Waves and Vortices near Outlet

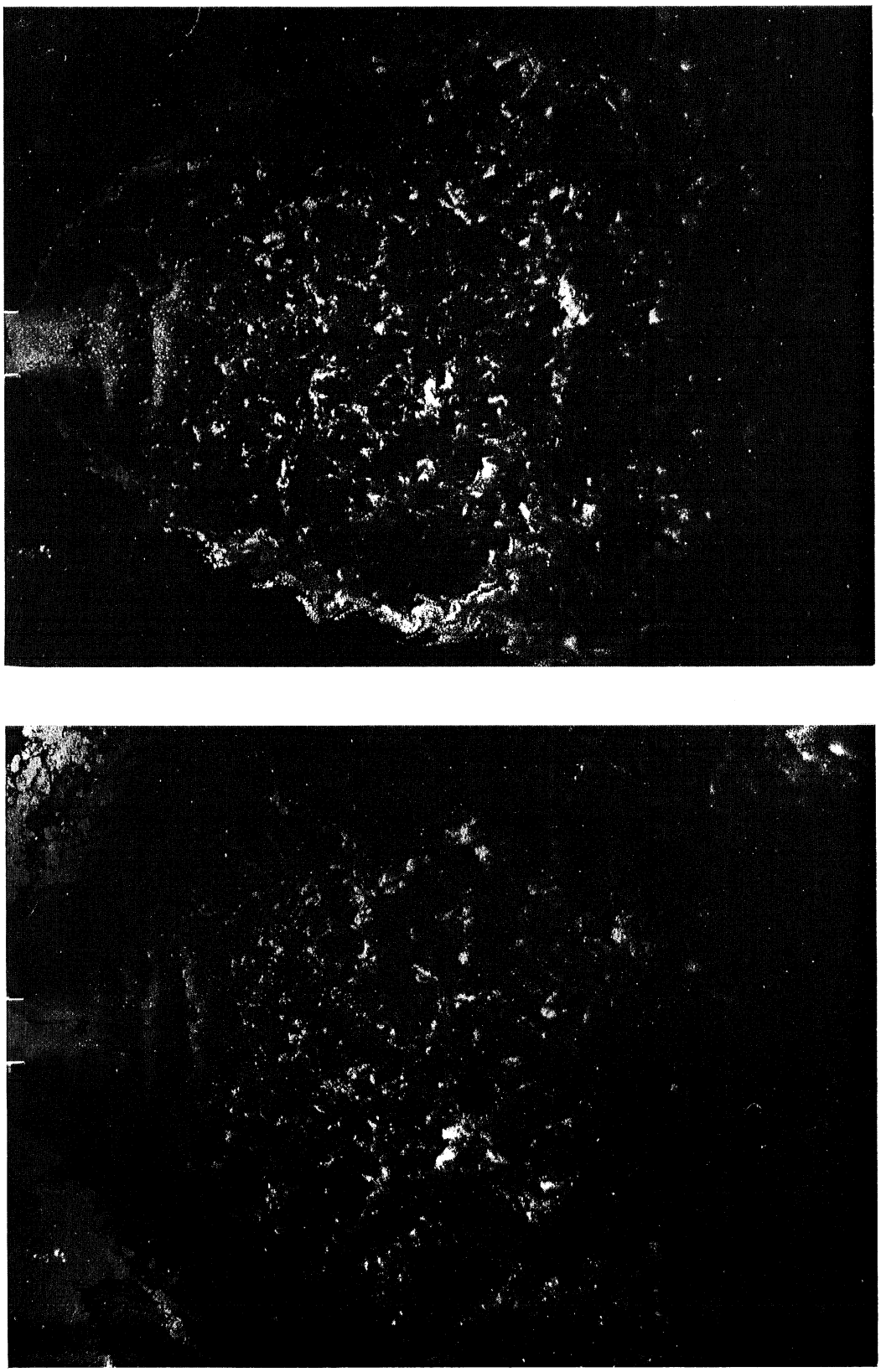

Fig. 28b - Examples of Surface Spreading Patterns showing Accumulation of Lycopodium Powder in Streaks near Outlet due to Internal Gravity Waves (Test 209)

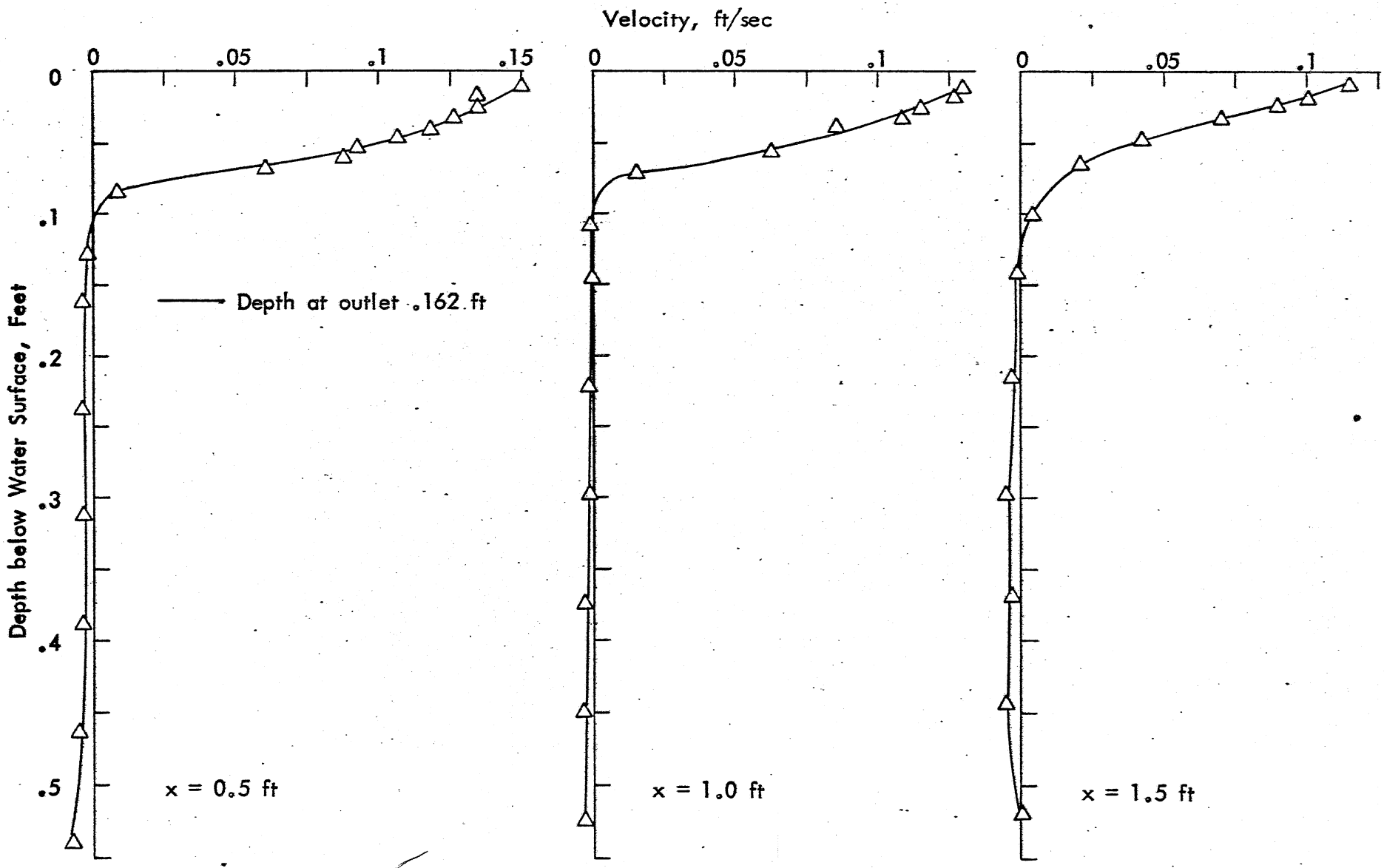

Fig. 29a - Velocity Component in x-direction for Test 215 at y = 0

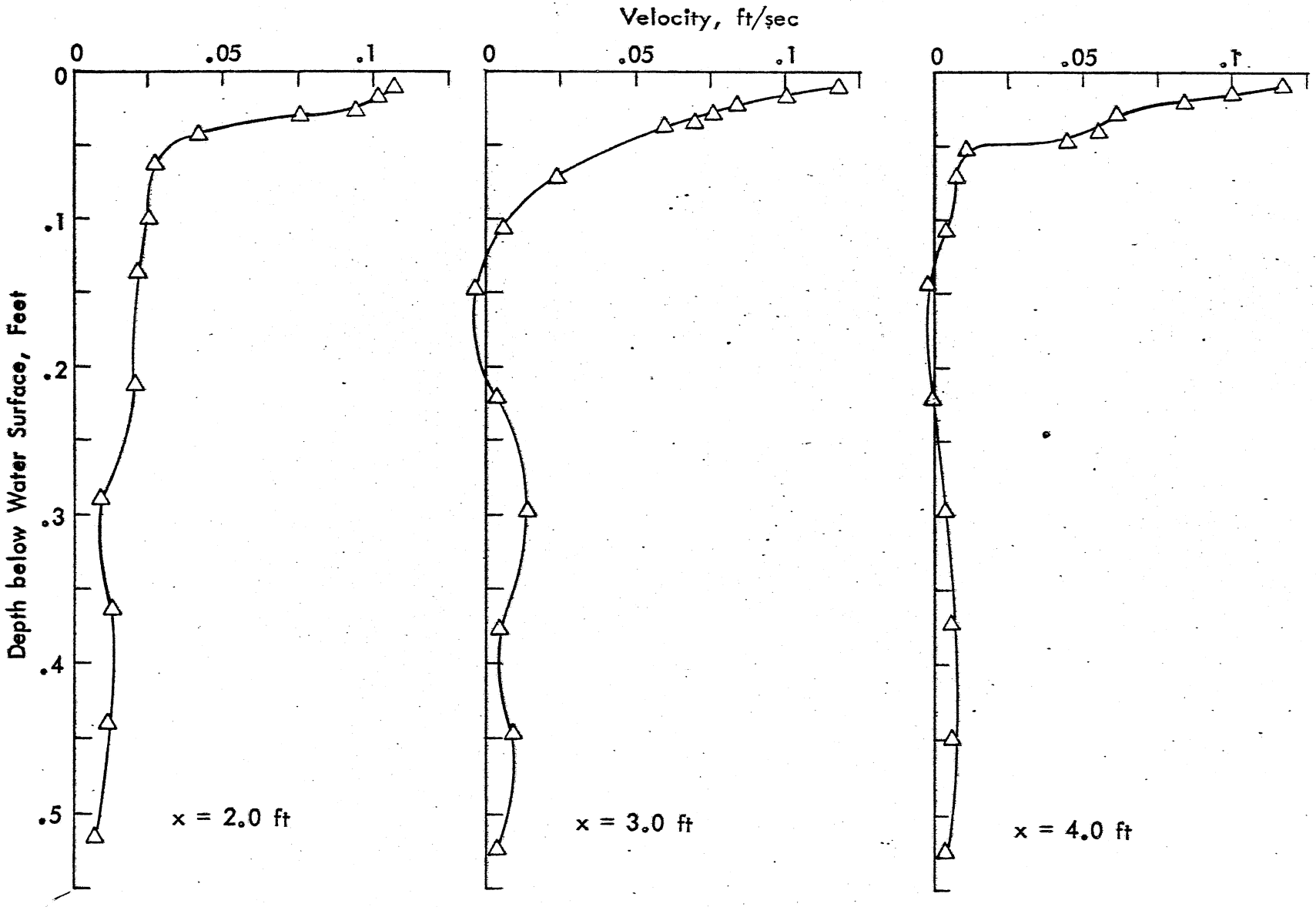

Fig. 29b - Velocity Component in x-direction for Test 215 at y = 0

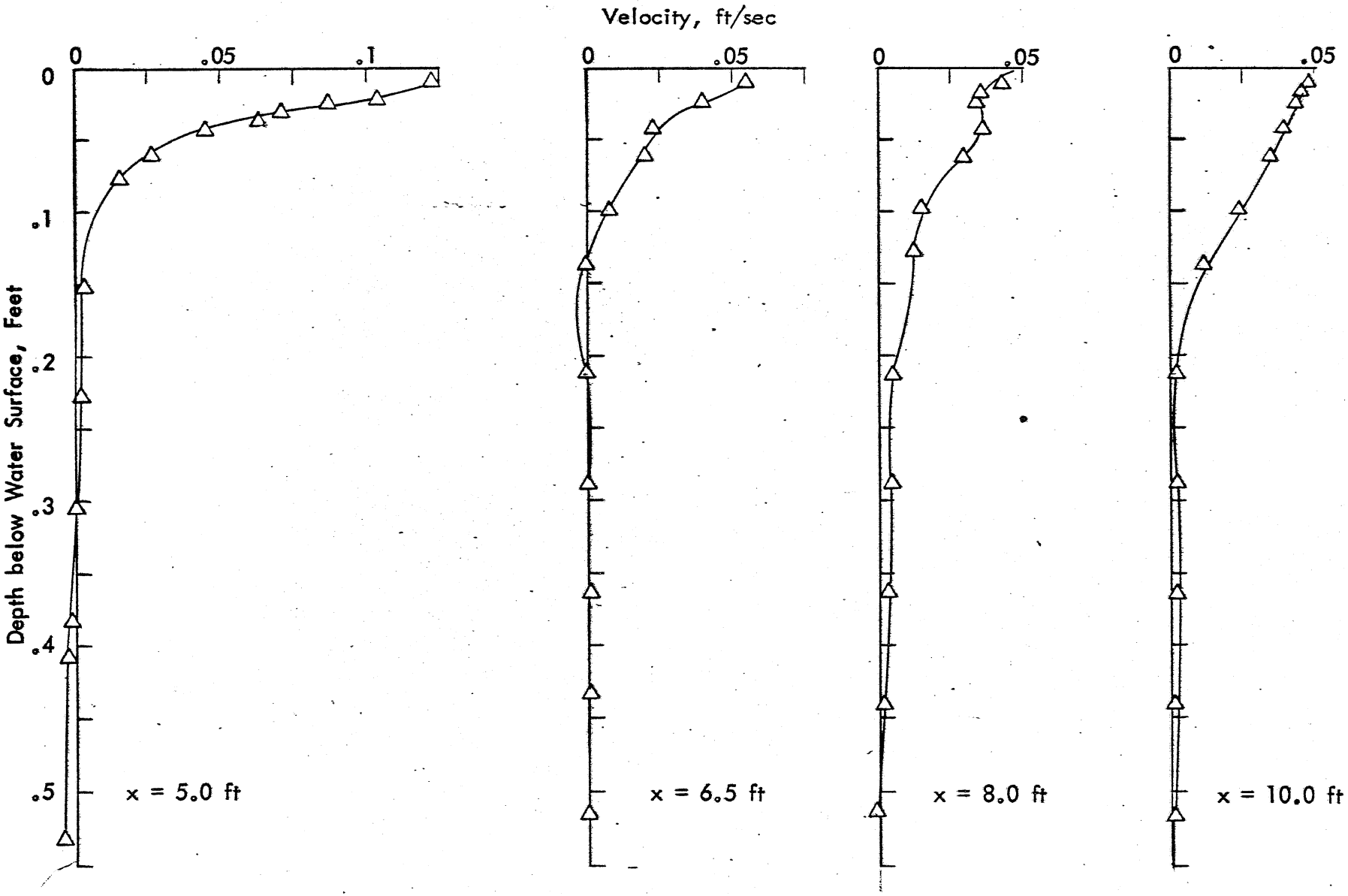

Fig. 29c - Velocity Component in x-direction for Test 215 at y = 0

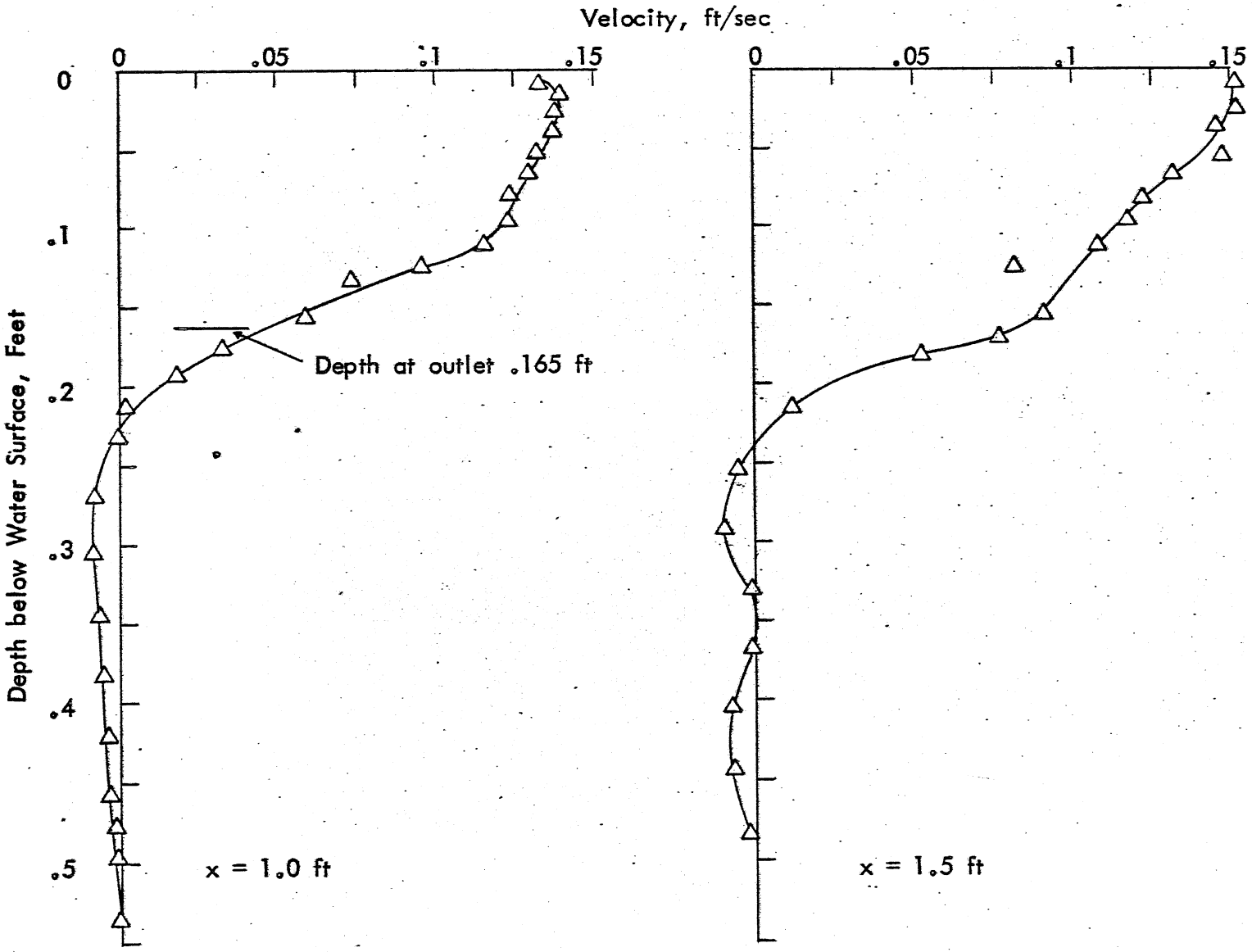

Fig. 30a - Velocity Component in x-direction for Test 207 at y = 0

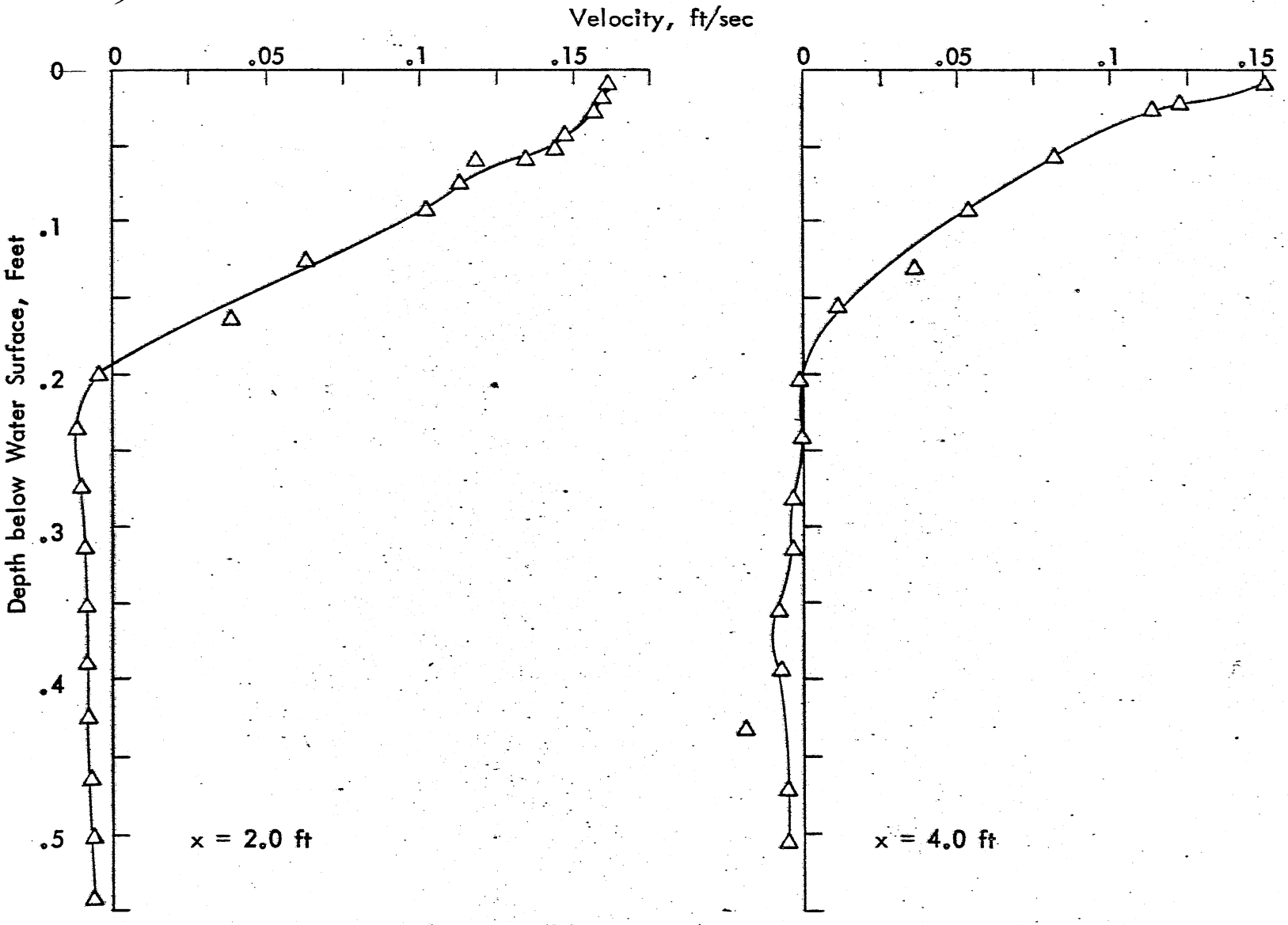

Fig. 30b - Velocity Component in x-direction for Test 207 at y = 0

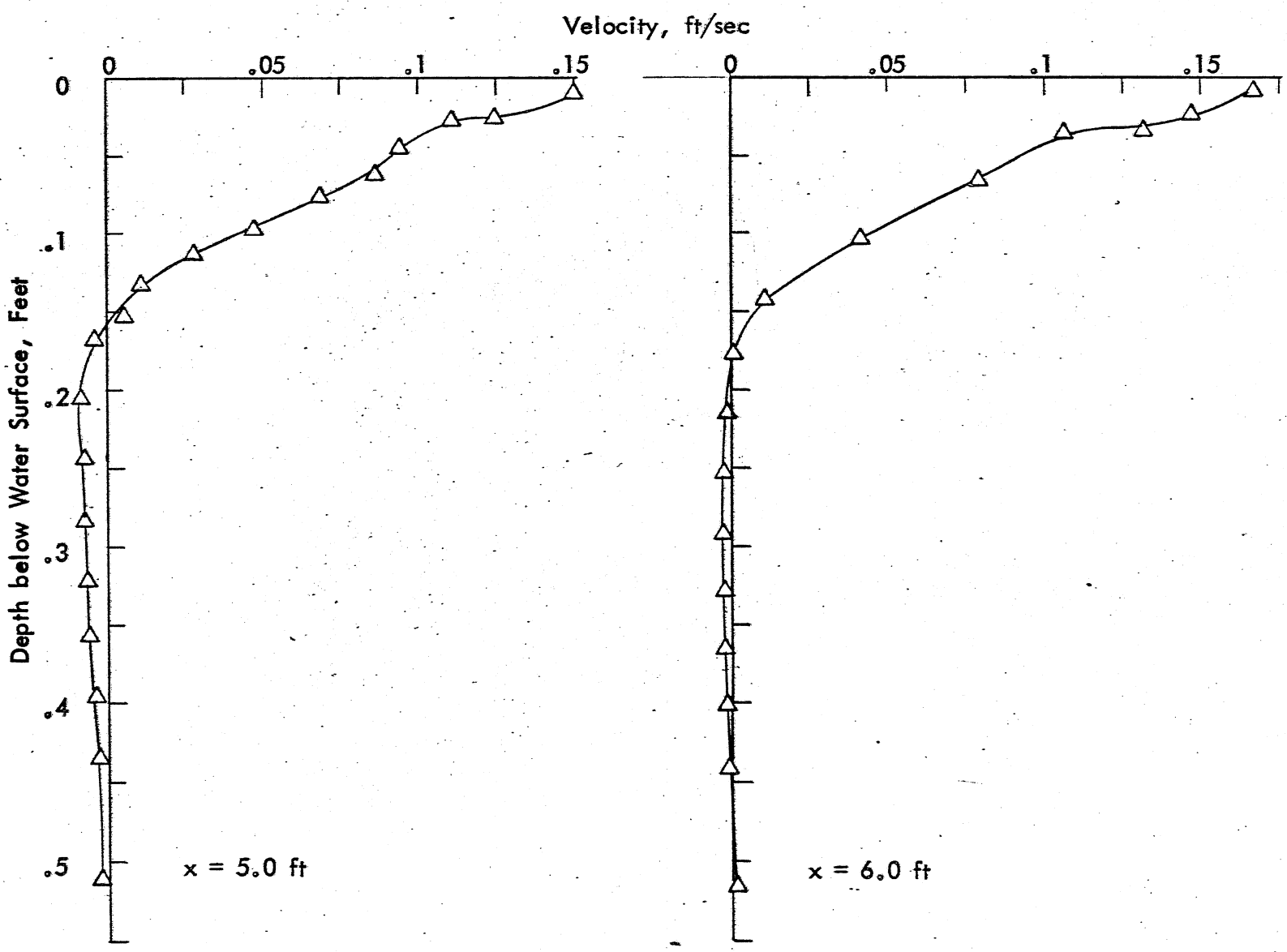

Fig. 30c - Velocity Component in x-direction for Test 207 at y = 0

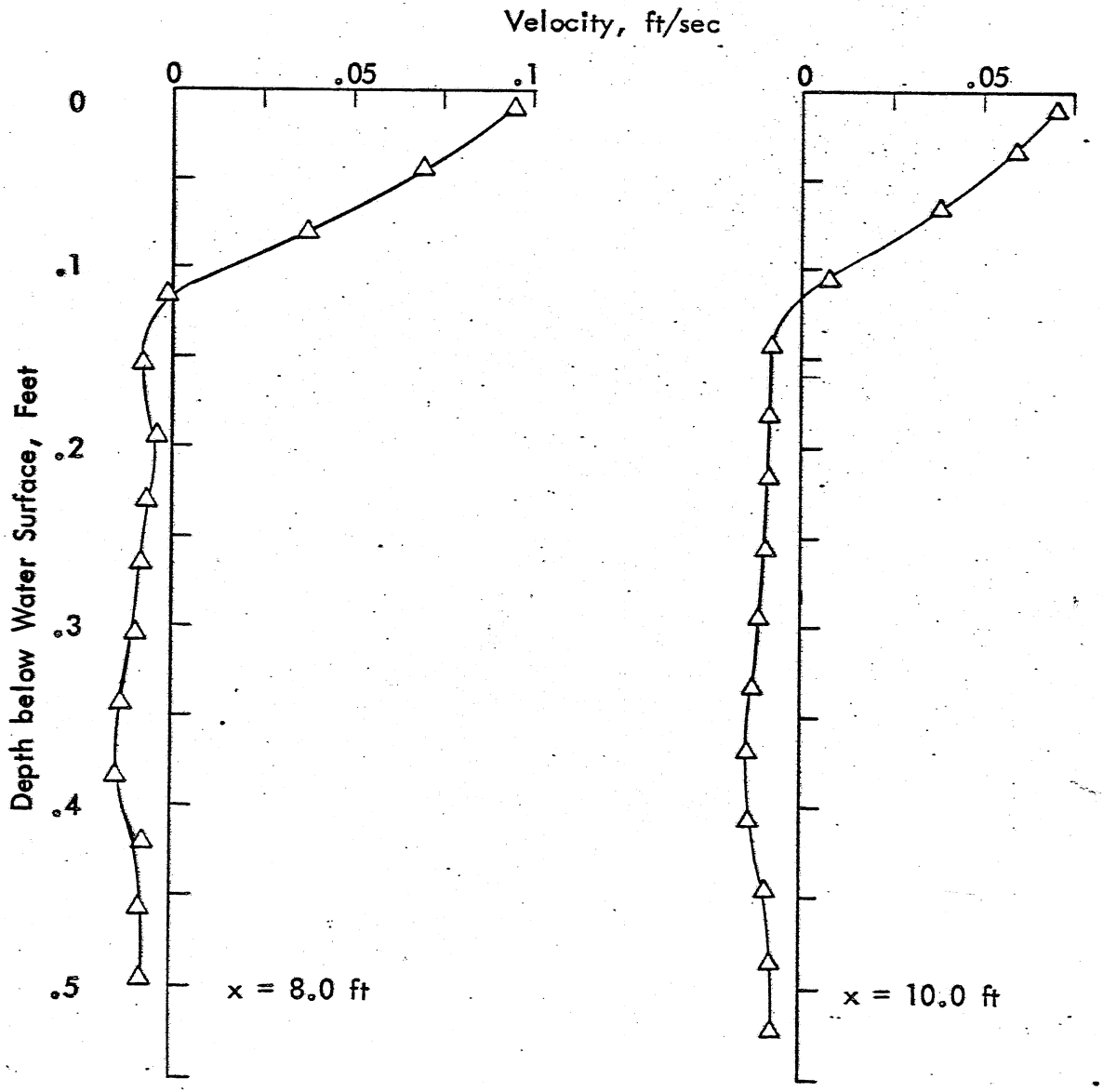

Fig. 30d - Velocity Component in x-direction for Test 207 at y = 0

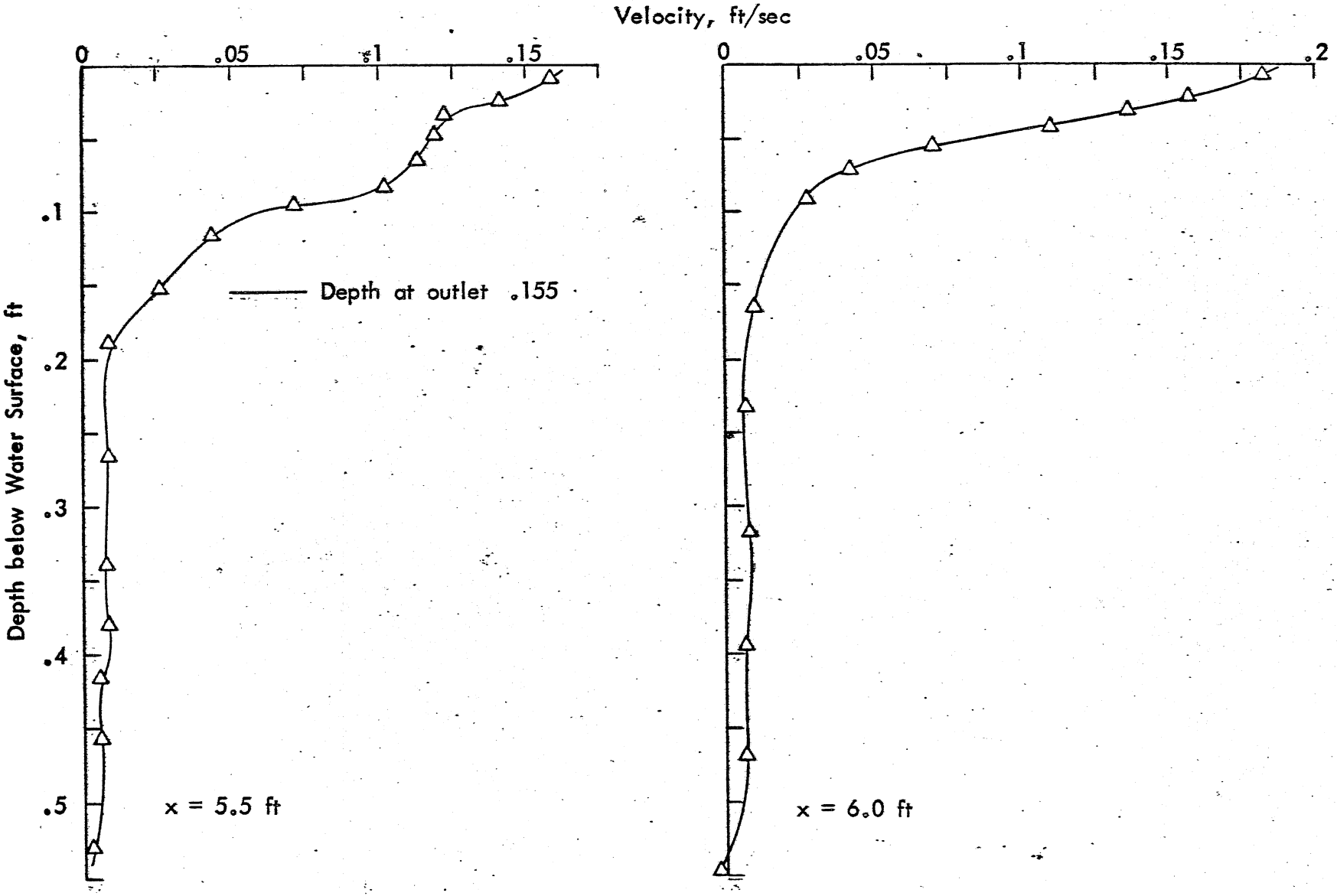

Fig. 31a - Velocity Component in x-direction for Test 214 at y = 0

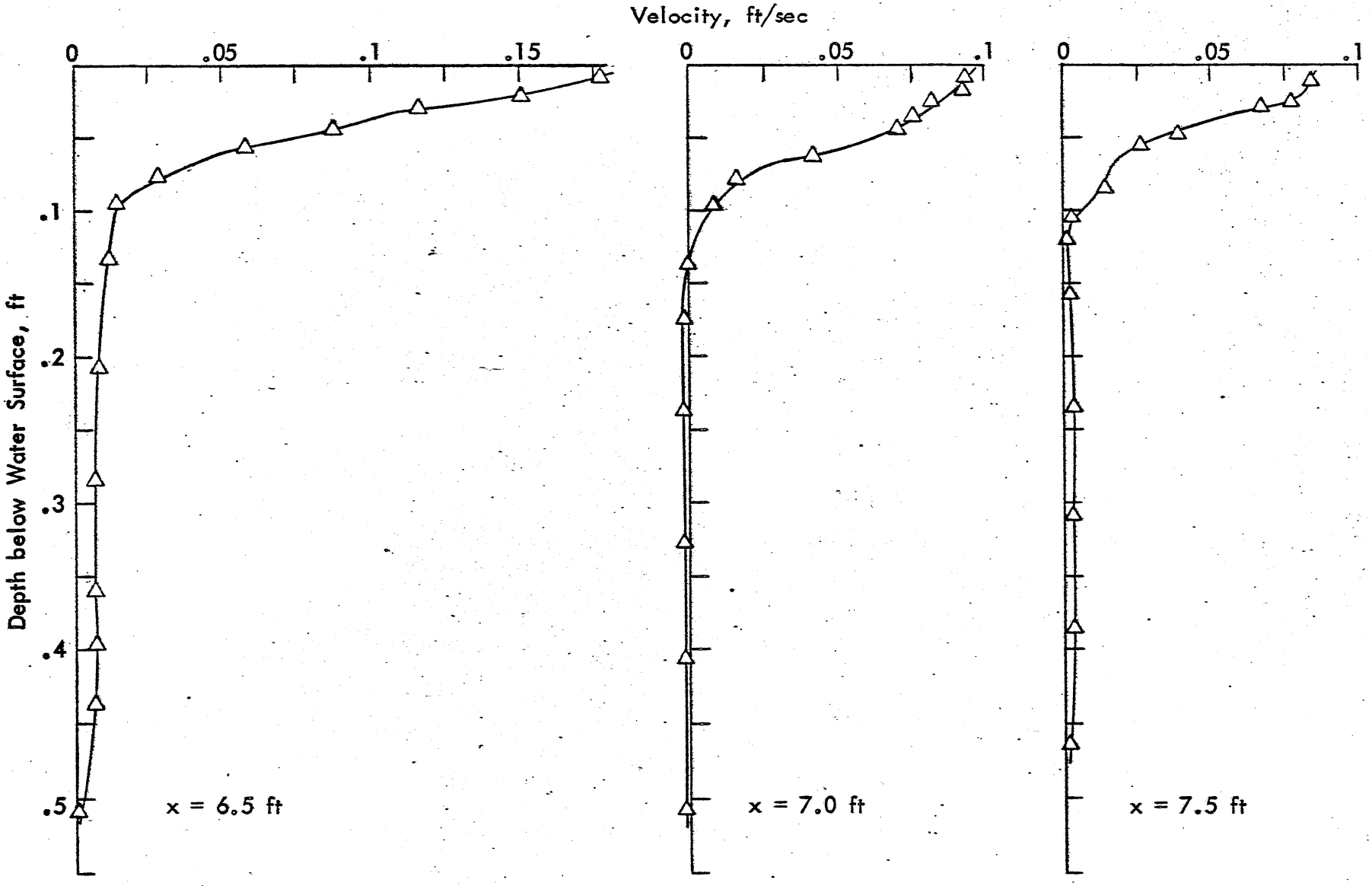

Fig. 31b - Velocity Component in x-direction for Test 214 at y = 0

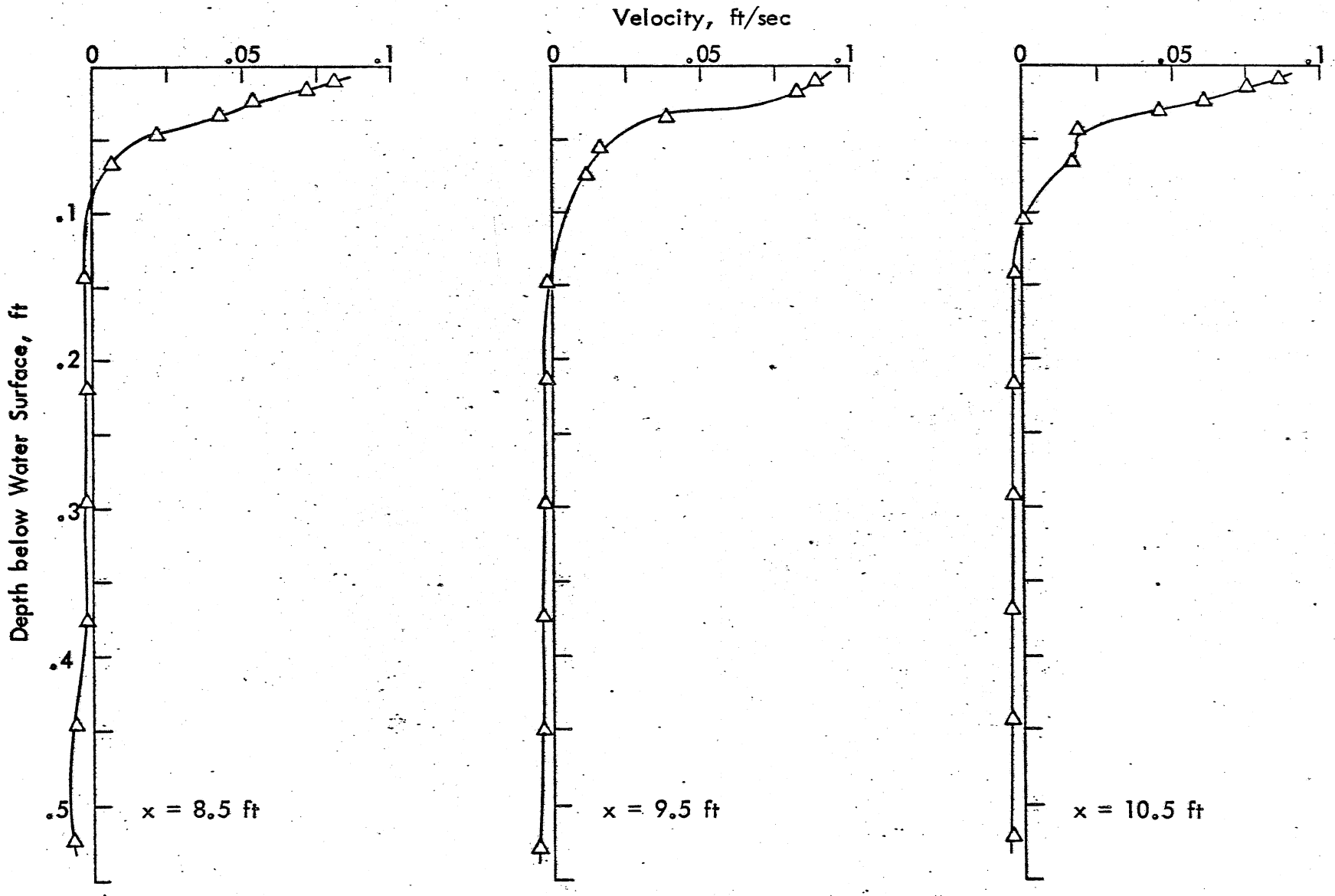

Fig. 31c - Velocity Component in x-direction for Test 214 at y = 0

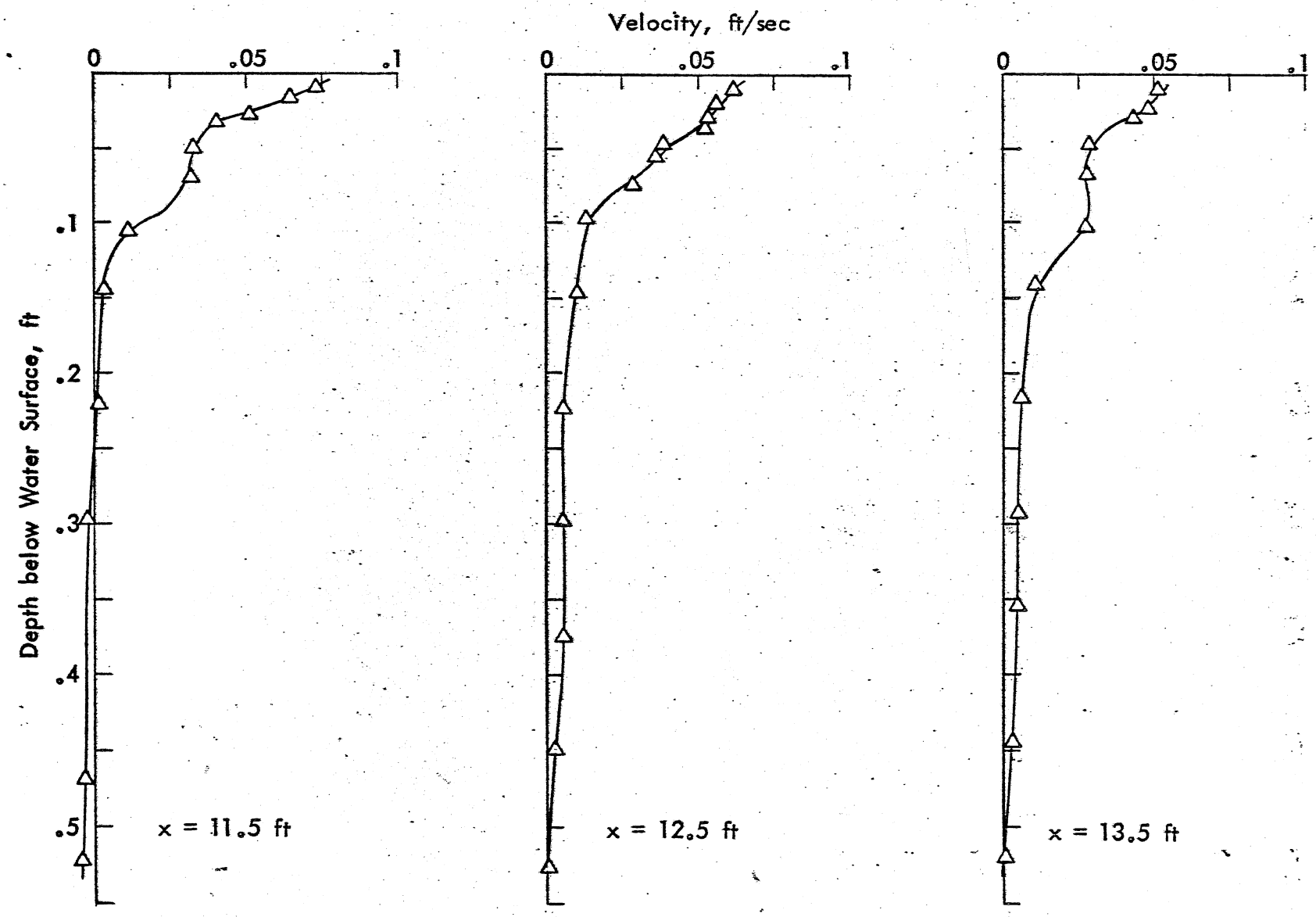

Fig. 31d - Velocity Component in x-direction for Test 214 at y = 0

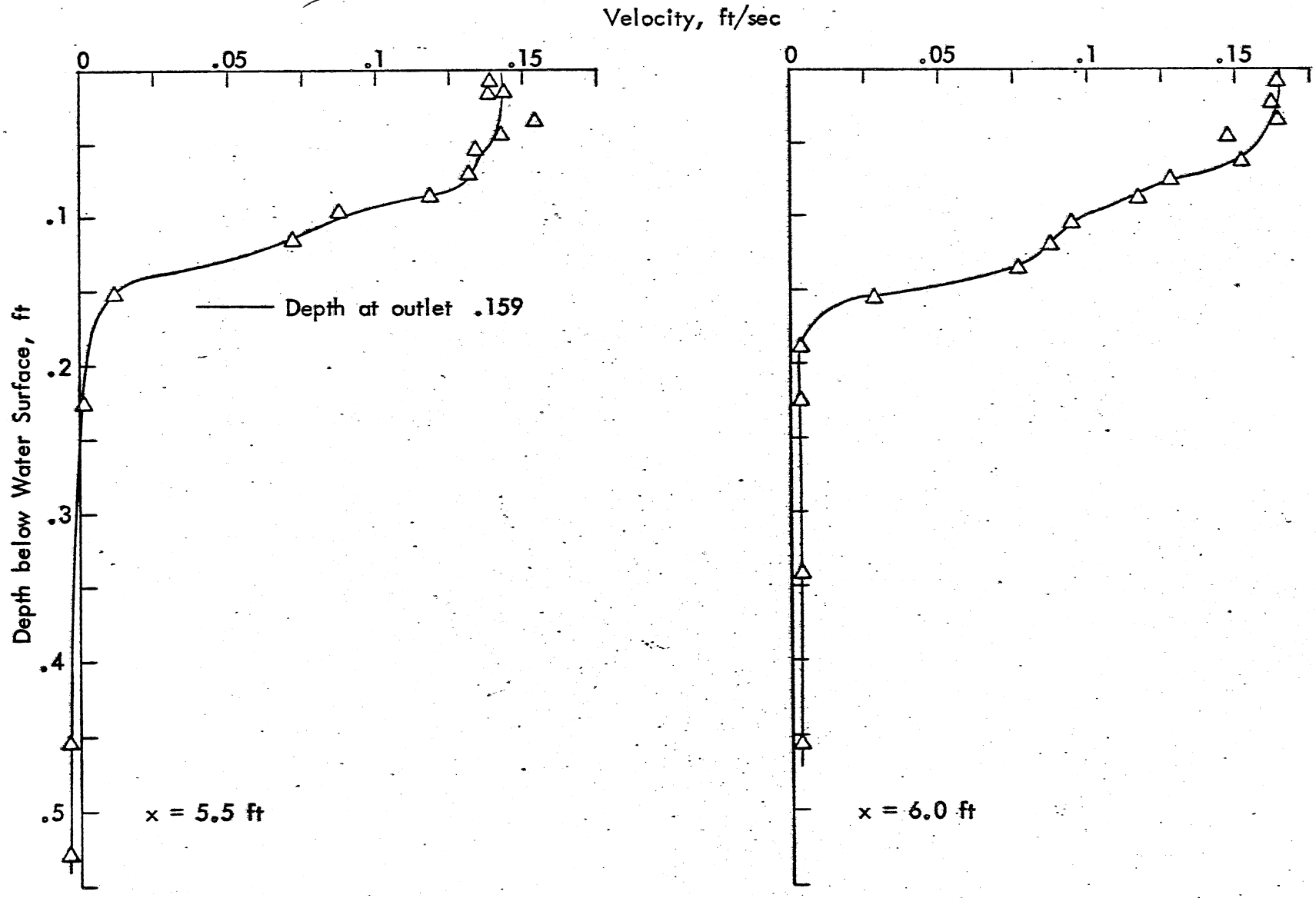

Fig. 32a - Velocity Component in x-direction for Test 211 at y = 0

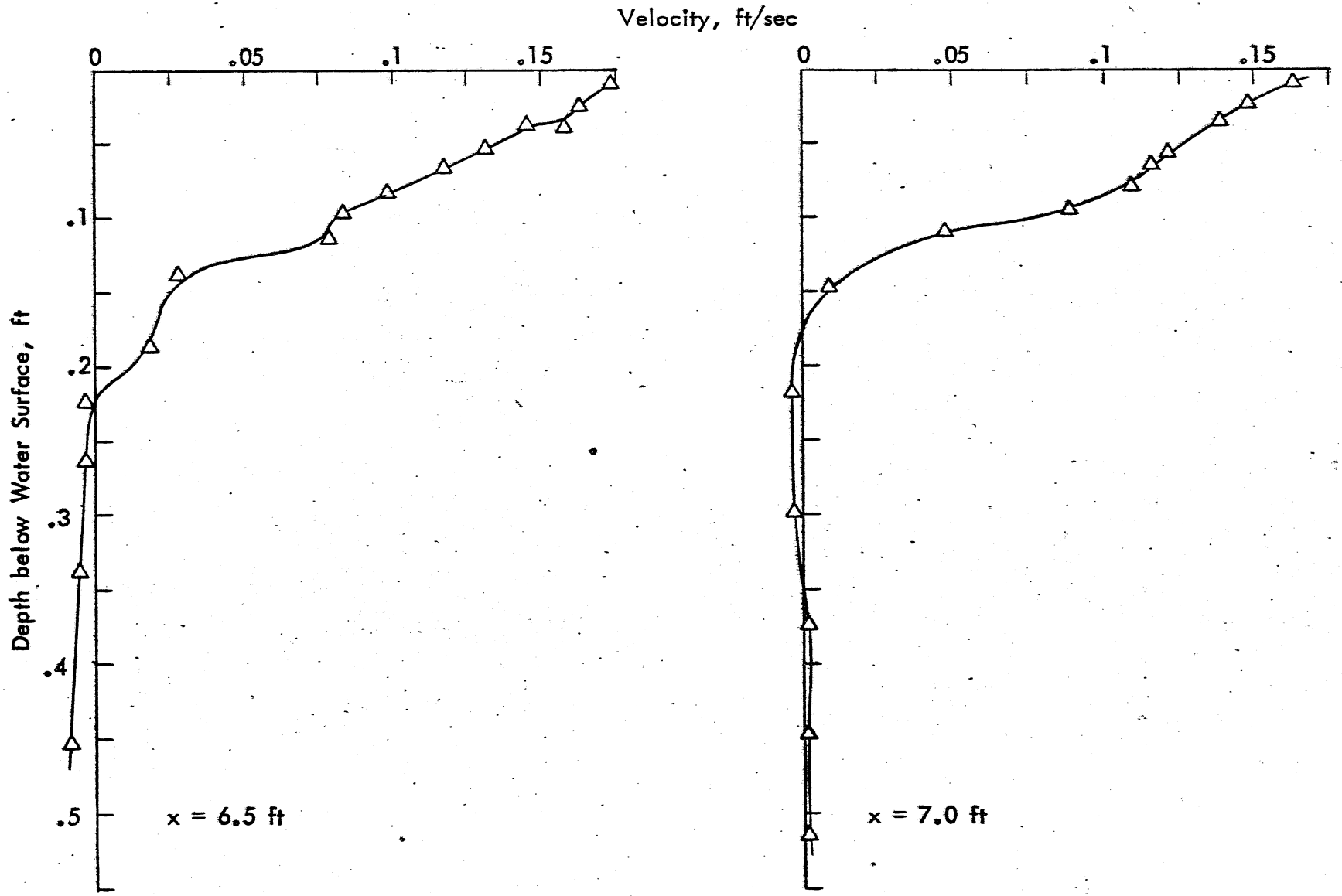

Fig. 32b - Velocity Component in x-direction for Test 211 at y = 0

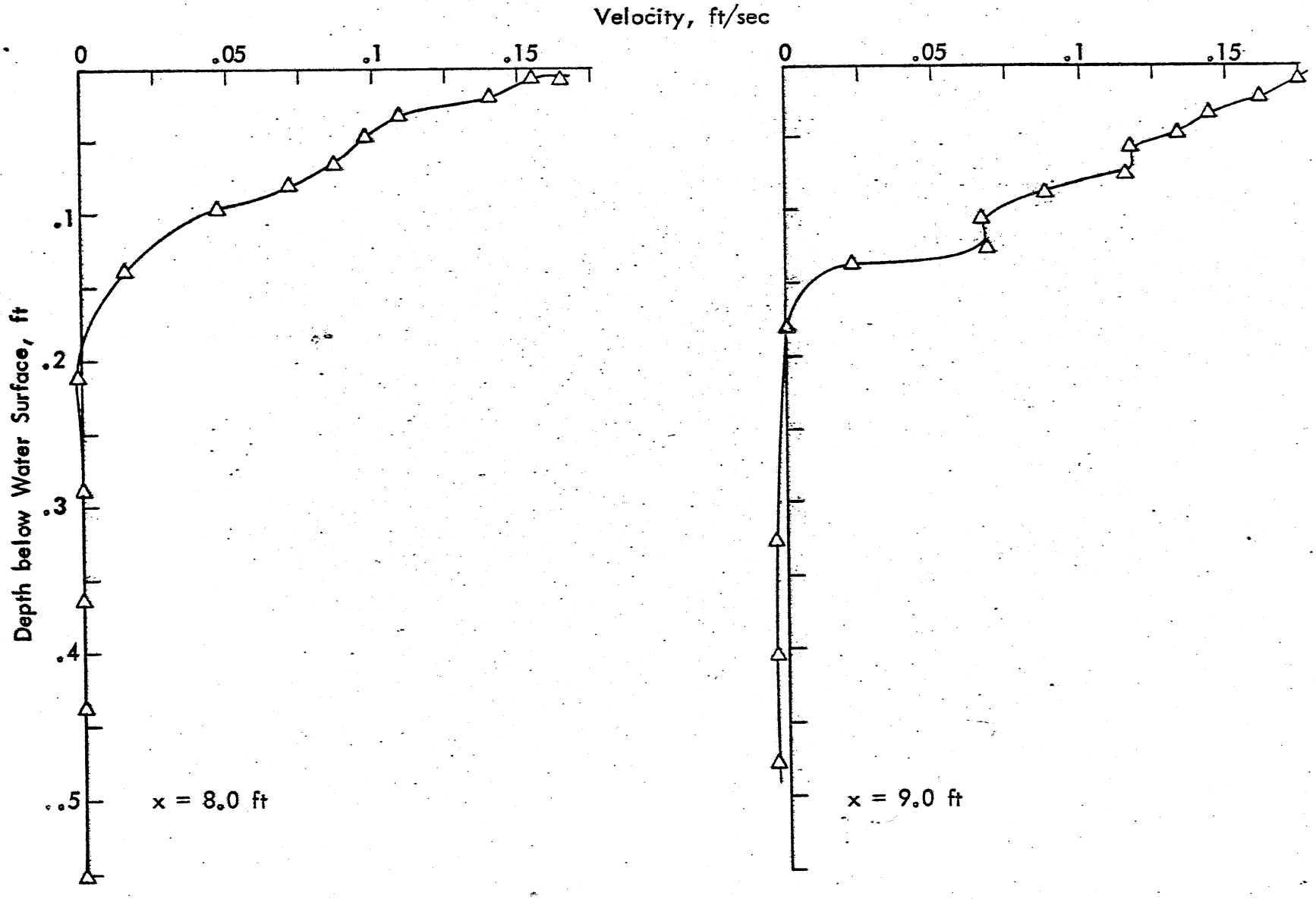

Fig. 32c - Velocity Component in x-direction for Test 211 at y = 0

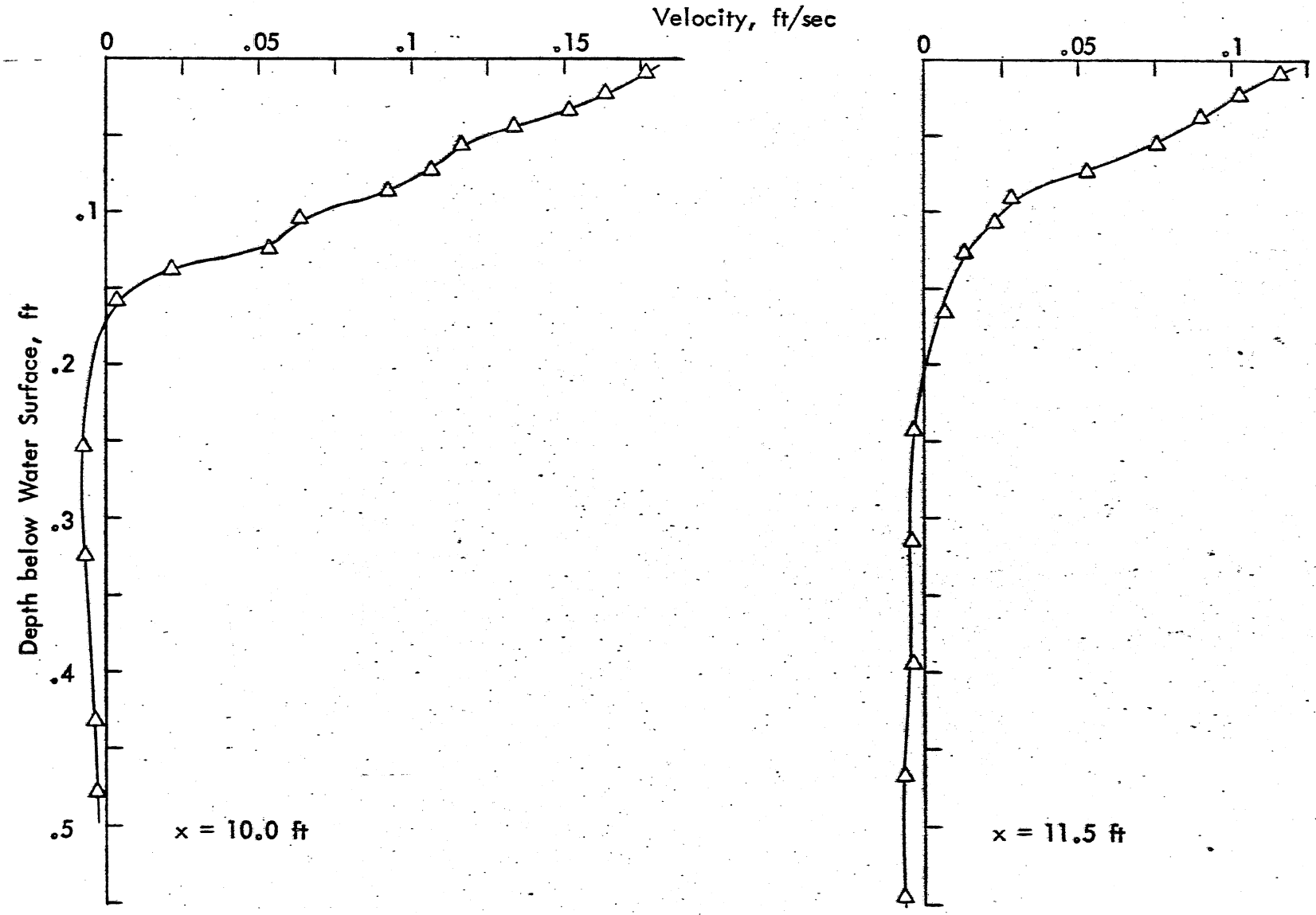

Fig. 32d - Velocity Component in x-direction for Test 211 at y = 0

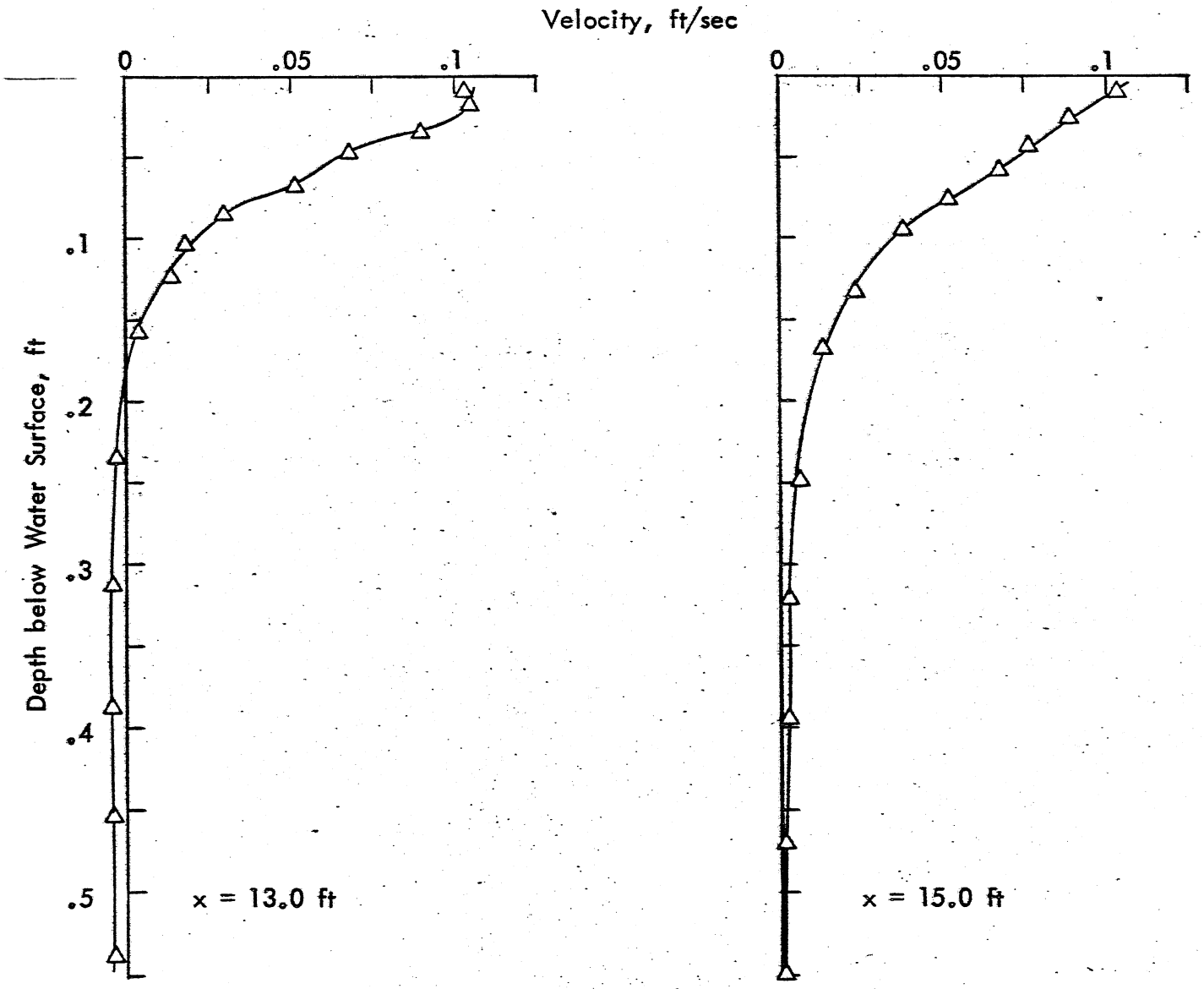

Fig. 32e - Velocity Component in x-direction for Test 211 at y = 0

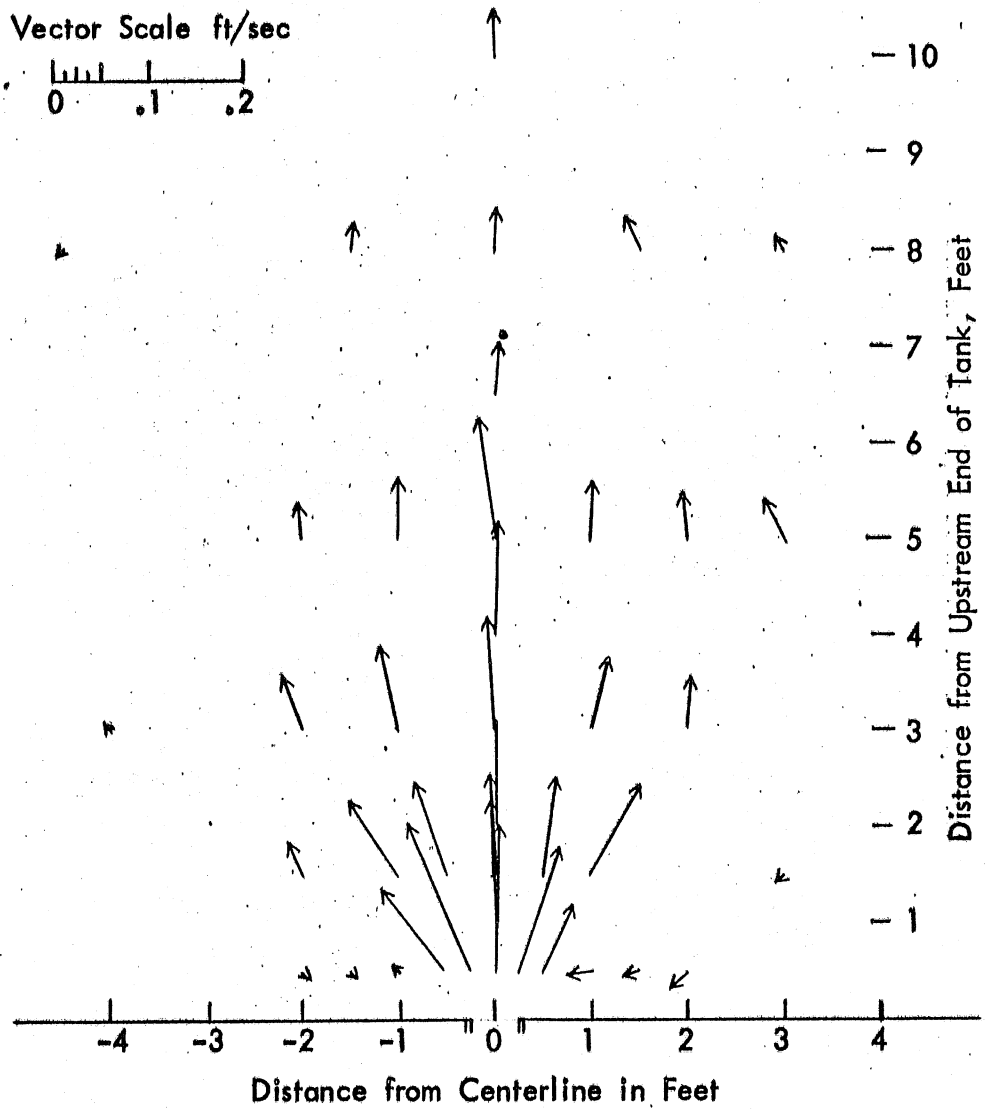

Fig. 33a - Velocity Vectors for Test 215 at Water Surface

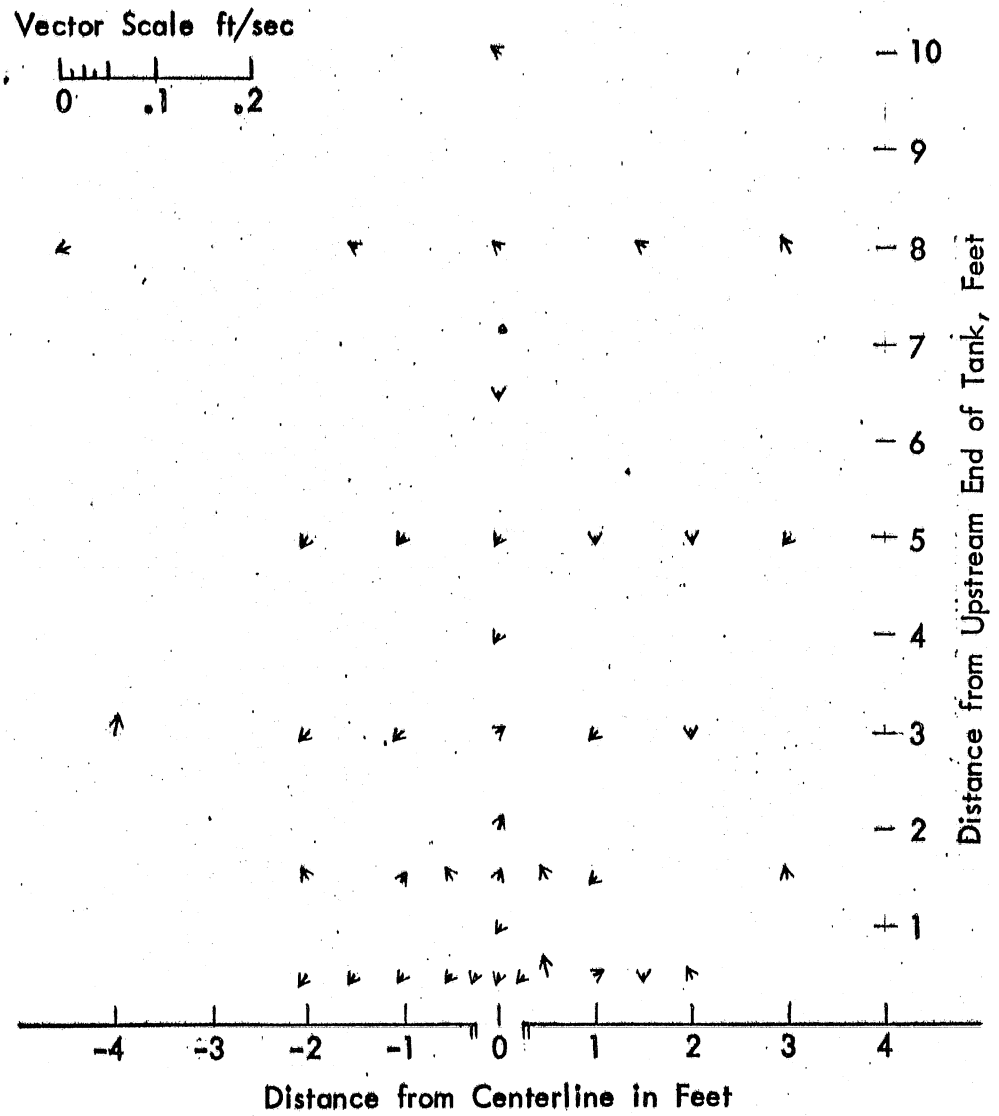

Fig. 33b - Velocity Vectors for Test 215 at z = 0.2 ft

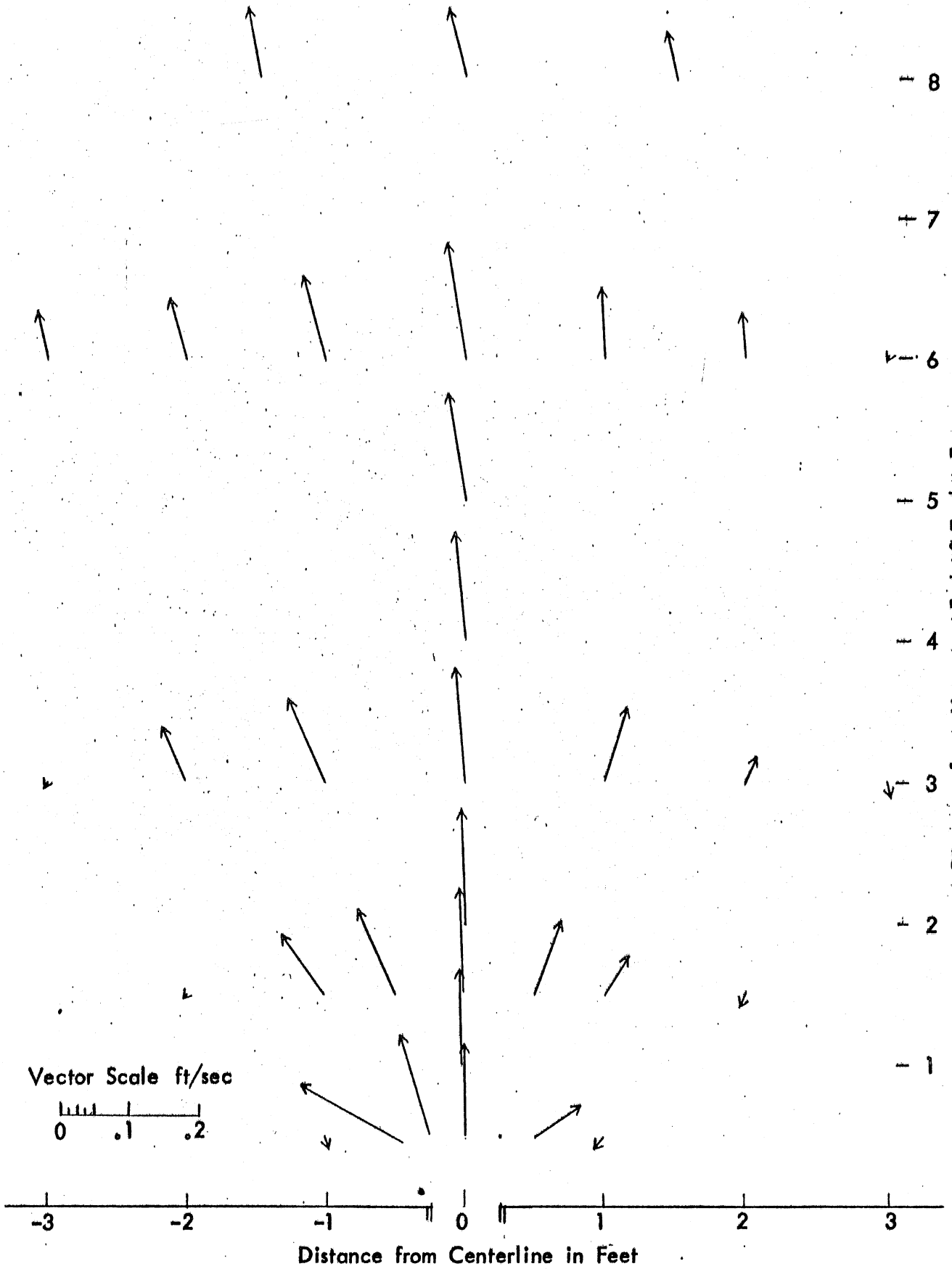

Fig. 34a - Velocity Vectors for Test 207 at Water Surface

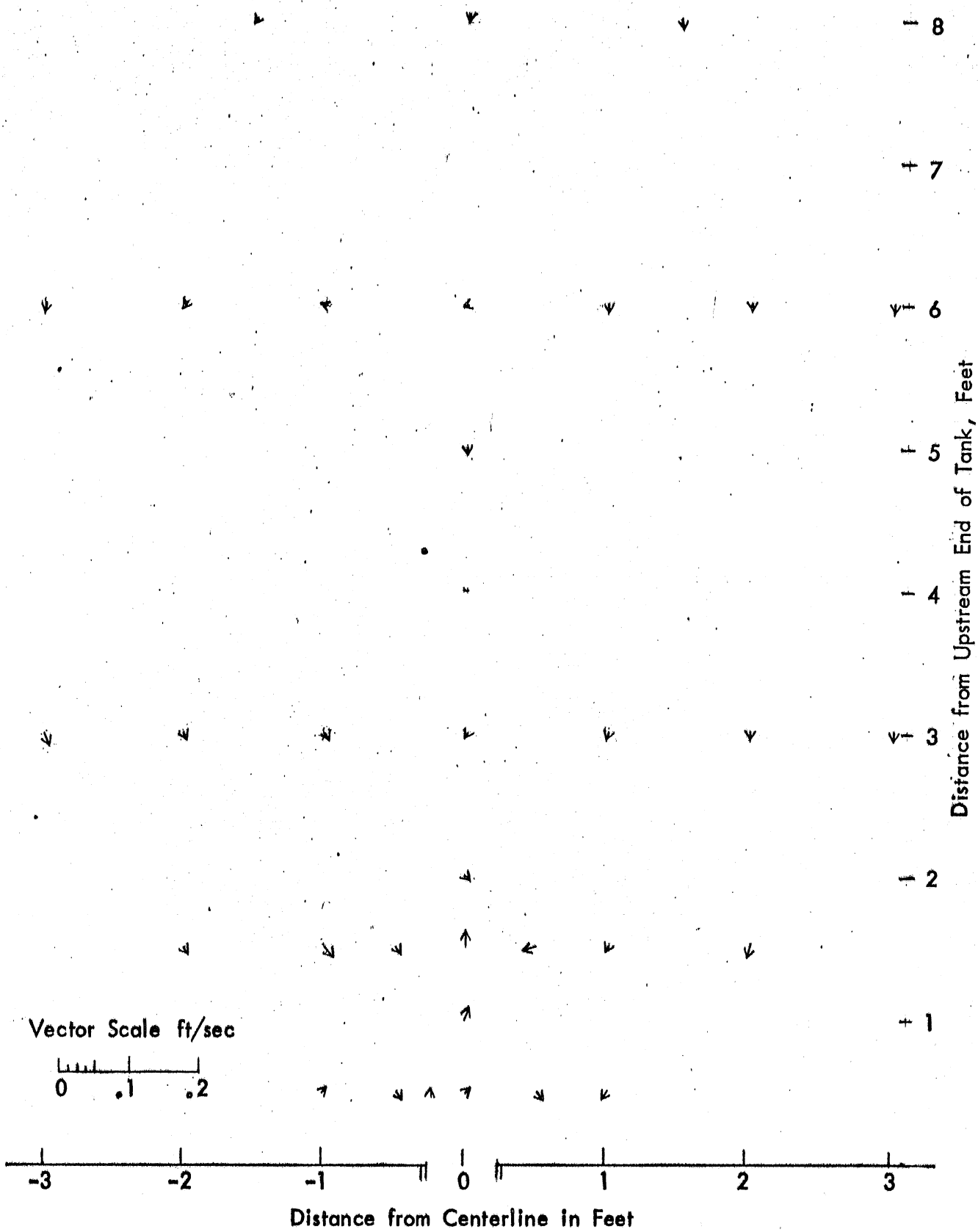

Fig. 34b - Velocity Vectors for Test 207 at z = 0.2 ft

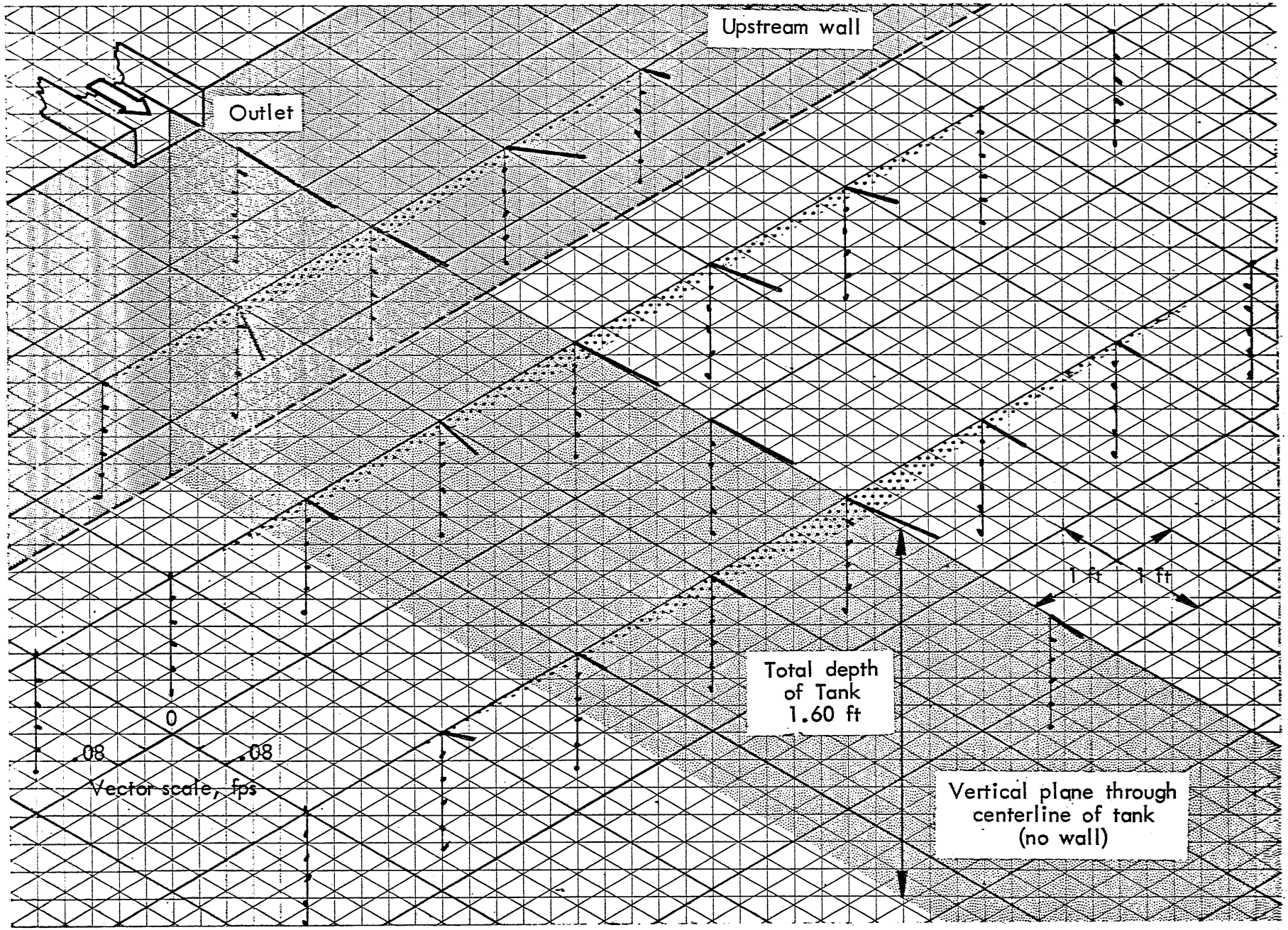

Fig. 35a - Velocity Field near the Outlet for Test 215. Lengths of bars are proportional to velocity magnitudes. Heavy dotted areas refer to velocity components $u > 0$.

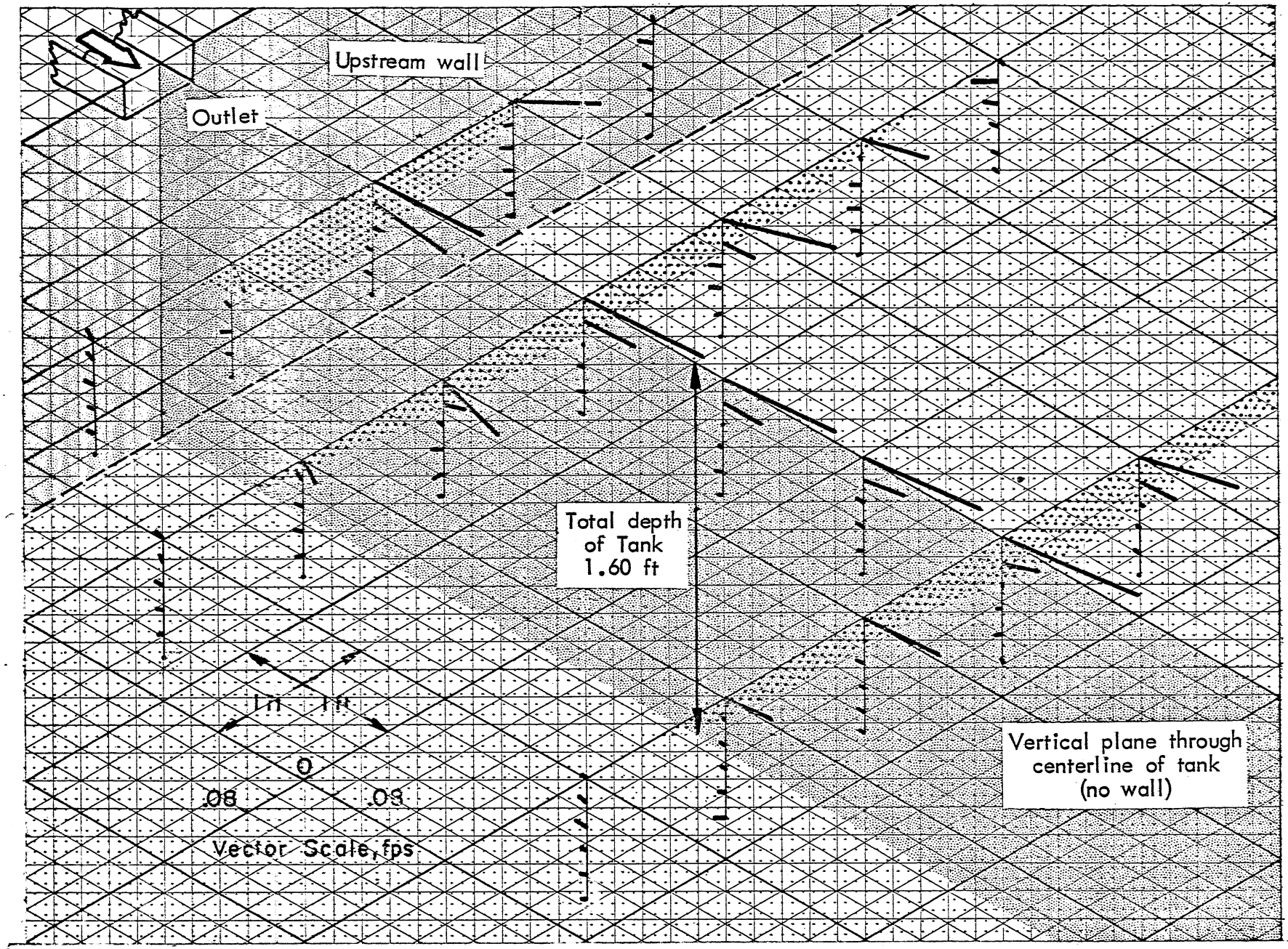

Fig. 35b - Velocity Field near the Outlet for Test 207. Lengths of bars are proportional to velocity magnitudes. Heavy dotted areas refer to velocity components $u > 0$.

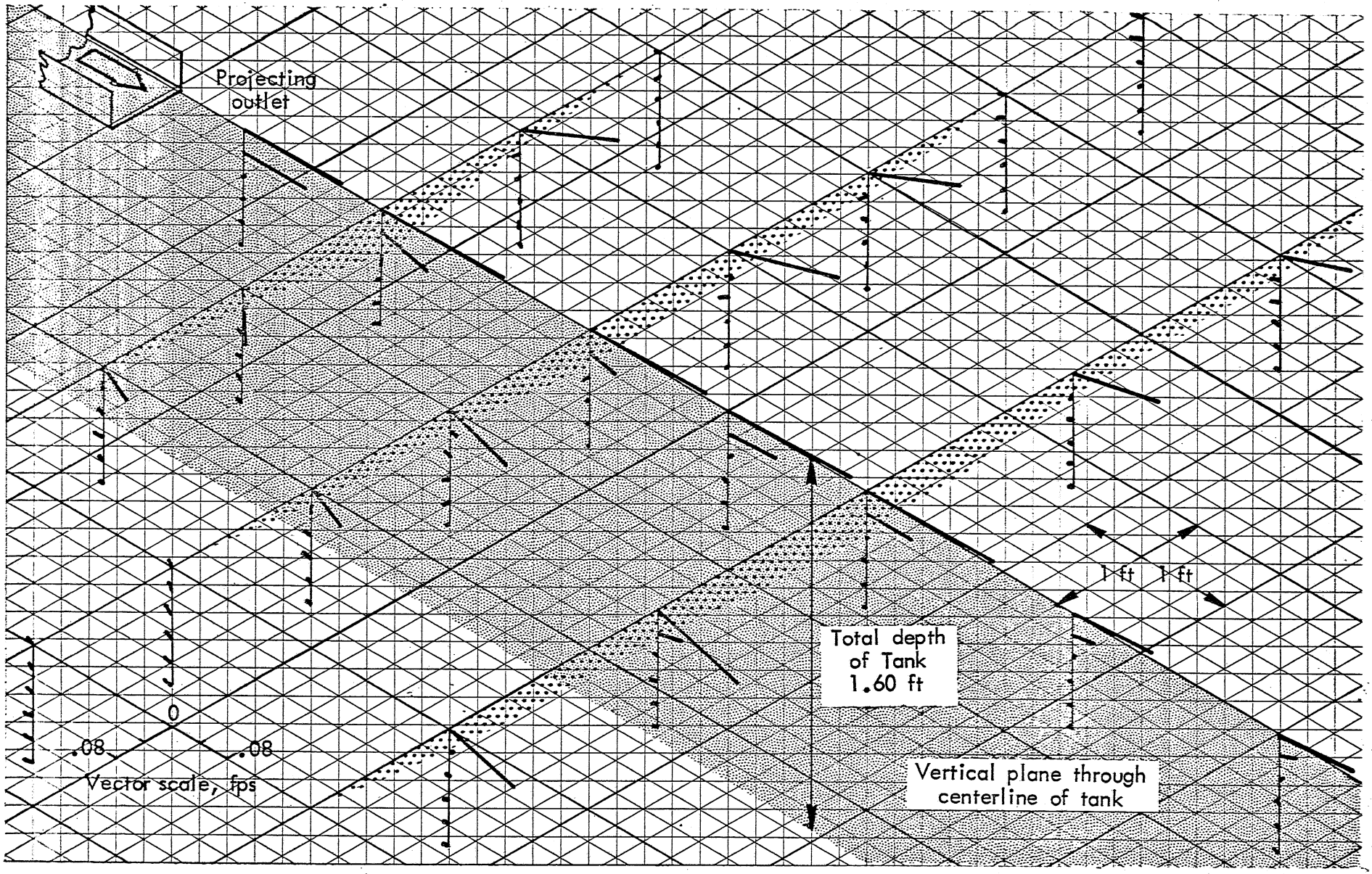

Fig. 35c - Velocity Field near the Outlet for Test 211. Lengths of bars are proportional to velocity magnitudes. Heavy dotted areas refer to velocity components $u > 0$.

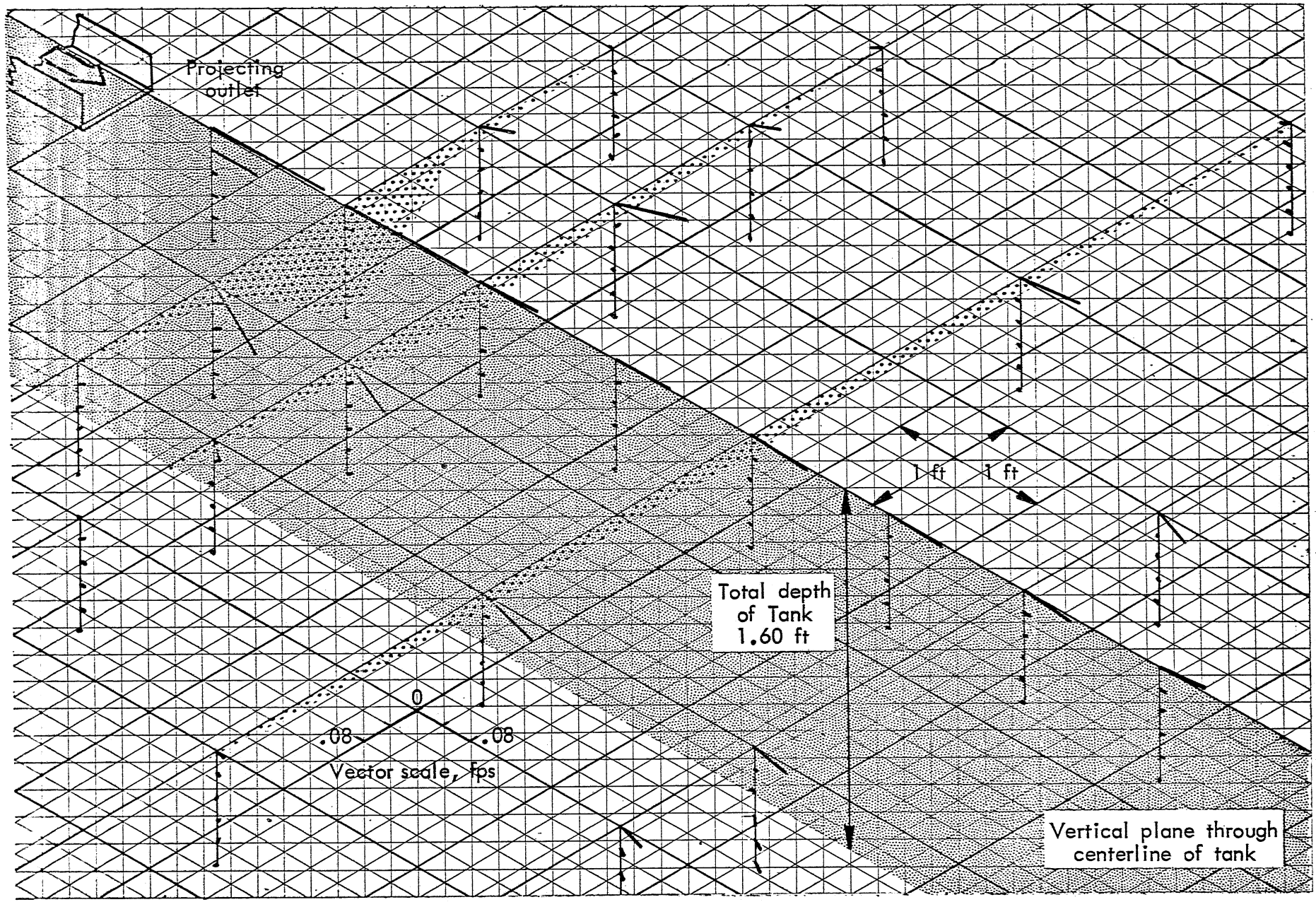

Fig. 35d – Velocity Field near the Outlet for Test 214. Lengths of bars are proportional to velocity magnitudes. Heavy dotted areas refer to velocity components $u > 0$.

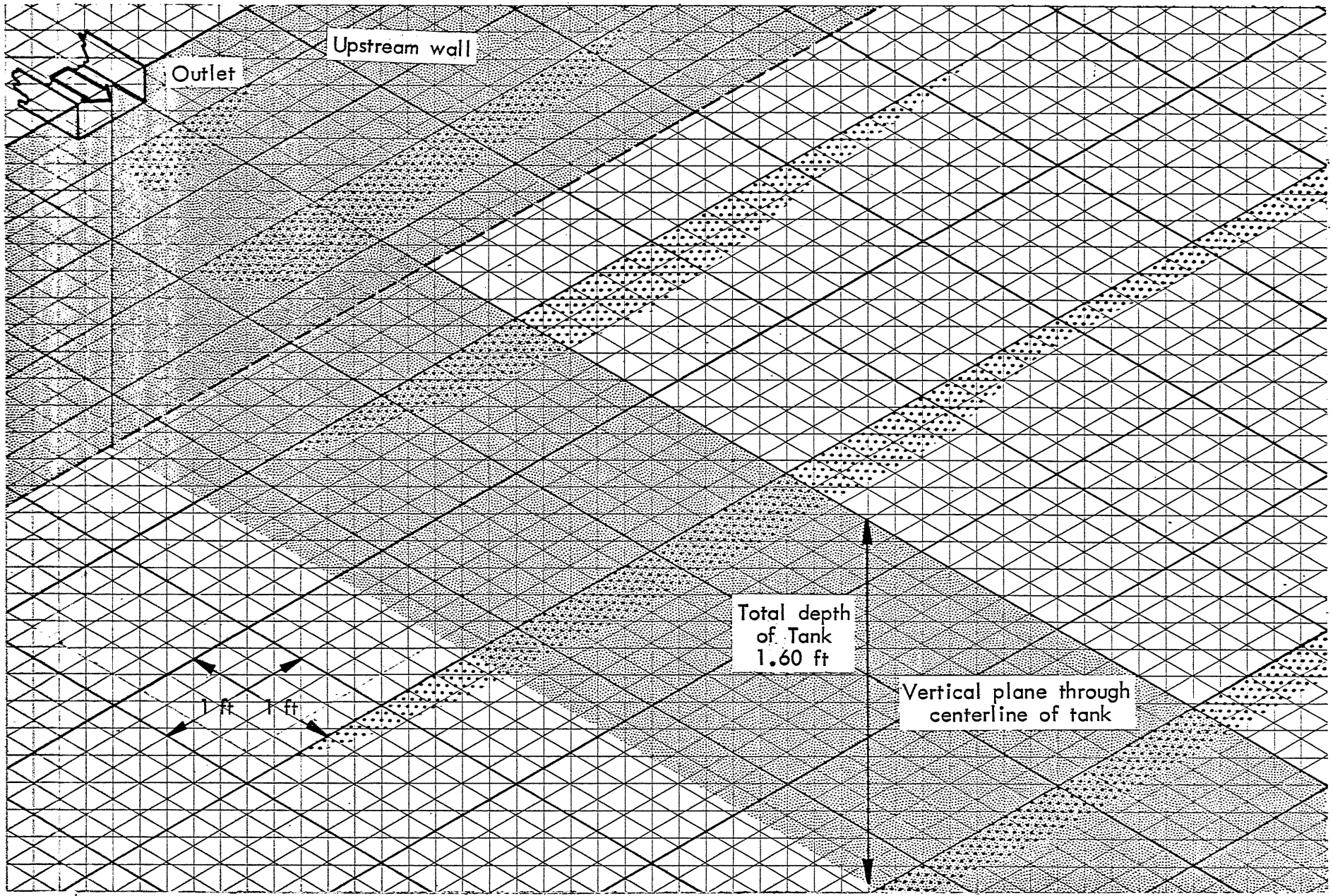

Fig. 36a - Surface Layer near Outlet for Test 216. Heavy dotted areas refer to velocity components $u > 0$.

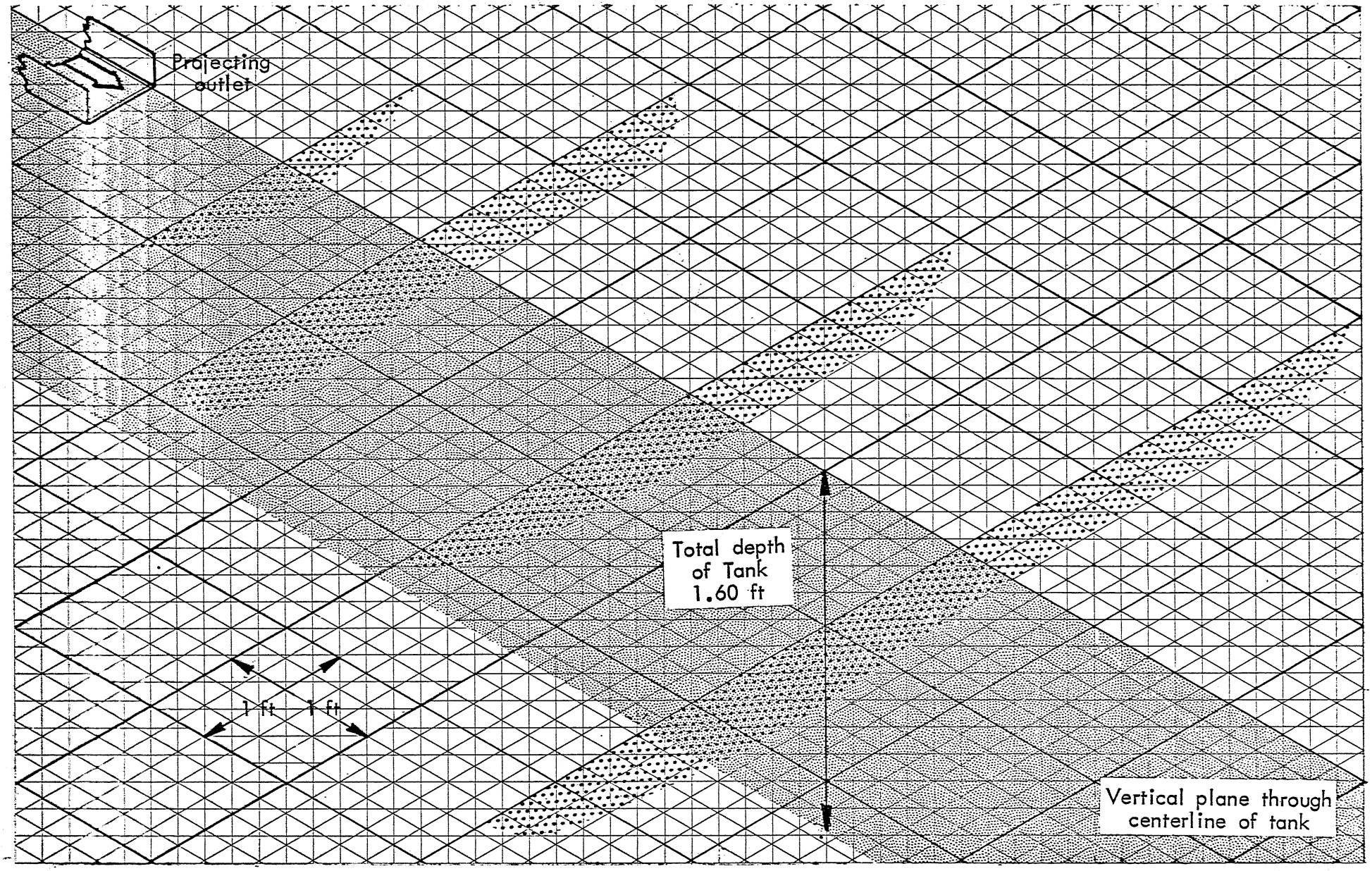

Fig. 36b – Surface Layer near Outlet for Test 217. Heavy dotted areas refer to velocity components $u > 0$.